Article:

Armit, RJ, Betts, PG, Schaefer, BF et al. (2 more authors) (2014) Provenance of the Early Mesoproterozoic Radium Creek Group in the northern Mount Painter Inlier: Correlating isotopic signatures to inform tectonic reconstructions. Precambrian Research, 243. 63 - 87. ISSN 0301-9268

https://doi.org/10.1016/j.precamres.2013.12.022

Elsevier Editorial System(tm) for Precambrian Research
Manuscript Draft

Manuscript Number: PRECAM3819R1

Title: Provenance of the Early Mesoproterozoic Radium Creek Group in the Northern Mount Painter Inlier: Correlating isotopic signatures to inform tectonic reconstructions

Article Type: Research Paper

Keywords: Radium Creek Group; Mount Painter Inlier; U-Pb maximum depositional ages; Hf isotopes; isotopic fingerprinting; Palaeogeographical reconstructions

Corresponding Author: Mr Robin John Armit, BSc Hons

Corresponding Author's Institution: Monash University

First Author: Robin John Armit, BSc Hons

Order of Authors: Robin John Armit, BSc Hons; Peter G Betts, Ph.D; Bruce F Schaefer, Ph.D; Matthew J Pankhurst, Ph.D; David Giles, Ph.D

Abstract: New in-situ zircon LA-ICPMS geochronologic and Hf-isotope data from the Radium Creek Group within the Mount Painter Inlier provide important temporal constraints on the Early Mesoproterozoic palaeogeography of eastern Proterozoic Australia. The entire Radium Creek Group was deposited in a single basin forming phase, and has a maximum depositional age of 1595 ± 3.7 Ma. Detrital zircon from these metasedimentary rocks have U-Pb age populations at ca. 1595 Ma, 1660-1680 Ma, 1710-1780 Ma, ca. 1850 Ma and ca. 2500 Ma. These grains are characterised by isotopically diverse and evolved sources, and have crystallised within predominantly felsic igneous host-rocks. The relative age spectra and isotopic character has more similarity with the Gawler Craton than the Arunta Block, Curnamona Province or the Mount Isa Inlier. These observations suggest that the Mount Painter Province was adjacent to the Gawler Craton in the Early Mesoproterozoic. Our data supports a coherent South Australian Craton at ca. 1595 Ma and a contiguous continental mass that included the North and South Australian cratons. The Mount Painter Inlier occupied a complex plate tectonic setting in the overriding plate of two convergent margins.

Cover letter

Randall Parrish
Editor
Precambrian Research

Dear Randall,

We have revised the manuscript titled "Provenance of the Early Mesoproterozoic Radium Creek Group in the Northern Mount Painter Inlier: Correlating isotopic signatures to inform tectonic reconstructions" co-authored by Robin Armit, Peter Betts, Bruce Schaefer, Matthew Pankhurst and David Giles for consideration for publication in Precambrian Research.

We thank you for the review of this manuscript. We have improved the manuscript in accordance with your recommendations and in particular address more fully the key points of debate outlined in the introduction. We have also included regional maps and simplified the local geological interpretations in order to make this paper more appealing to the readers of Precambrian Research.

We have outlined clearly how we have dealt with each and every comment raised by reviewers or editor in a tabulated list of changes in the file named "Revision notes.docx". We have also included a marked up version of the revised manuscript showing all of the changes made.

We hope this manuscript can still be considered for publication in Precambrian Research.

Yours Sincerely,

Robin Armit

PhD Candidate

arc linkage Project # LP0882000 "Unearthing the marginal terranes of the South Australian Craton: Keystone of Proterozoic Australia."

School of Geosciences
Monash University
P.O. Box 28E
VIC 3800
robin.armit@monash.edu
tel: +61 3 9905 4973

Revisions

General comments – editor

As you might imagine, papers like this often appear full of local names and regional geology, and many readers unfamiliar will be confused, as some of the reviewers are. You need to make things less complex and confusing so that your paper appeals to more readers.

We have included more detailed regional geology figures (Fig. 1a-c) that provides the reader with a clearer sense of the spatial and temporal distributions of geological terranes discussed in this manuscript. We have also simplified the geological nomenclature where possible and assigned geological units to clearly defined domains. This should make the arguments easier to follow and more appealing to international readers. A greater focus on the larger scale implications has been included to make this study more relevant to an international audience.

Can I just remind you that earlier in the manuscript you state the key problems are
The key points of debate are;
58 1) the location and polarity of subduction systems,
59 2) the timing of major depositional and collisional events,
60 3) the interpretation of the spatial positions of the North Australian and South Australian
61 Cratons through time with respect to one another (as a result of 1 and 2).
But your conclusions don't really very effectively come back to these larger issues

We have developed the discussion section (4.6) and the conclusion extensively to more effectively tackle these larger issues. We have also included 2 new figures by way of Fig. 2 and Fig. 13 that show a number of the current palaeogeographical reconstruction models for the early Mesoproterozoic eastern Australia and a new model incorporating the findings of this study.
These revisions include:
"The implication of this interpretation is that the North and South Australian cratons were contiguous at ca. 1595 Ma placing the Mount Painter Inlier at the nexus of two convergent margins characterised by subduction zones that dip towards the continent interior. Perturbations in the dynamics of these convergent margins resulted in rapid tectonic switches following deposition of the Radium Creek Group. Our data provides a critical constraint for palaeogeographic reconstruction for eastern Australia at the Palaeo- to Mesoproterozoic transition."

Reviewer 1

Lines 32-33. The second sentence in the introduction does not really say anything informative. Why is this approach better? I think that the introduction could be much more powerful if it focused on the tectonic/paleogeographic problems rather than on methods that have been previously been proven to be useful for this purpose.

Revision 1 – Removed second line.

Revision 2 – removed ancient supercontinents as this method works for all reconstructions not just ancient ones.

Line 34. Remove "our." It is unclear what the group is you are referring to.

Revision 3 – removed "our"

Lines 39, 40. See above.

Revision 4 – removed "our" twice
replaced with "the" and "on", rephrased line 40 to remove majority. Now reads "understanding the Proterozoic record of Australia underpins the knowledge of how this continent has evolved, and informs on global tectonics through time"

Line 40-41 - rephrase

Revision 5 – Rephrased with "Central to Proterozoic Australia reconstruction models is the link between the South Australian Craton and the Northern Australian Craton"

Line 42. The word nexus here and throughout is not used correctly and should be changed. This line reads like there is a relationship between Paleoproterozoic and Mesoproterozoic. You want to say this is an important time interval for Australian evolution so state that more clearly. E.g. ……particularly at the boundary between Paleoproterozoic and Mesoproterozoic times.

Revision 6 – replaced "nexus" and rephrased as "particularly at the boundary between the Palaeoproterozoic and Mesoproterozoic times."

Line 44. Remove: "it was positioned in a complex paleogeographic environment," and join with the next sentence.

Revision 7 – removed this sentence and joined it to next sentence to read "Current geologic/tectonic understanding of the Palaeo-Mesoproterozoic of eastern Australia suggests it was situated adjacent to two convergent margins"

Line 45: Please be more specific here - at what time (Palaeo-Mesoproterozoic is 1.5 Ga)? What do you mean by eastern Australia in these content? Betts and Giles (2006) show some convergence between SAC and NAC, for example. Etc.

Revision 8 – reworded to define the period to 1700-1500 Ma and eastern Australia to include the North and south Australia cratons. Now reads as "The tectonic model of Betts and Giles (2006) for ca. 1700-1500 Ma Palaeo-Mesoproterozoic of eastern Australia incorporating both the North and South Australia cratons suggests it was situated adjacent to, and were affected by, two convergent margins (Betts and Giles, 2006), which had a plume-related continental hotspot track superimposed upon them (Betts et al., 2007; 2009)."

Line 52: "intra-continental back-arc rift system" is nonsense. Either intra-continental, or back-arc.

Revision 9 – removed back-arc system and reworded for clarity to "whereby eastern Proterozoic Australia evolved between ca. 1730 and 1640 Ma by a series of large intra-continental rift system along the margins of the South Australian and North Australian cratons"

Line 53. …was subsequently inverted between 1640 and 1600 Ma….

Revision 10 – changed ca. 1640-1600 Ma to "between ca. 1640 and 1600 Ma"

Line 57 - : instead of ;

Revision 11 – change made

Lines 80-83. This section sounds like a proposal not part of the introduction. Again change nexus - these are geological time terms not locations with relationships.

Revision 12- reworded paragraph to be part of the introduction and removed nexus. Paragraph now reads as" In this communication we investigate the provenance and depositional environment of sediments deposited in the Early Mesoproterozoic within the Mount Painter Inlier as they may provide constraints on the palaeogeography of both the Mount Painter Province and eastern Proterozoic Australia."

Line 96. This sentence is awkward and needs revision.

Revision 13 – Re-worded paragraph to read "A major crustal-scale south-east-dipping discontinuity between the Moolawatana Domain and the Curnamona Province has been interpreted from the deep seismic reflection and magnetotelluric survey (08GA-C1) by Korsch et al. (2010). This discontinuity has been interpreted as separating distinct basement blocks. The basement below the Moolawatana Domain on the north-western side of the discontinuity is termed the Warrakimbo Seismic Block by Korsch et al. (2010). This seismic block is characterised by markedly lower reflectivity than the Yarramba Seismic Province which is interpreted to be basement to the Curnamona Province south-east of the major discontinuity (Korsch et al., 2010)."

Line 103. Use of the word comprised in this sentence and throughout the manuscript is incorrect. Replace with "is composed of."

Revision 14 – Replaced comprised to "is composed of" throughout manuscript

Line 111. Multi-phased? = polyphase metamorphism

Revision 15 – changed to polyphase metamorphism

Line 175. Remove "in extensive detail." This term is qualitative -- one person's extensive detail might mean not enough to someone else (e.g. analysis of 1000 zircons per sample).
Revision 16– removed "in extensive detail"
Line 176. Change " , with the remainder from…" to: and one from…
Revision 17– Change made
Line 184-185. Omit the last sentence of the paragraph.
Revision 18– Sentence omitted
Line 186. "we studied", not "we included"
Revision 19 – change made
Line 189 (404). see comment on line 103.
Revision 20 – Changes made
Line 195. Revise to read: …detritus at the apparent time of Radium…. You have not yet established this in the manuscript.
Revision 21 – added "apparent" as this has not been established in the manuscript
Lines 405-410 (and general comment about each of the samples). Resolution of these apparent age peaks is overly precise especially when quoted at 1 sigma error. These are the values calculated by the unmix routine (e.g. 1674.6 ± 2.8 Ma), but are not that precise in reality. From one sample to another a peak shows up somewhere between 1660 and 1680 Ma, but not in the same place and with different errors. These are likely the same population. I suggest just mentioning approximately where the peaks in the age distributions occur. You might also consider not using the PDF function, but rather changing to using a kernel density plot (e.g., Vermeesh).
Revision 22 – Removed the overly precise values and replaced them with the approximate position of the peaks e.g. ca. 1660-1680 Ma etc. and updated the probability plots text in Fig. 6 to be consistent.
Line 592. 1591-155? Ma
Revision 23– changed to read "1591-1552 Ma"
Lines 608-610. Omit this paragraph.
Revision 24 – Paragraph omitted helping to shorten this section.
Lines 682-707. Some of these populations of U-Pb age and Hf-isotopic composition are pretty small (<4 grains) and may not be representative. This should be noted.
Revision 25 – added a paragraph at the end of section 4.3 it reads "It is important to note the small sample populations of zircons (n <4) representing the ca. 1710-1760 Ma, ca. 1850 Ma, ca. 1904 Ma events, it is therefore possible that the Hf isotopic signatures of these populations may not be truly representative. "
Line 810. Telescopes --- reduces??
Revision 26 – Replaced telescopes with reduces
Lines 859-876. How could the Mount Painter region have been at the edge of the Gawler Craton at 1587 Ma when you have stated that it was sutured to the Curnamona Province before 1595 Ma? In the next paragraph you suggest that extension switched rapidly to shortening and then extension again. This suggests an intracratonic setting not a passive/active margin. Part of this inconsistency relates to what appears to be a variable definition of the Gawler Craton and South Australia Craton throughout the manuscript. I suggest defining the geological provinces up front and then reconsidering inconsistent parts of this section.
Revision 27 – Removed the statement " the Mount Painter Province represents the eastern most marginal terrane of the Gawler Craton prior to ca. 1587 Ma. region have been at the edge of the Gawler Craton at 1587 Ma" and instead suggest that the Gawler Craton and Curnamona Province are likely co-located ca. 1595 Ma. *We still support convergent margin driven rapid tectonic settings and have developed this argument with "Repeated rapid switching from extension to shortening at convergent plate margins is common during transient episodes of flat subduction (Gutscher et al., 2002) or when subduction roll-back is interrupted by accretion of buoyant material such as an ocean plateau (Rosenbaum et al., 2005;*

Mason et al., 2010), plume-head (Murphy et al., 1998; Betts et al., 2009; 2012), arc terrane (Boutelier et al., 2003) or continental micro-continent (Moresi et al., in review), which are all characterised by local trench advance and shortening in the overriding plate. We propose that during the ca. 1595-1555 Ma interval, the Mount Painter Inlier was located in the overriding plate of one or more subduction zones and was subjected to tectonic mode switches caused by disruption of a convergent margin."

We have also defined the South, North and West Australian cratons in the introduction to remove the inconsistency related to the definition of the Gawler Craton versus South Australian Craton and followed this throughout the manuscript. "Proterozoic Australia can be considered following the geography-based nomenclature of Myer et al. (1996) in which the continent is divided into three major cratonic units, called the North, West and South Australian cratons (Fig. 1a). The South Australian Craton comprises the Gawler Craton and the Curnamona Province (Fig.1b-c)."

Reviewer 2 – Major comments

It becomes especially difficult when the authors discuss the Hf-isotope correlations between various geological formations and then make conclusions about correlation of various terranes without citing which formation belongs to a specific terrane

Revision 28 – Added more detailed regional map (Fig. 1a-c) which defines the geological domains and the geological formations that belong to each of these. Separation of the Hf isotope correlation figures into Fig 8, 11, 12 provides more clarity regarding which units and domains of the Gawler Craton are compared in the text. The text has been updated to match the domain names outlined in Fig. 1c and Fig. 11a and will provide for an easier assessment of the interpretations by the reader.

1. Section 4.3 should be shorten and re-written with references to Figure 7. In present state it is very difficult to follow, especially for non-Australians. The same (but to a less extend) is applicable to the section 4.5.

Revision 29 - Section 4.3 has been shortened where possible and re-written with reference to Figures 8, 11, 12 and the regional geological map in Fig. 1c. Section 4.5 has been split into a section "4.5 Comparison with regional datasets" and "4.6 Proterozoic tectonic implications". Section 4.5 has also be re-written with reference to Figure 8, 11 and 12 as well as the regional geology map (Fig. 1c)

2. Figure 7 itself needs revision and more comprehensive figure captions. For example, Fig. 7e contains only a combined plot for the units of the Gawler Craton, so it is difficult to follow discussions about correlation between Radium Creek Group with some specific units in Gawler. Some suggestions are in the annotated text.

Revision 30 – The figure has been revised and separated into 3 different figures. Figure 8 contains the in-situ Hf plots for the Radium Creek Group in the Mount Painter Inlier Fig. 8a-b,d and the direct comparison with the samples of the Gawler Range Volcanics (uGRV) sample from the Gawler Craton, and the Frome Granite and Benagerie Volcanic Suite from the Curnamona Province in Fi. 8c). Figure 11 contains the larger datasets from the Gawler Craton. Fig 11a has the individual points for each geological domain and each author shown and compares these to the sampled from the Mount Painter Inlier. Fig. 11b shows the gridded field for all of the Gawler Craton in comparison to the point values for the Mount Painter samples. This will make is easier for a reader to follow the discussions regarding correlation between specific units in the Gawler Craton and the Mount Painter metasediments. Fig. 12 shows the Hf density field plots from the Arunta, Curnamona and Mt Isa terranes only. Breaking these figures into three separate figures makes each of the graphs easier to read.The text in section 4.3 and 4.5 has been re-written to reference these new figures.

3. The last part of discussion about paleogeographic reconstructions should be illustrated at least with sketches of these reconstructions.

Revision 31 – Illustrations of the most pertinent current reconstructions are added as Fig. 2a,b and discussed more fully in the introduction. A new figure (Fig. 13) has been added to develop on these existing models with the interpretations made in this paper. This section of the discussion has been *expanded to deal more effectively with the large scale issues introduced at the beginning of the manuscript.*

Reviewer 2 – revisions in annotated text (pdf)

Line 34 Remove "our"

Revision 32 – change made

Line 35 I would remove the end of the sentence "of ancient supercontinents". This method works for all reconstructions, not only reconstructions ofsupercontinents.

Revision 33 - RA - Removed "ancient supercontients"

RA - removed second line allowing for more focus on tectonic/palaeogeographic problems

Line 40 "majority" is a wrong word here. Rephrase.

Revision 34 - RA - rephrased and removed majority.

RA - Sentence now reads as "understanding the Proterozoic record of Australia underpins the knowledge of how this continent has evolved, and informs on global tectonics through time"

Line 42 "...particularly between the..." sounds better.

Revision 35 - RA - rephrased with "particularly at the boundary between the Palaeoproterozoic and Mesoproterozoic times."

Line 43 This sentence is meaningless, better remove it.

Revision 36 - RA - removed this sentence and joined with next sentence to read "Current geologic/tectonic understanding of the Palaeo-Mesoproterozoic of eastern Australia suggests it was situated adjacent to two convergent margins"

Line 45 Please be more specific here - at what time (Palaeo-Mesoproterozoic is 1.5 Ga)? What do you mean by eastern Australia in these content? Betts and Giles (2006) show some convergence between SAC and NAC, for example. Etc.

Revision 37 RA - reworded to define the period to 1700-1500 Ma and eastern Australia to include the North and south Australia cratons.

Now paragraph worded as "The tectonic model of Betts and Giles (2006) for ca. 1700-1500 Ma Palaeo-Mesoproterozoic of eastern Australia incorporating both the North and South Australia cratons suggests it was situated adjacent to, and were affected by, two convergent margins (Betts and Giles, 2006), which had a plume-related continental hotspot track superimposed upon them (Betts et al., 2007; 2009)."

Line 52 "intra-continental back-arc rift system" is nonsense. Either intra-continental, or back-arc.

Revision 38 RA - removed back arc system for clarity and reworded as "whereby eastern Proterozoic Australia evolved between ca. 1730 and 1640 Ma by a series of large intra-continental rift system along the margins of the South Australian and North Australian cratons"

Line 53 missing "between"

Revision 39 - RA- changed ca. 1640-1600 Ma to " between ca. 1640 and 1600 Ma"

Line 57 : instead of ;

Revision 40 – RA changed ; to :

Line 92: Add Flinders Ranges in South Australia and Moolawatana Domain in Fig. 1c

Revision 41- RA - added new figure as sub section of figure 1c with Flinders ranges and Moolawatana Domain shown

Line 93 show in map

Revision 42 RA - RA - added new figure as sub section of figure 1c with Flinders ranges and Moolawatana Domain shown

Line 105 XXXX-YYYY for Late Palaeoproterozoic dates

Revision 43 – removed "Late Palaeoproterozoic and section reads now as "These rocks have yielded Early Mesoproterozoic (1600-1580 Ma) maximum depositional U-Pb zircon ages

Line 107 If they are significantly younger than 1640 Ma, they cannot be Palaeoproterozoic...

Revision 44 - RA - Changed to read as' Early Mesoproterozoic max depositional....'

Line 117 Delete "either"

Revision 45 – RA - Paragraph removed as it is overly detailed for this communication

Line 122 This paragraph should be more explicit. It is hard to understand, especially without illustrations.

Revision 46 – RA -this paragraph has been removed as it is overly detailed for this communication

Line 125 Add this age range to the legend in Figure 2.

Revision 47 – RA- added to figure 2

Line 127 "Mount Neill" occurs two times in the same sentence.

Revision 48 – RA - rewritten this sentence as "The Mount Neill Suite was emplaced at ca. 1585-1557 Ma along the south-east margin of the inlier (Fig. 3). This suite incorporates the Box Bore and Mount Neill Granite (Elburg et al., 2012; Elburg et al., 2001; Fraser and Neumann, 2010). The slightly younger Moolawatana Suite was emplaced between ca. 1560 Ma and 1555 Ma (Stewart and Foden, 2001) on the northern side of the Inlier (Fig. 3).

Line 128 Add this age range to the legend in Figure 2.

Revision 49 – RA- added to figure 2

Line 129 Add this age range to the legend in Figure 2.

Revision 50 – RA- added to figure 2

Line 186 "we studied", not "we included"

Revision 51 – RA- change made

Line 189 – composed instead of comprised

Revision 52 – RA- change made

Line 195. Revise to read "detritus at the apparent time of Radium…. You have not yet established this in the manuscript.

Revision 53 - RA – added "apparent" as this has not been established in the manuscript

Line 197. ..are taken from... and kilometre with small K

Revision 54 - RA – change made and now reads "two samples are taken from drillholes ~150 kilometres to…"

Line 204. Tectonic unit instead of tectonic element… add "the" to make "which is the key"

Revision 55 - RA– Sentence re-worded as "They therefore contain information regarding the Early Mesoproterozoic evolution of Curnamona Province, which is a key to understanding the Mount Painter Inlier.."

Line 346. 30-100 um should be 30 to 100um

Revision 56 – RA – Change made

Line 592 ?

Revision 57 – RA – added a 2 to make the age range "1591-1552 Ma"

Line 593 General comment to the whole section 4.3 References to parts of Figure 7 (a, b,c etc.) are needed, otherwise it is difficult to follow.

Revision 58 - RA - To make this section easier to follow we have separated this figure into 3 (Figs 8, 11 and 12. Each of which have been cross referenced back to the text.

Line 626 "not dissimilar" means "similar"? It is hard to assess, as in Fig. 7c the combination of Gawler Range Volcanics, Frome Granite and Benagerie Volcanics is shown (see line 735).

Revision 59 – RA – changed "not dissimilar" to "are similar".
Separated this figure into 3 different figures, figs 8, 11, 12. This has increased the size of the figure (Fig. 8c) that includes the GRV, Frome granite and BVS making it easier to assess. Point size for each dataset has also been increased to show the comparison between these units more clearly.

Line 632 Shown in Fig. 7? Where?

Revision 60 – RA - added reference to Fig. 8c

Line 641 Shown in Fig. 7?

Revision 61 – RA - added reference to Fig. 8c

Line 646 Where is this mismatch demonstrated in Fig. 7?

Revision 62 – RA - added reference to Fig. 8c and re-written sentence to "This group is appreciably *more juvenile than the values for the upper Gawler Range Volcanics and Frome Granite (Fig. 8c). It is important to note that unlike the Radium Creek Group, we did not detect a more evolved and negative Hf component (-6 to -2) in this sample of Benagerie Volcanic Suite (Fig. 8c)."*

Line 763 - This is not obvious in the Fig. 7e at its present state.

Revision 63 – RA - added Fig. 11a-b to clarify this. This figure includes all of the U-Pb-Hf values for each of the terranes of the Gawler Craton as defined in Fig. 1c. and also separates these values based on the author the work is from.

Line 781. Why not shown in Fig. 7?

Revision 64 - RA – Now shown in Fig. 12b and referenced to this figure in the text.

Line 827 similar?

Revision 65 - RA – replaced 'not dissimlar' with 'similar'

Line 839 crust includes

Revision 66 - RA - added space between 'crust' and 'includes

Line 879: Figures would help a lot for this discussion of the reconstruction models

Revision 67 – RA - Figure added to show the proposed reconstruction space at this time (Fig. 13) as well as other models including the Betts and Giles 2006 model and the Wade et al. 2006 model (Fig. 2)

Line 881 Illustrations would help a lot.

Revision 68 – RA - This model is presented in a new Fig. 2. It is also adapted into the the proposed model in Fig. 13

Line 924 Choose another fonts - the text in the map is barely visible.

Revision 69 – RA - font changed to make labels more legible.

Line 927 Already shown

Revision 70 – RA - omitted 2nd reference to the gps location

Line 991 7a? 7b? etc. - please add

Revision 71 - RA - added these labels. Now as Fig. 8a,b,c and Fig 11a,b and Fig 12a,b,c.

Line 1022 Tables 1 and two seem to be switched in this PDF

Revision 72 – RA - These have been swapped to read correctly with the text

Table numbers missing?

Revision 73 – RA – added table number to table and checked in upload

Other changes made

RA - changed the last sentence of the abstract.
Now reads as "These observations suggest that the Mount Painter Province was adjacent to the Gawler Craton in the Early Mesoproterozoic. Our
data supports a coherent South Australian Craton at ca. 1595 Ma and a contiguous continental mass that included the North and South
Australian cratons. The Mount Painter Inlier occupied a complex plate tectonic setting in the overriding plate of two convergent margins."

Line 30 RA - moved this paragraph into section 1.4 Approach of this study.

Line 80 - RA - Paragraph re-written so that it is part of the introduction and less like a proposal. Now reads as "In this communication we investigate the provenance and depositional environment of sediments deposited in the Early Mesoproterozoic within the Mount Painter Inlier as they may provide constraints on the palaeogeography of both the Mount Painter Province and eastern Proterozoic Australia."

Line 96 RA - reworded paragraph and reads as "A major crustal-scale south-east-dipping discontinuity between the Moolawatana Domain and the Curnamona Province has been interpreted from the deep seismic reflection and magnetotelluric survey (08GA-C1) by Korsch et al. (2010). This discontinuity has been interpreted as separating distinct basement blocks. The basement below the Moolawatana Domain on the north-western side of the discontinuity is termed the Warrakimbo Seismic Block by Korsch et al. (2010). This seismic block is characterised by markedly lower reflectivity than the Yarramba Seismic Province which is interpreted to be basement to the Curnamona Province

south-east of the major discontinuity (Korsch et al., 2010)."
Line 184 – RA – Sentence omitted
Line 335 – RA - changed to correct reference (Griffin et al. 2000)
Line 336 - RA - Changed to correct reference (Nowell et al. 1998)
Line 404 - RA - removed isoplot unmix routine age and mentioned approx. peaks at ca. 1680 Ma and 1730 Ma
Line 407 – RA –sentence omitted as overly interpreted
Line 608 – RA - Paragraph omitted helping to shorten this section.
Line 679-681 - RA - removed sentence "In all of the Radium Creek Group...." To shorten this section and is a unneeded detail.
Line 685 RA - removed paragraph. This does not add to the manuscript and has been removed to shorten the section
Line 699-702 - RA - removed the sentence "A slightly older ca. 1904 Ma U...... This observations is overly interpreted and not crucial to the aims of the paper.
Line 729 – RA - This section has been renamed as "4.5 Comparison with regional datasets" and discusses and compares the U/Pb anf Hf regional datasets across eastern Proterozoic Australia. The discussion on tectonic implications is now in section 4.6
Line 745 – RA - removed the end of this sentence " which was accompanied by localised dep... Overly detailed for the outcomes of the communication
Line 805-809 – RA - removed the first 2 sentences This shortens the section as these interpretations are too detailed for the scope of the paper.
Line 852 – RA - split this section at line 852. Korsch et al..... is incorporated into the new section 4.6 Proterozoic tectonic implication. This section has also been expanded to more properly assess the large scale implications of the study.
Line 868 – RA - The paragraph has been re-written to remove the marginal terrane aspect and now reads as "Further, the isotopic and geochemical similarities between the Upper Gawler Range Volcanics and the Benagerie Volcanic Suite (Wade et al., 2012) suggests the lower crust in the footwall of the palaeo-Paralana Fault may represent the same crustal sources (e.g. Pankhurst et al., 2013) of magmatism as the central Gawler Craton. The correlation of the upper Gawler Range Volcanics with the Benagerie Volcanic Suite in the Curnamona Province (Wade et al., 2012) stitches the Gawler Craton and Curnamona Province together at ca. 1587 Ma."
Line 874 – RA - This section has been re-written to develop more expansively on the large scale implications and palaeogeographical reconstructions.
Line 885 – RA – Conclusion re-written to more fully develop the large scale reconstruction implications
Figure 1 – RA - updated figure to include 1a,1b and 1c. These layout the NAC, SAC and WAC positions in Proterozoic Australian palaeogeography (Fig. 1a) and provide detail on the geological terranes of both the Curnamona Province and Gawler Craton (Fig. 1c)
Figure 2 – RA - New Figure 2 added here. This figure outlines the Betts and Giles (2006) and Wade et al. 2006 reconstruction space in the early Mesoproterozoic.
Figure 3 – RA – Now as Figure 3. Date ranges added for intrusive suites. Text on image changed to arial to be clearer.
Figure 7 – RA- this figure has been moved into three different figures (fig 8, 11 and 12) and includes more detail for the Gawler terranes as well as bigger and more readable figure for the comparison of the RCG with the Gawler Range Volcanics etc. (Fig 8c)
Figure 11-13 – RA - Figures 11-13 added here. These include Fig 11- in situ zircons Hf isotopes of the Gawler Craton plot; Fig 12 - in situ zircons Hf isotopes of the Arunta Block, Curnamona Province and Mount Isa Inlier; Fig 13 - palaeogeographical reconstruction for the Mount Painter Inlier ca. 1595-1555 Ma.

Research Highlights

- The Radium Creek Group has a maximum depositional age of 1595 ± 3.7Ma.
- Zircons from the RCG have an isotopically diverse Hf isotopic fingerprint.
- The Radium Creek Group is interpreted to be derived from the Gawler Craton.
- The Curnamona Province and Gawler Craton were co-located at ca. 1595 Ma.
- The Mount Painter Inlier developed at the nexus of two convergent margins.

Provenance of the Early Mesoproterozoic Radium Creek Group in the Northern Mount Painter Inlier: Correlating isotopic signatures to inform tectonic reconstructions.

R.J. Armit[1,*], P.J. Betts[1], B.F. Schaefer[2], M.J. Pankhurst[3], D. Giles[4]

[1]School of Geosciences, Monash University, Clayton, VIC 3800, Australia

[2]GEMOC, Department of Earth and Planetary Sciences, Macquarie University, NSW 2109, Australia

[3]School of Earth and Environment, University of Leeds, Leeds, LS2 9JT, United Kingdom

[4]School of Earth and Environmental Sciences, University of Adelaide, SA 5005, Australia

*Corresponding Author: robin.armit@monash.edu

New in-situ zircon LA-ICPMS geochronologic and Hf-isotope data from the Radium Creek Group within the Mount Painter Inlier provide important temporal constraints on the Early Mesoproterozoic palaeogeography of eastern Proterozoic Australia. The entire Radium Creek Group was deposited in a single basin forming phase, and has a maximum depositional age of 1595 ± 3.7 Ma. Detrital zircon from these metasedimentary rocks have U-Pb age populations at ca. 1595 Ma, 1660-1680 Ma, 1710-1780 Ma, ca. 1850 Ma and ca. 2500 Ma. These grains are characterised by isotopically diverse and evolved sources, and have crystallised within predominantly felsic igneous host-rocks. The relative age spectra and isotopic character has more similarity with the Gawler Craton than the Arunta Block, Curnamona Province or the Mount Isa Inlier. These observations suggest that the Mount Painter Province was adjacent to the Gawler Craton in the Early Mesoproterozoic. Our data supports a coherent South Australian Craton at ca. 1595 Ma and a contiguous continental mass that included the North and South Australian cratons. The Mount Painter Inlier occupied a complex plate tectonic setting in the overriding plate of two convergent margins.

Keywords: Radium Creek Group, Mount Painter Inlier, U-Pb maximum depositional ages, Hf isotopes, isotopic fingerprinting, Palaeogeographical reconstructions

1. Introduction

Tectonic reconstruction models of Proterozoic Australia have been enthusiastically debated in the literature (c.f. Betts and Giles, 2006; Gibson et al., 2008; Giles et al., 2004; Korsch et al., 2009; Swain et al., 2008; Wade et al., 2006). This is because understanding the Proterozoic record of Australia underpins the knowledge of how this continent has evolved, which informs the view of global tectonics through time.

Proterozoic Australia can be considered following the geography-based nomenclature of Myer et al. (1996) in which the continent is divided into three major cratonic units, called the North, West and South Australian cratons (Fig. 1a). The South Australian Craton comprises the Gawler Craton and the Curnamona Province (Fig.1b-c). The South Australian Craton has a shared history with the North Australian Craton between ca. 1800 and 1550 Ma, suggesting that were contiguous during this interval. The South Australian Craton likely separated from the North Australian Craton during the Mesoproterozoic to form a discrete cratonic element (Giles et al., 2004). Consequently, the link between the South Australian Craton and the Northern Australian Craton, particularly at the boundary between the Palaeoproterozoic and Mesoproterozoic times is significant for determining the evolution of the Australian continent at this time.

Giles et al. (2004) interpreted a configuration of the Palaeoproterozoic Australia where the South Australian Craton was rotated 52^0 counter clockwise around an Euler pole in the North Australian Craton. This configuration aligned contemporaneous orogenic belts across the Gawler Craton, Arunta Inlier, Mount Isa Inlier and the Curnamona Province (Fig. 2a). Using the configuration of Giles et al. (2004), Betts and Giles (2006) suggested that between ca. 1700 and 1500 Ma, the contiguous North and South Australia cratons (Fig 2a) were situated adjacent to, and were affected by, two convergent margins. A plume-related continental hotspot track was also superimposed upon these cratons (Betts et al., 2007; 2009). In this model, the southern margin of the Australian continent evolved in the overriding plate of a north-dipping subduction, and the eastern margin of the continent sequentially evolved from a passive margin, to a convergent margin with west-dipping subduction.

Wade et al. (2006) presented an alternative model in which the South Australian Craton collided with the North Australian Craton between ca. 1590 Ma and 1560 Ma (Fig. 2b), chiefly supported by the identification of the ca. 1590 Ma continental-arc affinity rocks in the Musgrave Block of central Australia. In this model the continental arc rocks formed above a south-dipping subduction zone and the Gawler Craton evolved in a continental back-arc basin. Gibson et al. (2008) proposed a model whereby eastern Proterozoic Australia evolved between ca. 1730 and 1640 Ma by a series of large intra-continental rift systems along the margins of the South Australian and North Australian cratons. This system was subsequently inverted between ca. 1640 and 1600 Ma during accretion of the Georgetown-Mojave Block. These latter models consider the present-day distribution of Australia Palaeoproterozoic terranes to be representative of their distribution at the time of tectonism.

The key points of debate are:

1) the location and polarity of subduction systems,
2) the timing of major depositional and collisional events,
3) the interpretation of the spatial positions of the North Australian and South Australian Cratons through time with respect to one another (as a result of 1 and 2).

Increasing our knowledge of these tectonic settings will improve our understanding of the Palaeo-Mesoproterozoic evolution of Australia. Moreover, the knowledge will provide important constraints to larger-scale Nuna-Columbia supercontinent reconstructions.

1.2 A key terrane

The Mount Painter Inlier is situated within the northern, South Australian Craton margin (Fig. 1b-c), which makes it an ideal location to explore the links between the North and South Australian cratons. In addition, this inlier helps us investigate the interface between the Gawler Craton and northern Curnamona Province, which is currently poorly understood.

Recently, Armit et al. (2012) suggested that the Early Mesoproterozoic deformation events recorded in the Mount Painter Inlier appear to be more similar to those observed in the northern Gawler Craton and Mount Isa Inlier, rather than the southern Gawler Craton and Curnamona Province. According to that study, the Mount Painter region would be predicted to record an evolution more similar to that of the North Australian Craton rather than the South Australian Craton. If this is indeed the case, our interpretations of the relationships between these crustal elements and the reconstructions to place the Mount Painter Inlier in its correct location through time, require a substantial re-appraisal.

We investigate the provenance and depositional environment of sedimentary rocks deposited in the Early Mesoproterozoic within the Mount Painter Inlier as they may provide constraints on the palaeogeography of both the Mount Painter Province and eastern Proterozoic Australia.

1.3 Geological Background

1.3.1 Crustal architecture

The Radium Creek Group (Preiss et al., 2010; a nomenclature revised from the Radium Creek Metamorphics) outcrops within the Mount Painter and Mount Babbage inliers, which are located at the northern tip of the Flinders Ranges in South Australia (see Fig. 1c). These Inliers have been interpreted as part of the Moolawatana Domain (Fig. 1c) that defines the north-western extent of the Curnamona Province (Conor and Preiss, 2008; Parker et al., 1993; Teale and Flint, 1993).

A major crustal-scale south-east-dipping discontinuity between the Moolawatana Domain and the Curnamona Province has been interpreted from the deep seismic reflection and magnetotelluric survey (08GA-C1) by Korsch et al. (2010). This discontinuity has been interpreted as separating distinct basement blocks. The basement below the Moolawatana Domain on the north-western side of the discontinuity is termed the Warrakimbo Seismic Block by Korsch et al. (2010). This seismic block is characterised by markedly lower reflectivity than the Yarramba Seismic Province which is interpreted to be basement to the Curnamona Province south-east of the major discontinuity (Korsch et al., 2010).

1.3.2 Stratigraphy

Within the northern Mount Painter Inlier, the Radium Creek Group is composed of micaceous psammites, psammopelites, pelitic schists, phyllites, feldspathic quartzites and quartzofeldspathic gneisses (Fig. 3). These rocks have yielded Early Mesoproterozoic (1600-1580 Ma) maximum depositional U-Pb zircon ages (Elburg et al., 2012; Fanning et al., 2003; Fraser and Neumann, 2010). These ages appear to be significantly younger than the ca. 1720-1640 Ma Willyama Supergroup ca. 1720-1640 Ma (Conor and Preiss, 2008) from the southern part of the Curnamona Province and therefore previous correlations with the Radium Creek Group are considered erroneous (e.g. Teale, 1993). The Radium Creek Group has undergone polyphase metamorphism (Elburg et al., 2003; McLaren et al., 2002) and poly-deformation in the Early Mesoproterozoic and Palaeozoic (Armit et al., 2012).

1.3.3 Igneous suites

The metasedimentary rocks of the Mount Painter Province are intruded by a series of Early Mesoproterozoic igneous suites with A-type geochemical affinities (Elburg et al., 2012; Kromkhun et al., 2013). The Mount Neill Suite was emplaced at ca. 1585-1557 Ma along the south-east margin of the inlier (Fig. 3). This suite incorporates the Box Bore and Mount Neill Granite (Elburg et al., 2012; Elburg et al., 2001; Fraser and Neumann, 2010). The slightly younger Moolawatana Suite was emplaced between ca. 1560 Ma and 1555 Ma (Stewart and Foden, 2001) on the northern side of the Inlier (Fig. 3). The ca. 1552 Ma Hodgkinson Granodiorite (Fraser and Neumann, 2010) also intrudes the central part of the Inlier and outcrops as a linear NE-SW belt. Numerous metabasic bodies intrude the Radium Creek Group and are considered to be late Mesoproterozoic to Neoproterozoic in age (Wulser, 2009). Minor pegmatite lenses throughout the Radium Creek Group in the northern Mount Painter Inlier are most likely syn- to post- the Cambro-Ordovician Delamerian Orogeny (Elburg et al., 2003). Within the central part of the inlier, the peraluminous British Empire Granite and metaluminous Paralana Granodiorite are interpreted to have been emplaced during the Palaeozoic ca. 460-440 Ma (Elburg et al., 2003; McLaren et al., 2006).

1.3.4 Metasomatism

Lenses of peraluminous to hyperaluminous rock, composed of phlogopite-corrundum-kyanite bearing assemblages are present within the Radium Creek Group in the Mount Adams area proximal to the Mount Neill Granite (Shafton, 2006). This lithology is correlated with the Corundum Creek Schist Member (Shafton, 2006) originally mapped as part of the Radium Creek Metamorphics (Coats and Blissett, 1971). Elburg et al. (2011) interpreted these bodies as metasomatised igneous rocks which likely reflect intense alteration of the Mount Neill Suite.

1.3.5 Structure

The Inlier is bisected by the Paralana Fault Zone (Fig. 3) which separates sequences of the Radium Creek Group. This fault system is a major crustal-scale feature and has a predominantly steep, northwest-dipping geometry as interpreted from the 08GA-C1 deep seismic reflection survey (Korsch and Kositcin, 2010). Field observations indicate that the fault zone is defined by a corridor of high strain, which record demonstrable reactivations since the Early Mesoproterozoic (Armit et al., 2012) through to the Cenozoic (Elburg et al., 2012; Teasdale, 1993).

1.4 Approach of this study

Geochronology coupled with isotopic fingerprinting of ancient rock packages is a powerful tool for constraining reconstructions of Proterozoic terranes (e.g. Cawood et al. 1999; Halilovic et al. 2004; Nelson, 2001). This allows us to reconstruct links between cratonic elements with greater confidence, which improves global reconstructions.

This study aims to provide constraints on the timing and provenance of deposition of the Radium Creek Group. To achieve this we compare the isotopic and geochronological signatures of detrital zircon populations from these metasediments with that of neighbouring tectonic elements. Direct comparison of our new zircon age data with Precambrian terranes across eastern Australia can then be used to identify the most likely crustal element(s) those zircons, and thus sediments, are derived from.

In addition, the employment of trace element and Lu-Hf isotope system fingerprinting allows us to also compare the source (i.e. relative contemporary crust/mantle contribution) that different zircon populations have crystallised from (Blichert-Toft and Albarede, 1997). These data have the potential to discriminate between terranes that have similar chronology, but different magmatic source chemistry and antiquity, allowing a further level of discrimination between potential sources of detritus. Our approach is to assess the U-Pb-Hf-trace element signature of samples throughout the Radium Creek Group and compare them to that of zircon populations from potential source lithologies across a number of terranes, using both new data presented herein and published datasets from the Gawler Craton, Mount Isa Inlier, Curnamona Province and Arunta Block (Belousova et al., 2006b; Condie et al., 2005; Griffin et al., 2006; Hollis et al., 2010; Howard et al., 2009; Howard et al., 2011a; Howard et al., 2011b; Howard et al., 2011c; Szpunar et al., 2011).

Available whole rock Nd isotope datasets from across the region (Neumann, 2001; Schaefer, 1993; Wade et al., 2012) are also examined in order to further test observed temporal and spatial patterns with respect to relative inputs of juvenile material, which can provide insights into the provenance of the Radium Creek Group.

1.5 Samples

Four samples from the Mount Painter Inlier were investigated. Three of which (Z3, F and 123) are from the hanging wall (western side) of the Paralana Fault and one from the eastern (foot-wall) side (see Fig. 3). Sample Z3 is a sample of a fine-grained, mica rich, garnet + quartz psammopelitic horizon within the Brindana Schist (Fig. 4a-b). This horizon is located ~100 m to the west of the Paralana Fault and Mount Neill Granite Suite. Sample F is a medium-grained quartz + muscovite ± garnet layer within the Freeling Heights Quartzite ~6 km to the south-west of sample Z3 (Fig. 4c-d). 123 is a course grained quartz + muscovite layer of the Freeling Heights Quartzite (Fig. 4e-f). This sample location is ~2 kilometres south-west of sample F. 36 is a medium grained quartz + muscovite ± biotite ± garnet layer of the Mount Adams Quartzite (Fig. 4g-h), from the eastern side of both the Paralana Fault and the Mount Neill Granite Suite.

Additionally, we studied one sample from the Central Gawler Craton. Sample YD23A is a black, course-grained porphyritic (plagioclase + k-feldspar + iron oxide) sample (Fig. 4i-j) of the Pondanna member of the Upper Gawler Range Volcanics (uGRV; Allen et al., 2003; Blissett et al., 1993). The uGRV is a major capping sequence of the Gawler Felsic Large Igneous Province (Allen et al. 2012), and is composed of widespread and homogeneous felsic lava (due to high magmatic temperature and halogen enrichment, promoting efficient mixing via low magmatic viscosity: see Pankhurst et al. 2011a) that outcrops as monotonous sheets across the Central Gawler Craton. The emplacement of this voluminous felsic large igneous province (FLIP) was rapid (Pankhurst et al. 2011b), and occurred at ca. 1592 ± 3 Ma (Fanning et al., 1988). As such, this sample represents both a snapshot of Gawler Craton evolution as well as the principle source of Gawler Craton-derived detritus, at the apparent time of Radium Creek Group deposition.

Finally, two samples are taken from drillholes ~150 kilometres to the south of the Mount Painter Inlier, within the Curnamona Province (Fig. 1b-c). They have previously been dated using in-situ zircon U-Pb techniques by Jagodzinski & Fricke (2010). Sample R1707876 is from the Frome 12 Granite, Bimbowrie Suite, intersected in drillhole DDH Frome 12 (385176E, 6503512N). Sample

R1709059 is from rhyolite assigned to the Benagerie Volcanic Suite, intersected in DDH Frome 13 (393612E, 66528251N). Both of these samples are from igneous rocks emplaced within the Curnamona Province at ca. 1594-1587 Ma (Jagodzinski and Fricke, 2010). They therefore contain information regarding the Early Mesoproterozoic evolution of the Curnamona Province, as well as representing a potential contemporary source for detritus contributing to the Radium Creek Group.

2 Methods

2.1 Sampling for whole rock geochemistry and zircon extraction

Several kilograms of representative material were collected from each site (see Fig. 3-4). Weathered rinds and any obvious zones of alteration were discarded. These samples were then pulverised using a ceramic disc mill and sieved to collect the resulting fragments within an 18 to 250 μm size range. Magnetite within this fraction was removed using a hand magnet. Tetrabromoethane (TBE; 2.96g/ml) and Di-iodomethane (DIM; 3.3g/ml) heavy liquids were then used to separate minerals with high specific gravity (including zircon) from the predominantly lighter medium. A further magnetic separation step followed using the heavy fraction. We used a Frantz magnetic separator set at 1.4 Amps, 15^{o} forward and 25^{o} side tilt.

2.2 Zircon mounting, imaging and in-situ targeting

Zircons were hand-picked from the non-magnetic fraction using a binocular microscope and suspended in an epoxy resin mount for grinding, polishing and carbon coating. The mounts were imaged using a JEOL JSM 6300 SEM at Ballarat University (both back scatter electron and cathode luminescence images) on the Brindana Schist sample (sample Z3), and a JEOL JSM-840A SEM (back scatter electron images only) at the Centre for Electron Microscopy, Monash University on the uGRV sample (YD23a). A Cameca SX100 electron microprobe (back scatter electron and cathodoluminescence images) was used to image zircons from the Freeling Heights Quartzite (sample F, 123), Brindana Schist (sample Z3) and Mount Adams Quartzite (sample 36) at GEMOC, Macquarie University. These images (BSE and/or CL) were used to choose analysis spots for each grain. The most appropriate sites were those that best fit the criteria of adequate size, internal consistency and tractable petrographic context of crystal zonation domains.

2.3 Analytical methods

2.3.1 In-situ major and trace element chemistry

Electron microprobe (EMP) analysis for in-situ zircon major and trace-element (HfO_2, SiO_2, ZrO_2, Y_2O_3) geochemistry was conducted on samples from the Freeling Heights Quartzite (samples F) and Mount Adams Quartzite (sample 36) using a Cameca SX100 Electron Microprobe fitted with 5 wavelength dispersive spectrometers (WDS) and Princeton Gamma-Tech (PGT) energy dispersive system (EDS). The microprobe was operated at an accelerating voltage of 15 kV with a beam current of 20 nA, a 1-2 µm beam diameter, and a dwell time of 60 seconds acquisition after 60 seconds background. The analyses were conducted at the same site within each zircon grain chosen for both the U-Th-Pb-trace and Hf-isotope analyses.

2.3.2 U-Th-Pb

In-situ zircon U-Th-Pb isotope analysis was conducted at Macquarie University using a HP 4500 quadrupole inductively coupled plasma mass spectrometer (ICPMS) attached to a New Wave UV213 Laser system for samples Z3, F, 123 and 36. Analysis of zircon from sample YD23a was undertaken at Monash University by laser ablation (LA) -ICPMS attached to a Thermo X-series quadrupole coupled with a New Wave 213 nm, Nd: YAG laser. A laser spot size between 30-40 µm was used depending on the size and morphological complexity of each zircon. Ablation sites were chosen to best represent populations from each of the distinct zircon morphologies that could be characterised from BSE and CL images of the zircon grains (see Fig. 5). The lasers at both Macquarie University and Monash University were operated using a 5 Hz repetition rate with 11-13 $mJcm^{-2}$ laser energy at the sample with a 60-120 s acquisition period including 15 ms dwell for Pb^{206}, U^{238}; 10ms for Pb^{204}, Pb^{208}, Th^{232} and 30 ms for Pb^{207}. The dwell times for sample YD23a (undertaken on the Monash University LA-ICPMS) differed slightly with a shorter 10 ms dwell for Pb^{204} and 25 ms for Pb^{206}, Pb^{207}, Th^{232} and U^{238}.

2.3.3 In-situ Lu-Hf

We targeted zircons for Hf isotope analysis that represented each distinct U-Pb age population within each sample. Hf isotopes were only measured from grains with U-Pb ages that were <10% discordant. The specific sites were chosen to be adjacent to the same pit and within the same internal domain, ablated for U-Pb isotopic analysis (identified by BSE and CL images: Fig. 5).

The in-situ zircon Lu-Hf isotope analytical technique used in this study follows that described by Griffin et al., (2004); Griffin et al., (2006); Griffin et al., (2002). Analysis was conducted at GEMOC, Macquarie University using a New Wave/Merchantek LUV213 (Nd: YAG) laser-ablation system attached to a Nu Plasma multicollector ICPMS via Ar/He gas delivery. The ICPMS was tuned using a 1 ppm solution of the JMC475Hf standard spiked with 80 ppb Yb, which yielded a typical total Hf beam of 10-14 x 10^{-11} Å (Jackson et al., 2004).

The analyses in this study were carried out using a 40 to 55 µm beam diameter with a 5Hz repetition rate and ~0.6 mJ/pulse which produced a total Hf signal of 1-6 x 10^{-11} Å. Following 60 s of background measurement, 80-120 s of acquisition time per analysis produced ≤ 50 um deep pits.

During the analytical run, Mud Tank Zircon standard was analysed as an internal monitor (Table 1). These measurements yielded an average corrected $^{176}Hf/^{177}Hf$ ratio of 0.282527 ± 0.000029 (n=14, 2σ), which is within the error of the long term average 0.282532 ± 0.000033 (n=984, 2σ) and 0.282523 ± 0.000043 (n=2190, 2σ) (Pearson, N.J. Pers comms, 2010). In addition, the 91500 zircon standard was analysed, and yielded a corrected average $^{176}Hf/^{177}Hf$ ratio of 0.282322 ± 0.000059 (n=4, 2σ) which is within error of the long term average of 0.282307 ± 0.000058 (n=632, 2σ) (from Pankhurst et al., 2013). In addition and where possible, multiple ablations of the same domain in our unknown samples (quasi repeat analyses) returned ε Hf values that were indistinguishable from the original analyses (1σ <0.05 ε Hf).

2.3.4 Whole-rock geochemistry

Splits (~250 g) of sample Z3 and sample F were crushed using a hydraulic press and then further in an agate mill to produce a powder of each sample. A portion (15 g) of each powder was analysed for major elements using a Bruker-AXS S4 Pioneer XRF Spectrometer and processed through Bruker-AXS Spectra-plus software, at the Advanced Analytical Centre at James Cook University. This is the same method and laboratory that determined the whole rock data from sample Y23a (see Pankhurst et al. 2011a). Trace (including rare-earth element) data were acquired from high-pressure digestions using HF. This step was followed by an HCl digestion at one atmosphere before drying down and converting to nitric complexes using HNO_3. These samples were then taken up in dilute HNO_3, spiked with a Li, In and Bi internal standard before analysing the solutions using a quadrupole ICPMS at Monash University.

2.4 Data treatment

2.4.1 U-Th-Pb isotope ratios

U-Th-Pb isotopic ratios were calculated using GLITTER software (e.g. Van Archerbergh et al., 1999) and the U-Pb ages were calculated using Isoplot 4.15. The procedure for data reduction procedure follows that of Griffin (2004) and Jackson et al. (2004) and in each case GEMOC GJ-1 zircon (TIMS normalisation values of Jackson et al. (2004) are: $^{207}Pb/^{206}Pb$ 608.3 Ma, $^{206}Pb/^{238}U$ 600.7 Ma and $^{207}Pb/^{235}U$ 602.2 Ma) was used to correct for U-Pb fractionation. In addition, the 91500 zircon standard was analysed within each run as a monitor of the reproducibility and accuracy for both LAM-ICPMS instruments used (Table 2). A correction for ^{204}Pb was applied following the method described in Anderson (2002). This correction had a negligible effect on the majority of the analyses. Absolute ages and their individual errors were calculated using Isoplot 4.15 (Ludwig, 2008), and age populations were assessed with the unmix function (to unmix superimposed Gaussian distributions) as appropriate.

2.4.2 Zircon trace element data

A cameca Φpz correction procedure was applied to the EMP dataset to calculate oxide percentages from raw counts. The trace element concentration data (Y, Hf) were combined with U, Th, Lu, Yb concentration data acquired during the LAM-ICPMS analysis, and used to model potential magmatic source rock type (c.f. Belousova et al., 2002) for each grain, and by extension, on age populations. These data were collated for selected grains from sample F (n=16) and sample 36 (n=18) that satisfy our selection criteria: grains were chosen to represent each of the U-Pb detrital age populations brackets, and were limited to igneous crystals only, by using geochemical data as a filter (Th/U ratios of >0.5 normally indicate an igneous origin; Cowley and Fanning, 1992).

2.4.3 Lu-Hf isotope ratios

Measured masses 172, 175, 176, 177, 178, 179 and 180 were normalised to ^{179}Hf/^{177}Hf = 0.7325 using an exponential correction for mass bias. Interference of ^{176}Lu on ^{176}Hf was corrected using a ^{176}Lu/^{175}Lu ratio = 0.02669 (Claoué-Long et al., 2008) and measuring the interference-free ^{175}Lu value to calculate ^{176}Lu/^{177}Hf. Interference of ^{176}Yb on ^{176}Hf was corrected using a ^{176}Yb/^{172}Yb ratio of 0.5865 (see Griffin et al., 2000), determined by spiking the JMC475 Hf standard with Yb, and measuring the interference-free ^{172}Yb (Jackson et al., 2004). Repeated analysis of standard zircons (see 3.2.3 above) with a variety of ^{176}Lu/^{177}Hf and ^{176}Yb/^{177}Hf ratios (see Griffin et al., 2004) establishes the accuracy and precision of the Lu and Yb corrections.

The measured ^{176}Lu/^{177}Hf ratios for each of the zircons analysed were used to calculate initial ^{176}Hf/^{177}Hf ratios. Numerous proposed decay constants exist for ^{176}Lu (e.g. Bizzarro et al., 2003; Blichert-Toft et al., 1997; Scherer et al., 2001 ; Soderlund et al., 2004). We have used a value of 1.865E^{-11}/yr for all Hf isotope calculations (Scherer et al., 2001; Soderlund et al., 2004). Chondritic values of ^{176}Lu/^{177}Hf = 0.282772 and ^{176}Hf/^{177}Hf = 0.0332 (Blichert-Toft and Albarede, 1997) are used for calculating ε Hf and model ages.

The mean 2se precision of ^{176}Hf/^{177}Hf ratios presented in this study is ± 0.00002 which equates to ±0.7 ε Hf). The majority of the analyses returned a 2se uncertainty range between <1-5% contributing an uncertainty of between 0.05 and 0.25 ε Hf. This uncertainty reflects the within-grain variation in Lu/Hf observed in zircons and the analytical uncertainties (Belousova et al., 2006a).

Further discussion on the precision and accuracy of this method are expanded upon in Griffin et al. (2002; 2004).

Calculation of depleted mantle model ages (T_{DM}) for each zircon analysis were made using the measured $^{176}Lu/^{177}Hf$ and modelled values for $^{176}Hf/^{177}Hf_i$ = 0.279718 at 4560 Ma and $^{176}Lu/^{177}Hf$ = 0.0384 (Griffin et al., 2000). These values produce a depleted mantle model with $^{176}Hf/^{177}Hf_{(present-day)}$ = 0.28325, comparable to average MORB (Nowell et al., 1998). These single-stage model ages provide a minimum age on the source material from which the zircon crystallised. In addition, two stage model ages or crustal model ages (T_{DM}^{c}) were calculated. These models assume that a zircon's parental magma was formed from average continental crust and therefore use a $^{176}Lu/^{177}Hf$ ratio of 0.015 (Griffin et al., 2004) (Geochemical Earth Reference Model database) that was initially derived from the depleted mantle.

3 Results

3.1 Zircon descriptions

The zircon grains (n=57) from sample Z3 are rounded and reddish-brown. Typical diameters range from 30 to 100 µm. In ~90% of these zircons, morphologies are characterised by oscillatory zoned cores (Fig. 5a-b) with isometric overgrowths and rims (6 rims >30 µm in thickness). The additional 10% zircons have isometric morphologies with <15 µm overgrowths.

Zircons from sample F (n=138) are predominantly brown, subhedral grains and are slightly larger than those in sample Z3 (~80% >70µm). The morphology of these zircons is predominantly characterised by oscillatory zoned cores (~75% of grains) with variable, weak to strongly zoned rims and isometric overgrowths (Fig. 5c-d).

Grains of zircon separated from sample 36 (n=32) are reddish-brown in colour and have a typical diameter range from 40-110 µm. The grains are subhedral and ~80% have oscillatory zoned cores (Fig. 5e-f). The remainder have isometric cores. ~10% of the grains have very thin overgrowths (<10 µm).

The zircons separated from sample 123 (n=33) are indistinct in terms of colour, shape and size from the grains in sample F. Approximately 90% of the grains have oscillatory zoned cores. Very thin (<10 µm) rims/overgrowths are apparent on ~30% of the grains (Fig. 5g-h).

The zircon grains from sample YD23a (n=29) are brown in colour, subhedral in shape, exhibit blunt pyramidal terminations, and vary in size between 100-300 µm. All of the zircon grains from this sample display oscillatory zonation and do not show any evidence for any metamorphic overgrowths (Fig. 5i-j).

Description of the Curnamona Province zircons from R1707876 (Frome Granite) and R1709059 (Benagerie Volcanic Suite) can be found in Jagodzinski & Fricke (2010).

3.2 U-Th-Pb zircon geochronology

Results from LA-ICPMS U-Pb dating of zircon are presented in Table 3. The complete dataset is provided in Supplementary Appendix A. Probability density plots and concordia plots for each of the samples analysed in this study are shown in Fig. 6-7.

3.2.1 Z3 (Radium Creek Group - Brindana Schist)

A total of 78 zircon U-Pb analyses were conducted on 60 separate zircon grains. Data were gathered from both the cores and regions with clear oscillatory zoning for completeness (Fig. 6a-b). Six analyses from this total dataset were interpreted as metamorphic zircon growth (see Armit et al., 2012). Armit et al. (2012) described these zircons as exhibiting isometric rims and overgrowths, yet only 3 of these analyses returned Th/U ratios <0.3 (an order of magnitude lower than the detrital igneous zircon cores presented here) and were less than 10% discordant. These metamorphic overgrowths have weighted mean $^{207}Pb/^{206}Pb$ age of 1552 ± 32 Ma (2σ).

Fifty-four analyses from the remaining 72 are within 10% concordancy. The probability density plot for this sample has two major zircon population peaks (Fig. 6). The younger population consists of a group of 19 zircons which have a weighted mean $^{207}Pb/^{206}Pb$ age of 1595.7 ± 9.2Ma (n = 19, MSWD = 0.38, 2σ). An older population of 21 zircons has a weighted mean $^{207}Pb/^{206}Pb$ age of 1708 ± 17 Ma (n = 21, MSWD = 1.9, 2σ). This peak consists of two separate populations at ca. 1680 Ma and at ca. 1740 Ma. Three zircons with an age range of between ca. 1790 and ca. 1850 Ma were present in the sample. Archaean to earliest Palaeoproterozoic aged detrital zircons were also present in the sample and exhibit an age range of between ca. 2370 and ca. 2900 Ma.

3.2.2 F (Radium Creek Group – Freeling Heights Quartzite)

A total of 148 U-Pb zircon analyses were conducted for this sample across 138 grains. Four of these analyses were located on zircon overgrowths/rims with isometric and/or 'fir-tree' and/or sector zoned morphology that were >30μm wide, and therefore could return signals uncontaminated by neighbouring domains, these are discussed in Armit et al. (2012). One hundred of the analyses from the remaining 144 igneous detrital zircon fraction were within 10% concordancy. The probability density plot of concordant analyses (<10% discordant) for this sample has 3 major peaks (Fig. 6c-d).

The youngest population consists of 17 zircon grains and has a weighted mean $^{207}Pb/^{206}Pb$ age of 1591.7 ± 7.8 Ma (n =17, MSWD = 1.9, 2σ). An older peak is composed of two distinct populations (Isoplot unmix routine) at ca. 1680 Ma and at ca. 1730 Ma. A single grain from this sample returned a ca. 1841 Ma age. Eighteen analyses returned an age plateau between 2240 Ma and 2600 Ma.

3.2.3 123 (Radium Creek Group - Freeling Heights Quartzite)

U-Pb analysis was conducted on 40 separate detrital igneous-sourced zircons. Nine analyses were more than 10% discordant. Probability plots for the 31 remaining analyses are displayed in figure 6e-f. A tight cluster of late Mesoproterozoic zircon ages (n=8) have a weighted mean $^{207}Pb/^{206}Pb$ age of 1590 ± 6 Ma (n = 8, MSWD = 0.95, 2σ). The remaining, older ages are characterised by Palaeoproterozoic populations at ca. 1660 Ma, ca. 1710 Ma and 1770 Ma. An Earliest Palaeoproterozoic population is also present and returns a weighted mean $^{207}Pb/^{206}Pb$ age of 2490.1 ± 9.9 Ma (n=4, MSWD = 0.41, 2σ).

3.2.4 36 (Radium Creek Group – Mount Adams Quartzite)

Thirty-nine analyses were conducted on 38 zircon grains for U-Pb ages from this sample of the Mount Adams Quartzite (Fig. 6g-h). One analysis is >10% discordant. The youngest distinguishable population from the remaining 38 analyses is a cluster at 1592 ± 10 Ma (n = 8, MSWD = 1.4, 2σ). Other population peaks are evident at ca. 1680 Ma, ca. 1710 Ma and ca. 1740 Ma. An older, Earliest Palaeoproterozoic population has a weighted mean $^{207}Pb/^{206}Pb$ age of 2477.1 ± 11 Ma (n=3, MSWD = 2.2, 2σ).

3.2.5 YD23a (upper Gawler Range Volcanics)

A total of 33 analyses were conducted on 29 separate zircons grains. 26 of these are ≤10% discordant. No concordia age or intercept age could be satisfactorily determined using the entire population. In addition, the weighted mean $^{207}Pb/^{206}Pb$ age for the entire group (Fig. 7) produced an MSWD >8. The very high MSWD implies the presence of inherited zircon populations. These are calculated using probability plots and unmixing models to have ages of ca. 1680 Ma and ca. 1760 Ma. These analyses correlate with dark core regions in CL images, which independently suggest that they should not be included in a weighted crystallisation age calculation. Instead we prefer the weighted mean $^{207}Pb/^{206}Pb$ age of 1595 ± 19 Ma (n = 17, MSWD = 0.046, 2σ), which is consistent with the previously published age of the Yardea Dacite (upper Gawler Range Volcanics: 1592 ± 3 Ma; Fanning et al., 1988) as well as the lower units of the Gawler Range Volcanics 1591± 3 Ma (Fanning et al., 1988).

3.3 In-situ Lu-Hf

A total of 74 zircon grains were analysed from the Radium Creek Group. This included 37 grains from the pelitic Brindana Schist, 18 from the overlying Freeling Heights Quartzite and 19 from the Mount Adams Quartzite (Fig. 8a-b). Twenty-five grains were analysed from the upper Gawler Range Volcanics (Central Gawler Craton; YD23a) (Fig. 8c). Twenty-two grains with 2 repeats [from the same domain] were analysed from the Frome Granite (Fig. 8c), and 13 zircon grains from the rhyolitic Benagerie Volcanic Suite (Fig. 8c) (Curnamona Province; R1707876 and R1709059 respectively). These results are presented in Table 3 and summarised in Figure 8a-d (the full dataset is presented in Appendix A).

3.3.1 Z3 (Radium Creek Group - Brindana Schist)

Hf isotope ratios measured from the ca. 2900 Ma (Archaean) zircon grain has a ε $Hf_{(t)}$ value of +7.27 and a crustal model age (T_{DM}^{c}) of 2880 Ma (Fig 8a-b). Early Palaeoproterozoic zircon grains that are dated at 2300 and 2500 Ma have ε $Hf_{(t)}$ of -4.89 and -1.11, and T_{DM}^{c} at 3110 Ma to 3240 Ma respectively (Fig. 8a-b). Zircon grains with ages between 1765 Ma and 1850 Ma (n=3) possess an ε $Hf_{(t)}$ range from -4.9 to -2.89 and T_{DM}^{c} ages between 2660 and 2800 Ma. Zircon grains with ca. 1710-1760 Ma dates have initial ε Hf values that are scattered between -6.58 and +2.74 (n=6). T_{DM}^{c} ages for these ca. 1710-1760 Ma zircons range from 2280 to 2840 Ma. A continuum of initial ε $Hf_{(t)}$ values from -4.21 to +5.8 characterise zircon grains with ages ca. 1630-1690 Ma (n=11) and correspond to T_{DM}^{c} ages between 2000 and 2630 Ma. The youngest population ca. 1595 Ma has a ε $Hf_{(t)}$ range between -6.7 and +2.77 (n=14) (Fig. 8a) and T_{DM}^{c} from 2150 to 2750 Ma (Fig. 8b).

3.3.2 F (Radium Creek Group – Freeling Heights Quartzite)

The ca. 2500 Ma zircon grains (n=2) have ε $Hf_{(t)}$ values of -5.15 and +1.29 (T_{DM}^{c} values of 3.38 and 2970 Ma respectively) (Fig. 8a-b). A single grain with an age of ca. 1841 Ma has a ε $Hf_{(t)}$ of -2.56 and a T_{DM}^{c} of 2680 Ma. A ca. 1730 Ma population s (n=8) records ε $Hf_{(t)}$ values ranging from -9.4 to -0.53, T_{DM}^{c} for this group are 2480 to 3030 Ma. Zircons with U-Pb ages of ca. 1680 Ma (n=3) have a range of ε $Hf_{(t)}$ values from -9.91 to 0 and T_{DM}^{c} from 2390 to 3000 Ma. An early Mesoproterozoic population ca. 1595 Ma (n=4) have ε $Hf_{(t)}$ values ranging from -6.11 to +2.44 (Fig. 8a) and T_{DM}^{c} between 2170 and 2720 Ma (Fig. 8b).

3.3.3 36 (Radium Creek Group – Freeling Heights Quartzite)

This sample includes grains from 5 discrete age populations. All but the youngest (the early Mesoproterozoic population) have negative ε $Hf_{(t)}$ values (Fig. 8a). The oldest grain ca. 2948 Ma has a ε $Hf_{(t)}$ value of -9.46 and a T_{DM}^{c} of 3970 Ma. A ca. 2500 Ma population (n=2) has initial ε Hf values of -2.77 and -0.93 (T_{DM}^{c} values of 3220 and 3070 Ma respectively). Ca. 1850 Ma (n=2) zircon grains have ε $Hf_{(t)}$ values of -6.32 and -3.24 (Fig. 8a) with T_{DM}^{c} of 2730 and 2940 Ma respectively (Fig 8b). Grains at ca. 1710-1740 Ma (n=4) return a tight cluster of initial ε $Hf_{(t)}$ values that range between -3.63 and -2.07. This group have T_{DM}^{c} from 2540 to 2670 Ma. A ca. 1677 Ma (n=3) population have a ε $Hf_{(t)}$ value range of -3.82 to -1.07 and T_{DM}^{c} between 2450 and 2630 Ma. A ca. 1595 Ma (n=7) population have a spread of ε $Hf_{(t)}$ values ranging from -5.37 to +2.79 (Fig 8a) and corresponding T_{DM}^{c} of 2130 to 2690 Ma (Fig 8b).

3.3.4 YD23a (upper Gawler Range Volcanics)

This sample has 4 U-Pb age clusters. The principle age population (ca. 1595 Ma, n=20) ranges between -4.51 and -0.82, T_{DM}^{c} range of 2380-2620 Ma with an outlier that returned a ε $Hf_{(t)}$ value of +3.01 and 2250 Ma T_{DM}^{c} (Fig. 8c). ε $Hf_{(t)}$ of grains older than ca. 1710 Ma (n=4) range between +1.61 and +2.81, T_{DM}^{c} ranges from 2300-2430 Ma. ε $Hf_{(t)}$ values of ca. 1680 Ma (n=2) zircon grains are -1.14 and -0.98, T_{DM}^{c} ages of 2440 and 2450 Ma (Fig. 8c).

3.3.5 R1707876 (Curnamona Province: Frome Granite – Bimbowrie Suite)

The dominant population at 1594 ± 8 Ma (n=22; Jagodzinski and Fricke, 2010) have ε $Hf_{(t)}$ values ranging from -5.29 to +1.02 and T_{DM}^{c} between 2260 and 2670 Ma (Fig 8c). A single older grain ca. 1640 Ma has an ε $Hf_{(t)}$ value of -2.7 and T_{DM}^{c} of 2.53 Ga. A young grain ca. 1557 Ma has a distinctly positive ε $Hf_{(t)}$ value of +5.96 and T_{DM}^{c} of 1920 Ma.

3.3.6. R1709059 (Curnamona Province: Benagerie Volcanic Suite)

The single population ca. 1587 Ma calculated for this rhyolite (Jagodzinski and Fricke, 2010) recorded a range of ε $Hf_{(t)}$ values from -1.7 to +4.0 and T_{DM}^{c} between 2070 and 2440 Ma (Fig. 8c).

3.4 In-situ trace element chemistry

The modelled rock type for each zircon analysed using the classification scheme of Belousova et al. (2002) are shown in Table 4 and are shown graphically in Figure 9. In both samples modelled (F and 36), three modelled rock types for all of the zircons analysed were distinguished. These were low SiO_2 granitoids, granitoids (70-75 wt% SiO_2) and dolerites.

The ca. 1595 Ma zircons in sample F (Freeling Heights Quartzite) were modelled as originating from low SiO_2 granitoids (n=2) and from moderate SiO_2 content (70-75 wt%) granitoids (n=1). The ca. 1650-1680 Ma population was modelled as dolerite and 70-75 wt% granitoid (n=2). A subset of 8 zircons from the ca. 1700-1740 Ma zircon population indicates a predominantly granitoid source rock (n=5), although two zircons modelled as being sourced from dolerite (n=2) and 1 from a low SiO_2 granitoid. The ca. 1800-1850 Ma and earliest Palaeoproterozoic populations were modelled as wholly 70-75 wt% SiO_2 granitoid derived. The overall modelled rock type source distributions for this sample are 62.5% granitoid (70-75 wt% SiO_2 content) derived (n=10/16) and 18.75% from both dolerite and low SiO_2 (<65 wt%) granitoids.

The ca. 1595 Ma zircons in sample 36 (Mount Adams Quartzite) model as being derived from both low (n=2) and moderate (n=3) SiO_2 content granitoids. The ca. 1650-1680 Ma grains in this sample are evenly sourced from dolerite and 70-75 wt% SiO_2 granitoid rock types, which is identical to sample F. The ca. 1700-1740 Ma grains in this sample (n=3) are similar to those from that in sample F, as two are modelled as granitoid (70-75 wt% SiO_2), and the third as dolerite sourced zircon, but lack zircons derived from low SiO_2 granitoids. It is possible this is due to sample size. One zircon in the 1800-1850 Ma population is derived from a low silica granitoid, and the other to a moderate SiO_2 content granitoid. The Archaean portion of the zircons analysed from this sample are sourced from a granitoid with 70-75 wt% SiO_2 content (n=3) or from a dolerite (n=1). The total modelled rock type source distributions for this sample was 61.1% granitoid (70-75 wt% silica content) derived (n=11/18), 22.2% dolerite derived (n=4/18) and 16.67% from low silica granitoids (n=3/18).

3.5 Whole rock geochemistry

Complete major and trace element data is presented in supplementary appendix B. Major element data defines sample Z3 as shale and sample F as subarkose according to the classification of Herron (1998). Th/Sc ratios for each of sample Z3 and sample F are 2.506 and 2.23 respectively. The samples display negative Eu/Eu* anomalies (Taylor & McLennan, 1985) of 0.41 for sample Z3 and 0.575 for sample F. Sample Z3 has a La/Yb_n value of 6.05 and sample F has a value (La/Yb_n) value of 1.08.

4 Discussion

4.1 Implications of new Radium Creek Group U-Pb zircon ages

In-situ U-Pb zircon dating of the Radium Creek Group units yielded a distinct Early Mesoproterozoic population within analytical uncertainty of each other. The 4 samples in this study yield a weighted mean average $^{207}Pb/^{206}Pb$ age of 1595.5 ± 3.7 Ma (n=41), which can be interpreted as the maximum depositional age of the Radium Creek Group. This robust age is within error of the SHRIMP IIe U-Pb maximum depositional ages of 1600 ± 8 Ma (Palaeoproterozoic suite 4; Teale, 1993) and 1591 ± 6 Ma (Palaeoproterozoic suite 5; Teale, 1993) for quartzofeldspathic gneisses sampled in the Paralana Creek ~10 kilometres to the south of the current study (Fraser and Neumann, 2010). Since we find these early Mesoproterozoic depositional ages to be prominent throughout the Radium Creek Group, we interpret a geological framework involving a single phase of deposition for the entire package (Coats and Blissett, 1971; Elburg et al., 2001) at ca. 1595 Ma rather involving two distinct phases as previously interpreted (Paul, 1998; Teale 1993). This single depositional episode model is consistent with the structural framework interpreted by Armit et al. (2012) who described an upwards coarsening sequence from basal pelitic units (Brindana Schist) conformably overlain by quartzites and conglomerates of the Freeling Heights Quartzite (Fig. 10).

The overall detrital zircon U-Pb population distributions (Fig. 6) for all 4 Radium Creek Group samples in this study, are very similar to each other; with significant U-Pb age contributions at ca. 1595 Ma, ca. 1660-1680 Ma, ca. 1710-1780 Ma and ca. 2500 Ma. Moreover, the in-situ zircon geochemistry of zircons from both the hanging wall (Freeling Heights Quartzite; sample F) and the footwall (Mount Adams Quartzite; sample 36) of the Paralana Fault is remarkably similar (Fig. 9). Modelling of these zircon grain's geochemistry classifies the population as predominantly derived from felsic magmatism, but both units also have a small component of more mafic derived magmatic zircons of ca. 1660-1680 Ma and ca. 1710-1780 Ma age.

Our data support the suggestion of comparable provenance for these units, and by extension, the Radium Creek Group across the fault. The most straightforward explanation is that entire group shares the same provenance. On this basis we interpret a source terrane for the Radium Creek Group that contains ca. 1595 Ma intermediate to felsic magmatic rocks and reworked older Archaean to Palaeoproterozoic mafic to felsic magmatic material.

In addition, a subordinate U-Pb population at ca. 1850 was discovered in both the Freeling Heights Quartzite (Sample F) and the Mount Adams Quartzite (sample 36). These quartzites have been previously interpreted as distinct units; the Mount Adams Quartzite forming an older unit in the stratigraphy (Coats and Blissett, 1971). The lower Freeling Heights Quartzite has also been interpreted to be significantly older than the upper Freeling Heights Quartzite and Mount Adams Quartzite on the basis of stronger deformation recorded in these lower horizons (Paul et al., 1999). Our data suggest these differences in deformation intensity may be due to factors other than a time break, as the indistinguishable maximum depositional ages for these two units and the similarities in both the dominant and subordinate U-Pb detrital populations (i.e. ca. 1850 Ma) would suggest that these quartzites are likely to be lateral correlatives to each other. The greater deformation intensity observed within the lower parts of the Freeling Heights Quartzite could instead be explained by the location of the Freeling Heights Quartzite in the hangingwall of the Paralana Fault, whilst the Mount Adams Quartzite is restricted to the footwall (Fig. 3). Strain partitioning related to protracted shearing along the Paralana Fault is suggested to result in the development of more intense deformation in the proximal parts of hangingwall to the fault.

The lower horizons of the Freeling Heights Quartzite are slightly more micaceous than the upper part of the unit and to the Mount Adams Quartzite (Armit, 2007). In particular, proximal to the contact with the underlying Brindana Schist, the Freeling Heights Quartzite contains large micaceous pods in which strain has been localised during Mesoproterozoic and Palaeozoic deformation (Armit et al., 2012) producing a stronger structural fabric than is evident at the meso-scale in the upper horizons of the Freeling Heights Quartzite and in the Mount Adams Quartzite. According to this single deposition framework the entire ca. 1595 Ma Radium Creek Group is deformed by ca. 1591-1585 Ma deformation and is not sub-divided into pre- and post-deformational sequences (c.f. Fanning et al., 2003; Paul, 1998; Paul et al., 1999).

4.2 Whole rock geochemistry

Th/Sc ratios for sample Z3 and sample F are higher than Post Archaean Australian Shale (PAAS, The/Sc = 0.91; Taylor & McLennan, 1985) which supports the interpretation from the in-situ zircon geochemistry that both of these samples were most likely sourced from a region dominated by felsic material (Bhatia & Cook 1986; Cullers & Berendsen 1998). The samples display moderately negative Eu/Eu* anomalies (0.41 for sample Z3 and 0.575 for sample F) when compared to PAAS (0.65; Taylor & McLennan, 1985). This indicates their source was also characterised by negative Eu anomalies, a ubiquitous affinity of A-type magmatic suites. La/Yb_n ratios of 6.05 for sample Z3 indicate it is slightly LREE enriched. Sample F displays significant HREE enrichment (La/Yb_n value of 1.08), which is most likely due to accumulation of previously mobile HREE in garnets that grew as a result of regional metamorphism at ca. 1591-1552Ma (Armit et al. 2012).

4.3 In-situ Hf Isotopes

Hf isotope signatures of the Radium Creek Group samples are fairly diverse and most likely reflect both less evolved and substantially more evolved signatures (Fig. 8a-b). Within each U-Pb age population, considerable overlap in the Hf isotope ratios is present across the three Mount Painter samples (Table 3). These data strengthens the argument that both the pelitic and more quartz-rich units of the Radium Creek Group are of the same provenance.

The ca. 1595 Ma U-Pb population within the Radium Creek Group samples (n=25, this study) in the northern Mount Painter Inlier is consistent with the spread in Hf isotope ratios of the Early Mesoproterozoic aged grains (n=4) in sample ARK661 (Fig. 8c-d), from the southern Mount Painter Inlier (Elburg et al. 2012). This strengthens for the interpretation of a similar provenance for all of the Early Mesoproterozoic metasediments in the Mount Painter Inlier. Our larger dataset both confirms the maximum depositional age for the Radium Creek Group, and demonstrates for the first time a clear bimodal $\varepsilon\ Hf_{(t)}$ signature for this population. Mixing between an evolved component ($\varepsilon\ Hf_{(1595)}$ -6.7 to -1.17, n=16) and a more juvenile component ($\varepsilon\ Hf_{(1595)}$ 0 to +2.79, n=9) is consistent with this pattern (Fig. 8d).

The magmatic pulse that generated the detrital source material of the Radium Creek Group must have contained a juvenile component, but also recrystallised more evolved material. Contemporaneous melting of various mantle and crust is consistent with the bimodal Hf isotope data in the resultant sedimentary packages. The Early Mesoproterozoic U-Pb age population peak (ca. 1595 Ma) within the age spectra of neighbouring felsic-dominated magmatic rocks; the upper Gawler Range Volcanics (sample YD23a), Frome Granite and Benagerie Volcanic Suite, therefore invite ε $Hf_{(t)}$ comparison with the Radium Creek Group (Fig. 8c).

The predominantly negative ε $Hf_{(1595Ma)}$ values (-4.51 to -0.82) of the upper Gawler Range Volcanics zircons (Fig. 8c) would suggest (prima facie) that it was formed from moderately evolved crustal material. However the single, positive ε $Hf_{(1595Ma)}$ value implies more juvenile material was also involved to a degree. Pankhurst et al. (2013) report whole-rock Hf data for the small volume mafic components of the Gawler Range Volcanics which record a more primitive signal than we observe within our zircon population. This demonstrates that a juvenile component of the Gawler Range Volcanics can be detected, and that its weak contribution to subsequent basin detritus may be muted by lack of mafic outcrop in the hinterland.

The Hf isotope signature of the upper Gawler Range Volcanics is similar to that of the ca. 1595 Ma detrital zircons from the Radium Creek Group, as their absolute range of ε $Hf_{(1595Ma)}$ values overlap (Fig. 8c). However, the Radium Creek Group data extends to both more evolved and strongly negative ε $Hf_{(1595Ma)}$ values. This might reflect a sampling bias (e.g. Andersen et al. 2005) or that the source terrane of the Radium Creek Group ca. 1595 Ma zircon peak has a greater isotopic heterogeneity than the preserved Gawler Range Volcanics alone.

Zircon grains with ca. 1595 Ma ages from the Frome Granite (Bimbowrie Suite) indicate that this magma formed at least in part from reworked crust of ca. 2260-2670 Ma (Fig. 8c). The signature is similar to the range of ε $Hf_{(1595Ma)}$ values from the upper Gawler Range Volcanics grains, as they also record predominantly negative values to weakly positive (-5.29 to +1.02) (Fig. 8c). Similarly, this range of values falls within that of the Radium Creek Group. Importantly, >1650 Ma U-Pb populations are absent from our data. Moreover the Frome Granite intrusive age of 1594 ± 8 Ma (Jagodzinski and Fricke, 2010) would suggest that it would have been located within the crustal pile during the earliest Mesoproterozoic and hence unlikely to be actively eroding to provide the required detritus into a nascent ca. 1595 Ma basin now preserved in the Mount Painter Inlier.

The Hf isotope signature of the ca. 1595 Ma zircon populations in the Benagerie Volcanic Suite sample is defined by a relatively tightly clustered group of ε $Hf_{(1595Ma)}$ values (-1.73 to +4.0). This group is appreciably more juvenile than the values for the upper Gawler Range Volcanics and Frome Granite (Fig. 8c). It is important to note that unlike the Radium Creek Group, we did not detect a more evolved and negative Hf component (-6 to -2) in this sample of Benagerie Volcanic Suite (Fig. 8c).

The lack of a good match between the Benagerie Volcanic Suite and Radium Creek Groups zircon Hf isotope signature (Fig. 8c) implies that provenance of the metasediment within the Mount Painter Inlier is unlikely to include the Benagerie Volcanic Suite. The ca. 1587 Ma crystallisation age calculated for this sample (Jagodzinski and Fricke, 2010) is also slightly younger than the maximum deposition age (ca. 1595 Ma) of the Radium Creek Group (although within analytical uncertainty). Rather, this age has greater similarity with the age of the Mount Neill Suite magmatism in the Mount Painter Inlier (ca. 1585 Ma). This suite intrudes the metasediments following an episode of burial and deformation at ca. 1595-1585 Ma (Armit et al., 2012). Thus if the Benagerie Volcanic Suite are extrusive equivalents of the magmatic pulse that generated the Mount Neill Suite, it would not be feasible for these rocks to contribute to the source of the Radium Creek Group.

Thus a combination of Hf isotope data and geologic evidence, effectively remove the Curnamona Province felsic magmatic rocks with ca. 1595 ages (Frome Granite and Benagerie Volcanic Suite) from consideration as potential sources of the Radium Creek Group. The remaining sample is the Gawler Range Volcanics sample. The following discussion aims to explore this hypothesis.

The prominent ca. 1680-1660 Ma detrital zircon U-Pb population within the Radium Creek Group has a grouped ε $Hf_{(t)}$ value range of -9.91 to +5.8 (n=17). A similar spread of values is evident in ARK661 (Elburg et al., 2012) with ε $Hf_{(t)}$ values of between -7 to +6.7 (n=9) (Fig. 8c-d). A source terrane for this scattered and highly variable Hf isotope signature is likely to be composed of reworked, refractory ca. 3000-2400 Ma Archaean to Palaeoproterozoic crust which has mixed with significantly more isotopically primitive material ca. 1680-1660Ma.

Two zircons from the upper Gawler Range Volcanics have U-Pb ages ca. 1655 Ma and therefore match the age peak within the Radium Creek Group. These two grains record slightly negative ε $Hf_{(t)}$ values. While these are within the ε $Hf_{(t)}$ range for the corresponding Radium Creek Group age peak; it is difficult to ascribe much significance given the size of the data subset.

No pre-1650 Ma U-Pb population was identified from either the Frome Granite or Benagerie Volcanic samples (Jagodzinski and Fricke, 2010). It is worth noting that the absence of a ca. 1660-1680 age peak in these samples strengthens the argument that the pre-1650 Ma zircons in the Radium Creek Group cannot have been sourced from these magmatic suites.

Detrital zircons that define a U-Pb population at ca. 1710-1780 Ma in the Radium Creek Group have a relatively evolved Hf isotopic signature, although an appreciably juvenile signal is also present (ε $Hf_{(t)}$ ranges between -9.4 to +2.74; n=18). Any potential sources for this detritus are interpreted to be composed of predominantly reworked and refractory ca. 3030-2680 Ma Archaean to Palaeoproterozoic crust that has mixed with slightly more isotopically juvenile material (T_{DM}^{c} of 2280 Ma) at ca. 1710-1780 Ma.

The three zircons ca. 1710-1780 Ma from the upper Gawler Range Volcanics all record positive ε $Hf_{(t)}$ (+1.61 to +2.73), which is similar to the small (n=2; +0.08, +2.73) juvenile component within the ca. 1710-1780 Ma Brindana Schist of the Radium Creek Group (Fig. 8c). Unlike the Radium Creek Group however, we did not detect a more evolved Hf component of ca. 1710-1780 Ma age in sample YD23a. Larger U-Pb-Hf zircon datasets for the upper Gawler Range Volcanics may resolve this Hf isotope mis-match.

All of the ca. 1850 Ma zircons analysed (n=4) from the Radium Creek Group in this study have isotopically evolved Hf signatures, interpreted as reworked ca. 2680-2940 Ma Archaean material (Fig. 8a). The six Hf isotope analyses from ca. 2500 Ma zircon grains have a ε $Hf_{(t)}$ value range between -5.15 and +1.29 reflecting reworked >2970 Ma Archaean crust. Archaean zircon in sample ARK661 (n=5) have overlapping to moderately more juvenile Hf isotopic signatures with respect to the other sample of Radium Creek Group and are characterised by ε $Hf_{(t)}$ values ranging between -0.35 and +4.12 (Fig. 8d) (T_{DM}^{c} range of 2820-3110 Ma). This most likely reflects a large isotopic heterogeneity in the Archaean component of the source terrane for the metasediments in the Mount Painter Inlier.

It is important to note the small sample populations of zircon grains (n <4) representing the ca. 1710-1780 Ma and ca. 1850 Ma ages. It is therefore possible that the Hf isotopic signatures of these populations may not be truly representative.

4.4 Whole rock Nd isotopes

Whole rock Nd isotope ratios of the Freeling Heights Quartzite and Yaglin Phyllite units of the Radium Creek Group (Neumann, 2001; Schaefer, 1993) have been recalculated to 1595 Ma to reflect the maximum depositional age of these units determined in this study. The result is negative $\varepsilon Nd_{(1595)}$ values of -5.19 to -3.25 (Freeling Heights Quartzite) and -4.36 (Yaglin Phyllite). This is consistent with the predominantly negative in-situ Hf isotopic signature presented in this study for the ca. 1595 Ma Radium Creek Group.

The $\varepsilon Nd_{(1585)}$ values of the felsic upper Gawler Range Volcanics range from -4.3 to -1.8, and as such are indistinguishable from those of the Benagerie Volcanic Suite (Wade et al., 2012). The felsic rocks of the lower Gawler Range Volcanics contain more variable values of $\varepsilon Nd_{(1585)}$, and range from evolved ($\varepsilon Nd_{(1585)}$ of -7) to less evolved ($\varepsilon Nd_{(1585)}$ of -0.2) signals (Wade et al., 2012). The Radium Creek Group contains slightly more evolved $\varepsilon Nd_{(1595)}$ (e.g. -5.19 for the Freeling Heights Quartzite) and disperse $\varepsilon Hf_{(1595)}$ values than the upper Gawler Range or Benagerie Volcanic Suite. We suggest that isotopic correlation between the Radium Creek Group and the more diverse negative $\varepsilon Nd_{(1585)}$ values for the lower Gawler Range Volcanics is more consistent.

The in-situ zircon age spectra and contained $\varepsilon Hf_{(t)}$ coupled with geologic context and whole-rock εNd support a Gawler Craton dominated provenance for the Radium Creek Group. The Curnamona Province contains appropriate felsic magmatic rocks of a similar age to that of the maximum Radium Creek Group deposition age, however, several lines of evidence preclude a Curnamona Province provenance for the Radium Creek Group.

4.5 Comparison with regional datasets

The present location of the Mount Painter Inlier within the northern South Australia Craton (Fig. 1a-b) and relative proximity to both the Curnamona Province and the Gawler Craton (Fig. 1c) merits isotopic comparison between these terranes and with the North Australian Craton. Disperse U-Pb-Hf isotopic signatures from the detrital zircons in the Radium Creek Group supports a more complex provenance than from any one of the proximal magmatic suites (e.g. upper Gawler Range Volcanics, Frome Granite and Benagerie Volcanic Suite) analysed in this study (Fig. 8c).

The combined detrital zircon patterns of the Radium Creek Group strongly argue for provenance from a terrane that includes ca. 1595 Ma, ca. 1660-1680 Ma, ca. 1710-1780 Ma, 1850 Ma and Earliest Palaeoproterozoic to Archaean magmatic rocks or significant inherited populations. Major magmatic events in eastern Early Mesoproterozoic Australia ca. 1595 Ma are also recorded in the Arunta Inlier with the ca. 1603-1615 Ma Burt-Rungutjirba Suite (Zhao and McCulloch, 1995; Zhao and Bennett, 1995), in the Musgrave Block with the Musgravian Gneiss (Gum and Belousova, 2006; Kirkland et al., In Press; Wade et al., 2006), and in the Curnamona Province with the ca. 1600-1570 Ma Mundi Mundi, Cusin Creek plutons, Benagerie Volcanic Suite and Ninnerie Supersuite (Fanning et al., 1998; Jagodzinski and Fricke, 2010; Wade et al., 2011;2012). The Gawler Craton magmatism ca. 1604-1583 Ma is dominated by the voluminous felsic Gawler Range Volcanics and Hiltaba Suite (Fanning et al., 1988; Fanning et al., 2007) and localised deposition of clastic sediments (e.g. the upper Corunna Conglomerate) (Daly et al., 1998). Sedimentation in the Early Mesoproterozoic is also recorded across the North Australian Craton including the Upper McNamara Group in the

Mount Isa Inlier (Andrews, 1998; Krassay et al., 2000), the Favenc Package in the McArthur River area (Rawlings, 1999) and the Dargalong Metamorphics in the Georgetown Inlier (Withnall et al., 1997) (Fig. 1b).

Palaeoproterozoic basin evolution is widespread and broadly comparable across eastern Australia characterised by the Leichhardt, Calvert and Isa Superbasins in the Mount Isa Inlier (Jackson et al., 2000), the Etheridge Group in the Georgetown Inlier (Withnall et al., 1988), Willyama Supergroup in the Curnamona Province (Conor and Preiss, 2008), and the metasediments preserved in the central and northern Gawler Craton (Hand et al., 2007; Payne et al., 2006; Szpunar et al., 2011). The basins in the Curnamona and Gawler Craton have been interpreted to have a predominantly evolved, felsic magmatic ca. 1710-1780 Ma Arunta (Barovich and Hand, 2008; Payne et al., 2006) or northern Gawler Craton provenance (Howard et al., 2011c). Hf isotope datasets that include these 1710-1780 Ma metasediments and felsic intrusives from the Fowler, Spencer, Olympic domains (Fig. 1c) of the Gawler Craton (Fig. 11a-b) (Belousova et al., 2009; Howard et al., 2011a; Howard et al., 2011b; Howard et al., 2011c; Szpunar et al., 2011) closely correlate with the felsic derived 1710-1780 Ma zircons in the Radium Creek Group. This would suggest that ca. 1710-1780 Ma detrital zircons in the Radium Creek Group could have been sourced from felsic intrusives in the Gawler Craton (e.g. ca. 1736 Ma Middle Camp Granite and ca. 1755 Ma Wertigo Granite; Fanning et al. 2007; see Fig. 1c), re-worked ca. 1710-1780 Ma metasediments (e.g. Wallaroo Group and Moonabie Formation; see Fig. 1c) in the Gawler Craton, or from their protoliths in the northern Gawler Craton or Arunta Block.

However, potential ca. 1595 Ma felsic magmatic protoliths in the Arunta Block, such as the Burt-Rungutjirba Suite (Zhao, 1994) which has $\varepsilon Nd_{(1603-1615)}$ values of +0.91 to +2.49 is interpreted to be too juvenile to be a likely source of more evolved ca. 1595 Ma detritus in the Radium Creek Group. Moreover, comparison of the Hf isotopes of the Radium Creek Group detrital zircons with those of the Meso-Palaeoproterozoic Arunta Inlier (Hollis et al., 2010) shows little correlation between the disperse and generally negative, evolved $\varepsilon Hf_{(t)}$ in zircon characteristics of the Radium Creek Group and the predominantly juvenile $\varepsilon Hf_{(t)}$ values for zircons from the Arunta region (Fig. 12a). This would imply that the direct ca. 1595 Ma source of the detritus in the Mount Painter Province is unlikely to be the Arunta Block but does not preclude the incorporation and assimilation of ca. 1710-1760 Ma Arunta derived material with more refractory Archaean to Palaeoproterozoic crust, in the potential source terrane for the Radium Creek Group.

Correlation of the Radium Creek Group with the available Hf isotopic datasets (modern drainage samples) for the Curnamona Province (Condie et al., 2005) (Fig. 12b) and Mount Isa Inlier (Griffin et al., 2006) (Fig. 12c) is plausible. The dataset for the Broken Hill Block of the Curnamona Province however, does not include any analysis of older Early Palaeoproterozoic or Archaean zircon grains (Fig. 12b). A number of authors (e.g. Cooper, 1985; Page et al., 2005) have indicated the existence of Archaean to Palaeoproterozoic zircon populations in the Curnamona Province, but further Hf isotope work is required to provide robust comparison with the pre-1700 Ma zircons in the Radium Creek Group. The Late Palaeoproterozoic to Early Mesoproterozoic zircon grains that constitute this Broken Hill dataset (Fig. 12b) are characterised by predominantly more juvenile Hf isotopic values than the Radium Creek Group. This more isotopically juvenile Hf range is consistent with the primitive $\varepsilon Nd_{(1650)}$ values of -3 to 0 reported by Barovich et al. (2008) for the upper Willyama Supergroup for which a distinct south-western Laurentia (Barovich et al., 2008) or southwest Baltica (Howard et al. 2011a) provenance has been proposed.

The U-Pb ages and Hf isotopic compositions from Mount Isa Inlier (Griffin et al., 2006) and Mount Painter Province metasediments reflect both Archaean and Palaeoproterozoic phases of crustal reworking (Fig. 11c). Mesoproterozoic magmatism in the Mount Isa Inlier did not initiate until ca. 1550 Ma with the emplacement of the Williams and Naraku Batholiths (Page and Sun, 1998). It is therefore problematic to consider any major magmatic suites in the Mount Isa Inlier as the source of the dominant ca. 1595 Ma magmatic derived zircon population in the Radium Creek Group.

Instead, it is plausible that the ca. 1595 Ma zircons in the Radium Creek Group could have been derived from 1595 ± 6 Ma, 1589 ± 3 Ma minor tuffaceous horizons in the Lawn Hill Formation and Balbirini Dolomite of the McArthur Basin (Page et al., 2000). However they would most likely represent volumetrically insignificant contributions if the Mount Isa Inlier or McArthur Basin were actively eroding ca. 1595 Ma and shedding material into the Mount Painter Province. The zircon budget from these tuffs would likely be swamped by competing sources.

A paucity of isotopically juvenile felsic magmatism ca. 1660-1680 Ma in eastern Proterozoic Australia reduces potential source correlations for the Radium Creek Group. The ca. 1680 Ma felsic Tunkilla Suite in the Gawler Craton (Fig. 1c) (Payne et al., 2010) which exhibits a large isotopic variation ($\varepsilon Nd_{(1680)}$ -6.3 to +2.6) is one possible exception. Erosion ca. 1595 Ma of a crustal pile that included this ca. 1680 Ma felsic material as well as more refractory Archaean to Palaeoproterozoic precursors is considered to be consistent with the isotopic fingerprint of the Radium Creek Group.

The ca. 1600-1540 Ma Musgravian Gneiss in the Musgrave Block, is characterised by juvenile Nd and Hf isotopic compositions (Gum and Belousova, 2006; Kirkland et al., 2012; Wade et al., 2006) that are too juvenile to be considered as viable correlatives with the ca. 1595 Ma Radium Creek Group.

Therefore, it is unlikely that the Radium Creek Group represents derivation from a proposed ca. 1600-1540 Ma magmatic arc in the Musgrave Block.

Correlation of the felsic magmatic-derived ca. 1850 Ma zircon grains in the Radium Creek Group is permissible with Hf datasets from the Olympic (Belousova et al., 2009) and Spencer domains (Szpunar et al., 2011) (Fig. 11a) of the Gawler Craton (Fig. 1c). These grains reflect the emplacement of the felsic Donington Suite (Fig. 1c) in the Gawler Craton (Drexel et al., 1995) which has ε $Hf_{(1850)}$ value range between -4 and +5 (Reid et al., 2008; Szpunar et al. 2011). These data indicate both reworking of the ca. 2500 Ma material as well as some juvenile input ca. 1850 Ma.

These data are similar to the ca. 1850 Ma Mount Isa Inlier Hf dataset (Fig. 12c) (Griffin et al. 2006) which corresponds to the emplacement of the ca. 1856 Ma Kalkadoon Batholith and co-magmatic Leichardt Volcanics (Page, 1983), and reflects remelting of Late Archaean material ca. 2500 Ma. The ca. 1850 Ma event in the Mount Isa Inlier does, however, comprise a far greater degree of mafic rocks with very positive ε $Hf_{(1850)}$ and are isotopically similar to the depleted mantle at ca. 1850 Ma. No such mafic (Fig. 9) and primitive isotopic signature (Fig. 8a,d) was detected for zircons from the Radium Creek Group.

The Neoarchaean to Earliest Palaeoproterozoic zircon grains in the Radium Creek Group return a broad range of ε $Hf_{(t)}$ values (-5.15 to +4.12), consistent with derivation from a complex Archaean source terrane that comprises both reworked and juvenile components. Whilst this is largely similar to the Archaean Mount Isa Inlier (Fig. 12c; Griffin et al. 2006) and Gawler datasets (Belousova et al., 2009; Howard et al., 2011a;2011b), both the more evolved ε $Hf_{(t)}$ values and > ca. 2600 Ma U-Pb populations evident in sample ARK661 (Elburg et al., 2012), are more consistent with derivation from average Archaean Gawler Craton crust (Fig. 11a-b). This crust includes the Meso-Neoarchaean Middleback Group (Szpunar et al., 2011) preserved in Spencer and Cleve domains, granite gneisses (Fraser et al., 2010), and the Sleaford and Mulgathing complexes preserved in the Coulta and Christie domains of the Gawler Craton (Fig. 1c) (Cowley and Fanning, 1992; Fanning, 1997; Schaefer, 1998; Swain et al., 2005a).

Collectively the detrital zircon isotopic pattern of the Radium Creek Group requires a complex source terrane. This source must include a significant felsic Early Mesoproterozoic portion as well as Neoarchaean to Palaeoproterozoic material that has undergone phases of Late Archaean to Early Mesoproterozoic re-working. This older material must itself have incorporated some juvenile components.

We consider the Gawler Craton to be the most plausible source for this composite signature of the ca. 1595 Ma Radium Creek Group. In this scenario, the Mount Painter Province is likely to be proximal to, and receiving material from, the eastern and central Gawler Craton at ca. 1595 Ma. The most probable source would be sub-aerial exposures of voluminous ca. 1595 Ma felsic material associated with the Gawler Range Volcanics felsic large igneous province (FLIP) (Pankhurst et al., 2013), particularly zircon grains derived from the Lower Gawler Range Volcanics.

4.6 Proterozoic tectonic implications

Korsch et al. (2010) interpreted a distinctive seismic basement (termed the Warrakimbo Seismic Package) below the Mount Painter Province. We suggest that this basement is the eastern extension of the Gawler Craton and that the palaeo-Paralana Fault represents the eastern extent of the Gawler Craton. The palaeo-Paralana Fault is interpreted a moderately south-east-dipping, crustal-scale fault that separates the Warrakimbo and Yarramba seismic packages and has been interpreted as a major crustal boundary (Korsch et al. 2010).

Since we now consider the Freeling Heights Quartzite and the Mount Adams Quartzite to be lateral equivalents and stitch the Paralana Fault, the age of the tectonic boundary (possibly a suture) between the Warrakimbo and Yarramba seismic packages must pre-date ca. 1595 Ma. Further, the isotopic and geochemical similarities between the Upper Gawler Range Volcanics and the Benagerie Volcanic Suite (Wade et al., 2012) suggests the lower crust in the footwall of the palaeo-Paralana Fault may represent the same crustal sources (e.g. Pankhurst et al., 2013) of magmatism as the central Gawler Craton. The correlation of the upper Gawler Range Volcanics with the Benagerie Volcanic Suite in the Curnamona Province (Wade et al., 2012) stitches the Gawler Craton and Curnamona Province together at ca. 1587 Ma.

An extensional event ca. 1595 Ma as suggested by Stewart and Betts (2010) is consistent with this scenario and supported by the interpretation by Korsch et al. (2010). In this scenario the Radium Creek Group was deposited within an extensional basin setting following the Olarian-Wartakan orogenic system (Page et al., 2005; Hand et al., 2007; Stewart and Betts, 2010). This tectonic system could be quite far-reaching, and include the Mount Woods Inlier and northern Gawler Craton (Cutts et al., 2011; Forbes et al., 2012) across southern Proterozoic Australia. This extensional phase was followed by renewed crustal shortening and inversion of the Radium Creek Metamorphics (Armit et al., 2012), and may have affected the northern Gawler Craton (Kararan Orogeny: Hand et al., 2007), southern Curnamona Province (Rutherford et al., 2007), and the Mount Isa Inlier (e.g., Betts et al., 2006). Repeated rapid switching from extension to shortening at convergent plate margins is common during transient episodes of flat subduction (Gutscher et al., 2002) or when subduction roll-back is interrupted by accretion of buoyant material such as an ocean plateau (Rosenbaum et al., 2005; Mason et al., 2010), plume-head (Murphy et al., 1998; Betts et al., 2009; 2012), arc terrane (Boutelier et al., 2003) or continental micro-continent (Moresi et al., in review), which are all characterised by local trench advance and shortening in the overriding plate. We propose that during the ca. 1595-1555 Ma interval, the Mount Painter Inlier was located in the overriding plate of one or more subduction zones and was subjected to tectonic mode switches caused by disruption of a convergent margin.

The palaeogeographic reconstructions of Betts & Giles (2006) (Fig. 2a); Betts et al. (2002; 2009), Cawood and Korsch et al. (2008) and Wade et al. (2006) (Fig. 2b) are consistent the Mount Painter Inlier being positioned proximal to one or more plate margins at ca. 1595 Ma. The configuration of Wade et al. (2006) does not have the Gawler Craton and the Curnamona Province co-located between ca. 1600-1580 Ma (Fig. 2b). The model of Wade et al. (2006) proposes that the Gawler Craton was positioned in the overriding plate of the south-dipping subduction zone prior to collision with the North Australian Craton at ca. 1590 Ma (Fig. 2b). In our reconstruction, the Curnamona Province is also required to be co-located with the Gawler Craton and therefore must have evolved in a back-arc setting on the overriding plate of a south dipping subduction zone and separated from the Mount Isa Inlier before ca. 1580 Ma (Fig. 2b). In this model, the Radium Creek Group would have been deposited in a back-arc setting and subsequent shortening resulted from collision between North and South Australian cratons at ca. 1560 Ma. However, separation between the North and South Australian cratons seems unlikely because of the well-established correlation of the ca.1720 to 1640 Ma basin systems between the Curnamona Province and North Australian Craton (Giles et al., 2002; Page et al., 2005; Conor and Priess, 2008; Gibson et al., 2008). We therefore consider a south-dipping subduction zone along the northern edge of the South Australian Craton highly unlikely at the beginning of the Mesoproterozoic.

The palaeogeographic reconstructions of Betts et al. (2002) and Betts and Giles (2006) consider that North and South Australian cratons to be contiguous at ca. 1600 Ma. The South Australian Craton was positioned between a long-lived accretionary convergent margin along the southern edge of the Australian continent (Betts et al., 2011), and a convergent margin along the eastern edge of the continent (Betts et al., 2002). Both these subduction zones are interpreted to dip towards the interior of the Australian continent (Betts et al., 2009). Superimposed on this complex tectonic setting is a major plume-related magmatic event (Betts et al., 2007; 2009). Tectonic interpretation of the evolution of the North Australian and South Australian cratons suggest that protracted episodes of high temperature metamorphism and continental basin systems formed in a back-arc setting

(Giles et al., 2002; Cutts et al., 2013), which were interrupted by transient accretion events (Betts et al., 2011) at the plate margin. Betts et al., (2009) proposed that the Olarian-Wartaken orogenic event was driven by the accretion of a plume-head with the Australian continent, which was followed by an episode of crustal extension after the transfer of the plume to the overriding plate (see Betts et al., 2013), producing a voluminous FLIP (Pankhurst et al., 2013) and a hotspot track defined by dominantly A-type magmatism after ca. 1600 Ma (Betts et al., 2007). We suggest that the deposition of the Radium Creek Group occurred in an extensional basin sourced from the FLIP preserved on the Gawler Craton (Fig. 13a). The Radium Creek Group were buried to mid crustal levels and then exhumed to the upper crust between ca. 1592 and ca. 1585 Ma requiring rapid switches to crustal shortening (Fig. 13b) to renewed extension (Armit et al., 2012). This was followed by renewed crustal shortening at ca. 1570-1555 Ma (Rutherford et al., 2007; Armit et al., 2012) (Fig. 13c). We interpret the tectonic switching is driven by perturbations in the convergent margin. We are unable to assess the relative role of these convergent margins but may speculate that the earlier shortening events (ca. 1585 Ma) is related to accretion along the southern margin of the continent (Fig.13a-b), whereas ca. 1570-1555 Ma shortening is related to subduction along the eastern margin of the continent (Fig. 13c).

5 Conclusions

The Radium Creek Group consists of a single stratigraphic package deposited in the Early Mesoproterozoic with a maximum deposition $^{207}Pb/^{206}Pb$ age of 1595.5 ± 3.7 Ma (n=41). The isotopic fingerprint of the Radium Creek Group requires a source with diverse but predominantly felsic character and evolved isotopic sources reflecting poly-phased crustal reworking from the Archaean to the Early Mesoproterozoic. Detrital zircon patterns in the Radium Creek Group that contains peaks at ca. 2500 Ma, ca. 1850 Ma, 1710-1780 Ma and 1660-1680 Ma. These ages are consistent with derivation from the Gawler Craton as opposed to other tectonic elements of eastern Proterozoic Australia, suggesting the Curnamona Province and Gawler Craton were co-located at ca. 1595 Ma. The implication of this interpretation is that the North and South Australian cratons were contiguous at ca. 1595 Ma placing the Mount Painter Inlier at the nexus of two convergent margins characterised by subduction zones that dip towards the continent interior. Perturbations in the dynamics of these convergent margins resulted in rapid tectonic switches following deposition of the Radium Creek Group. Our data provides a critical constraint for palaeogeographic reconstruction for eastern Australia at the Palaeo- to Mesoproterozoic transition.

6 Acknowledgements

We would like to thank the reviewers of this paper for providing constructive feedback. We are grateful to Heathgate Resources Pty Ltd for accommodation, access and company in the field. Marge and Doug Sprigg (Arkaroola station) are thanked for access and accommodation. Also thanks to

Steve Hore and Wolfgang Preiss (Primary Industry and Resources, South Australia) for advice and base maps. We would also like to thank Caroline Venn, Massimo Raveggi, Kirsty Sheerin, Jerram Adams, Ahmed Saleem, Laurent Ailleres and Andy Tomkins (Monash University) for field support, ideas and discussions. Norm Pearson, Elenor Belousova and Rosanna Murphy (GEMOC) are thanked for their invaluable technical assistance. This work was supported in part by ARC LP0882000.

Figure Captions

Fig. 1: a) Map of Australia showing the geography-based nomenclature after Myer et al. (1996) in which the continent is divided into three major cratonic units, called the North, West and South Australian cratons draped over a composite of the bouguer gravity and first vertical derivative of the total magnetic intensity (TMI) map of Australia (geophysical data provided by Geoscience Australia); b) Map highlighting the location of the Mount Painter Block and other eastern Australian Proterozoic terranes in relation to the major geological provinces of Australia. These are draped across a composite total magnetic intensity (TMI) anomaly and first vertical derivative of the TMI map of Australia. This magnetic image was produced using a two kilometre grid spacing and by applying a low pass filter (upward continued six kilometres), which highlights the longer wavelengths/major structural elements of eastern Australia. Data provided by Geoscience Australia; c). Map showing the position of the Mount Painter Province (grey box) in respect to the major domains and Archaean to Mesoproterozoic geology of the Curnamona Province after Conor and Preiss (2008) and the Gawler Craton modified after Fairclough et al. (2003) and Hand et al. (2007).

Fig 2: a) Palaeogeographical reconfiguration model after Giles et al. (2004); Betts and Giles (2006) supporting a shared history for the South Australian Craton and the North Australian Craton between ca. 1800 and 1550 Ma. This configuration aligns contemporaneous orogenic belts across the Gawler Craton, Arunta Inlier, Mount Isa Inlier and the Curnamona Province.; b) Palaeogeographical reconfiguration model after Wade et al. (2006) in which the Gawler Craton and Curnamona Province are separated by a south-dipping subduction zone between ca.1600-1580 Ma with the Gawler Craton positioned in the overriding plate.

Fig. 3: Map of the Mount Painter Inlier showing sample locations and regional geology after Armit et al. (2012).

Fig. 4: a) Photograph of the steeply dipping, foliated psammopelites of the Brindana Schist unit at the base of Radium Creek Group, geo-pick shown for scale (sample Z3 363800E 6675681N); b) Photo-micrograph of a thin section of sample Z3 from the Brindana Schist in cross-polarised light, cut normal to the S_3 foliation. This view demonstrates overprinting, spaced foliations defined by muscovite ± biotite fabrics (sub-horizontal in photo-micrograph) and recrystallised polygonal quartz aggregate (microlithons); c) Photograph of the intensely crenulated, micaceous quartzite outcrop of the Freeling Heights Quartzite (sample F 357632E 6673138N); d) Photo-micrograph of a thin section of the Freeling Heights Quartzite in cross-polarised light. The section, taken normal to the S_3 foliation, highlights a spaced schistosity defined by muscovite with elongate relic quartz grains which display undulose extinction. A discrete crenulation cleavage overprints the existing schistosity; e) Photograph of quartzite unit of the Freeling Heights Quartzite (sample 123 355996E, 6672099N).

Cross-beds defined by heavy minerals and distinct compositional layering (compare with bottom right of picture) record reverse grading. This indicates that younging is upwards and towards the west (head of the geo-pick is orientated E-W); f) Photo-micrograph of sample 123 in cross-polarised light. The section was cut normal to the S_3 foliation and highlights two spaced and overprinting foliations defined by biotite ± muscovite and polygonal quartz-rich microlithons; g) Photograph of the fine-grained pinky-grey micaceous quartzite outcrop of the Mount Adams Quartzite (Sample 36; 357161E, 6668472N). Cross beds defined by heavy minerals indicate upward younging; h) Photo-micrograph of sample 36 in cross-polarised light shows fine grained muscovite, sercite and quartz-rich assemblage. A sub-horizontal spaced foliation, defined by fine-grained micaceous material, overprints an earlier mica fabric with polygonal undulose quartz and biotite microlithons; i) Photograph of a hand specimen from the Pondanna member of the upper Gawler Range Volcanics (573593E, 6405524N) showing porphyritic texture with phenocrysts of quartz and feldspar within a dark, aphanitic groundmass; j) Photo-micrograph of Sample YD23a from the Pondanna member of the upper Gawler Range Volcanics (573593E, 6405524N), section shows phenocrysts of k-feldspar, quartz, and pyroxene within a fine grained matrix .

Fig. 5: Cathodoluminescence and back scatter electron images (a-d & e-j respectively of representive zircon grains from each sample analysed in this study. The region ablated during analysis is indicated; a) Z1-29a,b zircon grains from sample Z3 (Brindana Schist). Z1-29a grain has a U-Pb age 1659 ±15 Ma and an εHf value of+5.80, Z1-29b grain has a U-Pb age of 1604 ± 16 Ma and a εHf value of -6.1; b) Z3-24 zircon grain from sample Z3 (Brindana Schist). This grain has a U-Pb age of 2369 ± 28 Ma and an εHf value of-4.89; c) F6 zircon grain from sample F (Freeling Heights Quartzite). This grain has a U-Pb age of 1670 ± 10 Ma and an εHf value of +0.01; d) F9 zircon grain from sample F (Freeling Heights Quartzite). This grain has a U-Pb age of 2539 ± 28 Ma and an εHf value of +1.29; e) 36-13 zircon grain from sample 36 (Mount Adams Quartzite). This grain has a U-Pb age of 1596 ± 8 Ma and an εHf value of -1.79; f) Back scatter electron image of 36-10 zircon grain from sample 36 (Mount Adams Quartzite). This grain has a U-Pb age of 1678 ± 29 Ma and an εHf value of -1.64; g) 123-17 zircon grain from sample 123 (Freeling Heights Quartzite). This grain has a U-Pb age of 1589 ± 9 Ma; h) 123-1 zircon grain from sample 123 (Freeling Heights Quartzite). This grain has a U-Pb age of 1712 ± 8 Ma; i) YD23a-7 zircon grain from sample YD23a (uGRV). This grain has a U-Pb age of 1596.2 ± 36 Ma and an εHf value of -2.74; j) YD23a-27 zircon grain from sample YD23a (uGRV). This grain has a U-Pb age of 1597.6 ± 47 Ma and a εHf value of -4.5.

Fig. 6: a) Probability plot of detrital zircons analysed from sample Z3. Inset: weighted mean $^{207}Pb/^{206}Pb$ (2σ) age plot for the youngest population in this sample, interpreted as the maximum depositional age.; b) Concordia plot for zircons analysed from sample Z3 ;c) Probability plot of detrital zircons analysed from sample F. Inset: weighted mean $^{207}Pb/^{206}Pb$ (2σ) age plot for the maximum depositional age of this sample; c) Zircon grains from sample F plotted on a U-Pb concordia plot; d) Concordia plot for zircons analysed from sample F; e) Detrital zircon probability plot from sample 123. Inset: weighted mean age $^{207}Pb/^{206}Pb$ ages (2σ) for the maximum depositional age ; f) Concordia diagram for zircons analysed from sample 123; g) Probability plots for zircon analysed from sample 36. Inset: weighted mean $^{207}Pb/^{206}Pb$ ages (2σ) for the maximum depositional age for this sample; h) U-Pb concordia plot for zircon analysed from sample 36.

Fig. 7: Weighted mean $^{207}Pb/^{206}Pb$ ages plot for sample YD23a showing the dominant population and older inherited grains. Inset: Tera-Wasserburg concordia plot shows the concordant (<10% discordant) analyses, as well as all data >10% discordant from this sample. Data error ellipses and error bars used are 1σ.

Fig. 8: a) Plot of ε $Hf_{(t)}$ versus $^{207}Pb/^{206}Pb$ ages for the Radium Creek Group samples; b) Plot of T_{DM}^{c} versus $^{207}Pb/^{206}Pb$ ages for the Radium Creek Group samples; c) Plot of ε $Hf_{(t)}$ versus $^{207}Pb/^{206}Pb$ ages for the Radium Creek Group samples including values for ARK661 sample from Elburg et al. (2012) compared with the values for the upper Gawler Range Volcanics, uGRV from the Gawler Craton (sample YD23a), and the Frome Granite of the Bimbowrie Suite (sample FG12) and Benagerie Volcanic Suite (sample BV) from the Curnamona Province (see Fig. 1c-d for sample locations). Insert shows a plot of T_{DM}^{c} versus $^{207}Pb/^{206}Pb$ ages for these samples; d) Field for the Radium Creek Group ε $Hf_{(t)}$ values plotted as gridded density and data points for comparison. Density grid constructed using cell size of 20 Myr in the X direction and 0.5 ε Hf units in the Y direction, a threshold level of 0.05 and a smoothing level of 3.

Fig. 9: Comparison of zircon crystallisation rock type, modelled from in-situ trace chemistry after Belousova et al. (2002) to determine the source rock type of zircon grains across the Paralana Fault. Sample F (357632E 6673138N) is from the Freeling Heights Quartzite to the west (Hangingwall) of the Paralana Fault. Sample 36 (357161E, 6668472N) is from the Mount Adams Quartzite to the east (Footwall) of the Paralana Fault. The modelled source rock type is predominantly felsic and indistinguishable across the Paralana Fault.

Fig. 10: Stratigraphic and structural framework of the Mount Painter Inlier using data from this study and Armit et al. (2012). Proterozoic magmatic ages determined using U-Pb geochronology by LA-ICPMS and SHRIMP where available. Mount Neill Granite and porphyry age from Teale (1987, unpublished), Elburg et al. (2003), Neumann (2001), Neumann et al. (2009) and Fraser and Neumann (2010). Northern Gawler tectonism from Payne et al. (2008), Fanning et al. (2007), Thomas et al. (2008), Swain et al. (2005b) and Skirrow et al. (2007). Southern Gawler tectonism from Stewart and Betts (2010), Webb et al. (1986) and Parker et al. (1993). Southern Curnamona Province tectonism from Conor and Preiss (2008), Forbes et al. (2008), Betts et al. (2002), Stüwe and Ehlers (1997), Forbes and Betts (2004), Forbes et al. (2004), Stevens et al. (1988), Wilson and Powell (2001), Page et al. (2000, 2005), Rutherford et al. (2007), Marjoribanks et al. (1980) and Clarke et al. (1987, 1995). Georgetown tectonism from Black et al. (1979), Withnall et al. (1996), Hills (2004), Cihan et al. (2006), Davis (1996), Betts et al. (2009), Boger and Hansen (2004), Black and Withnall (1993), Black et al. (1998), Withnall et al. (1988), Withnall et al. (1996), Blewett et al. (1998) and Bell and Rubenach (1983). Tectonism in the Eastern Fold Belt of the Mount Isa Inlier from Betts et al. (2006), MacCready et al. (1998), Giles et al. (2006a), O'Dea et al. (2006), Page and Sun (1998), Giles and Nutman (2002), Hand and Rubatto (2002), Giles and Nutman (2003), De Jong and Williams (1995), Betts et al. (2006), Connors and Page (1995) and O'Dea et al. (1997). West Fold Belt tectonism from O'Dea and Lister (1995), O'Dea et al. (1997), Lister et al. (1999), Hand and Rubatto (2002), Connors and Page (1995), O'Dea et al. (1997), MacCready et al. (1998), Betts et al. (2006) and Blenkinsop et al. (2008). Tectonism in the Arunta Block after (Claoué-Long et al., 2008; Collins and Shaw, 1995; Collins and Williams, 1995; Maidment et al., 2005; Scrimgeour et al., 2005). Stratigraphy after Armit and Betts(2011) and references therein.

Fig. 11: a) Plot of ε $Hf_{(t)}$ versus $^{207}Pb/^{206}Pb$ ages for Archaean to Mesoproterozoic zircon populations for the major domains of the Gawler Craton from Belousova et al. (2009); Howard et al. (2009;2010;2011a;2011b); Szpunar et al. (2011), compared with the samples from the Radium Creek Group (this study); b) Field for the Gawler Craton ε $Hf_{(t)}$ values from Belousova et al. (2009); Howard et al. (2009;2010;2011a;b); Szpunar et al. (2011) plotted as gridded density and data points for comparison with the samples from the Radium Creek Group plotted as points. Density grid constructed using cell size of 20 Myr in the X direction and 0.5 ε Hf units in the Y direction, a threshold level of 0.05 and a smoothing level of 3.

Fig. 12: a) Plot of ε $Hf_{(t)}$ versus $^{207}Pb/^{206}Pb$ ages for Archaean to Mesoproterozoic zircon populations from the Arunta Block (Hollis et al. 2010) displayed as a gridded density field compared with the samples from the Radium Creek Group shown as points; b) Plot of ε $Hf_{(t)}$ versus $^{207}Pb/^{206}Pb$ ages for Archaean to Mesoproterozoic zircon populations from the Broken Hill Block of the Curnamona Province (Condie et al. 2005) displayed as a gridded density field, compared with the samples from the Radium Creek Group shown as points; c) Plot of ε $Hf_{(t)}$ versus $^{207}Pb/^{206}Pb$ ages for Archaean to Mesoproterozoic zircon populations from the Broken Hill Block of the Mount Isa Inlier (Griffin et al. 2006) displayed as a gridded density field compared with the samples from the Radium Creek Group shown as points. All U-Pb dates shown as $^{207}Pb/^{206}Pb$ ages, Hf isotope values recalculated using a decay constant of $1.865E10^{-11}$/yr. Density grids for the Radium Creek Group, Gawler Craton, Curnamona Province and Mount Isa Inlier are constructed using cell size of 20 Myrs in the X direction and 0.5 ε Hf units in the Y direction, a threshold level of 0.05 and a smoothing level of 3.

Fig 13: a) Palaeogeographical reconstruction of eastern Proterozoic Australia at ca. 1595 Ma adapted after Giles et al. (2004); Betts and Giles (2006); Betts et al. (2006;2007;2009). In this model the Radium Creek Group are deposited in an extensional back-arc basin and sourced from the Felsic large igneous province (FLIP) preserved on the Gawler Craton; b) Rapid tectonic switching to shortening ca. 1585 Ma and back to extension is driven by perturbations in the convergent margins along the southern margin of Australia; c) Renewed crustal shortening at ca. 1555 Ma is related to subduction along the eastern margin of the continent.

Table 1: Lu-Hf values for standards run to determine instrumentation precision and accuracy.

Table 2: U-Pb values for standards run during the study acquisition period and longer-term averages indicating the level of reproducibility and instrument stability obtained.

Table 3: Summary of the U-Pb dating and Hf isotope analysis.

Table 4: Zircon crystallisation rock type, modelled rock type from in-situ trace element chemistry after Belousova et al. (2002).

References

Allen, S.R., Simpson, C.J., McPhie, J., Daly, S.J., 2003. Stratigraphy, distribution and geochemistry of widespread felsic volcanic units in the Mesoproterozoic Gawler Range Volcanics, South Australia. Australian Journal of Earth Sciences 50, 97-112.

Anderson, T., 2002. Correction of common Pb in U– Pb analyses that do not report 204Pb.Chemical Geology 192, 59-79.

Andersen, T., 2005. Detrital zircons as tracers of sedimentary provenance: limiting conditions from statistics and numerical simulation. Chemical Geology 216, 249-270.

Andrews, S.J., 1998. Stratigraphy and depositional setting of the upper McNamara Group, Lawn Hills region, Northwest Queensland. Economic Geology 93, 1132 – 1152.

Armit, R.J., Betts, P.G., 2011. Proterozoic Eastern Australia Time-Space Plot, in: Beeston, J.W. (Ed.), Geological Survey of Queensland, North-West Queensland Mineral and Energy Province Report. Queensland Department of Employment, Economic Development and Innovation, Brisbane, pp. 1-123.

Armit, R.J., Betts, P.G., Schaefer, B.F., Ailleres, L., 2012. Mesoproterozoic and Palaeozoic constraints on long-lived poly-deformation in the northern Mount Painter Inlier. Gondwana Research 22, 207-226.

Barovich, K., Hand, M., 2008. Tectonic setting and provenance of the Paleoproterozoic Willyama Supergroup, Curnamona Province, Australia: Geochemical and Nd isotopic constraints on contrasting source terrain components. Precambrian Research 166, 318-337.

Bell, T.H., Rubenach, M.J., 1983. Sequential porphyroblast growth and crenulation cleavage development during progressive deformation. Tectonophysics 92, 171-194.

Belousova, E., Griffin, W., O'Reilly, S., Fisher, N., 2002. Igneous zircon: trace element composition as an indicator of source rock type. Contributions to Mineralogy and Petrology 143, 602-622.

Belousova, E.A., Preiss, W.V., Schwarz, M.P., Griffin, W.L., 2006a. Tectonic affinities of the Houghton Inlier, South Australia: U-Pb and Hf-isotope data from zircons in modern stream sediments. Australian Journal of Earth Sciences 53, 971 - 989.

Belousova, E.A., Reid, A.J., Griffin, W.L., O'Reilly, S.Y., 2006b. Proterozoic rejuvenation of the Archean Crust tracked by U-Pb and Hf-isotopes in Detrital Zircon. Geochimica et Cosmochimica Acta 70, A44-A44.

Belousova, E.A., Reid, A.J., Schwarz, M.P., Griffin, W.L., Fairclough, M.C., 2006c. Crustal evolution of the Gawler Craton, South Australia: Application of the TerraneChron technique to detrital zircon from modern stream sediments,South Australia. Department of Primary Industries and Resources, pp. 1-198.

Belousova, E.A., Reid, A.J., Griffin, W.L., O'Reilly, S.Y., 2009. Rejuvenation vs. recycling of Archean crust in the Gawler Craton, South Australia: Evidence from U-Pb and Hf isotopes in detrital zircon. Lithos 113, 570-582.

Betts, P.G., Giles, D., Lister, G.S., Fricke, L.R., 2002. Evolution of the Australian lithosphere. Australian Journal of Earth Sciences 49, 661-695.

Betts, P.G., Giles, D., 2006. The 1800-1100 Ma tectonic evolution of Australia. Precambrian Research 144, 92-125.

Betts, P.G., Giles, D., Mark, G., Lister, G.S., Goleby, B.R., Aillères, L., 2006. Synthesis of the Proterozoic evolution of the Mt Isa Inlier. Australian Journal of Earth Sciences 53, 187-211.

Betts, P.G., Giles, D., Schaefer, B.F., Mark, G., 2007. 1600-1500 Ma hotspot track in eastern Australia: Implications for Mesoproterozoic continental reconstructions. Terra Nova 19, 496-501.

Betts, P.G., Giles, D., Foden, J., Schaefer, B.F., Mark, G., Pankhurst, M.J., Forbes, C.J., Williams, H.A., Chalmers, N.C., Hills, Q., 2009. Mesoproterozoic plume-modified orogenesis in eastern Precambrian Australia. Tectonics 28.

Bizzarro, M., Baker, J.A., Haack, H., Ulfbeck, D., Rosing, M., 2003. Early history of Earth's crust–mantle system inferred from hafnium isotopes in chondrites. Nature 421, 931-933.

Black, L.P., Gulson, B.L., 1978. The age of the Mud Tank carbonatite, Strangways Range, Northern Territory. Bureau of Mineral Resources. Journal of Australian Geology and Geophysics 3, 227–232.

Black, L.P., Bell, T.H., Rubenach, M.J., Withnall, I.W., 1979. Geochronology of discrete structural-metamorphic events in a multiply deformed precambrian terrain. Tectonophysics 54, 103-137.

Black, P.M., Gregory, P., Withnall, I.W., Bain, J.H.C., 1998. U-Pb zircon age for the Etheridge Group, Georgetown region, north Queensland: implications for relationship with Broken Hill and Mt Isa sequences. Australian Journal of Earth Sciences 45, 925-935.

Blenkinsop, T.G., Huddlestone-Holmes, C.R., Foster, D.R.W., Edmiston, M.A., Lepong, P., Mark, G., Austin, J.R., Murphy, F.C., Ford, A., Rubenach, M.J., 2008. The crustal scale architecture of the Eastern Succession, Mount Isa: The influence of inversion. Precambrian Research 163, 31-49.

Blewett, R.S., Black, L.P., Sun, S.S., Knutson, J., Hutton, L.J., Bain, J.H.C., 1998. U-Pb zircon and Sm-Nd geochronology of the Mesoproterozoic of Northern Queensland: implications for a Rodinian Connection with the Belt supergroup of North America. Precambrian Research 89, 101-127.

Blichert-Toft, J., Albarede, F., 1997. The Lu–Hf isotope geochemistry of chondrites and the evolution of the mantle–crust system. Earth and Planetary Science Letters 148, 243-258.

Blichert-Toft, J., Chauvel, C., Albarède, F., 1997. Separation of Hf and Lu for high-precision isotope analysis of rock samples by magnetic sector-multiple collector ICP-MS. Contributions to Mineralogy and Petrology 127, 248-260.

Blissett, A.H., Creaser, R.A., Daly, S.J., Flint, R.B., Parker, A.J., 1993. Gawler Range Volcanics, in: Drexal, J.F., Preiss, W.V., Parker, A.J. (Eds.), The Geology of South Australia, Volume 1: The Precambrian. Geological Survey of South Australia Bulletin, pp. 107-124.

Boger, S.D., Hansen, D., 2004. Metamorphic evolution of the Georgetown Inlier, northeast Queensland, Australia; evidence for an accreted Palaeoproterozoic terrane? Journal of Metamorphic Geology 22, 511-527.

Cawood, P.A., Nemchin, A.A., Leverenz, A., Saeed, A., Balance, P.F., 1999. U/Pb dating of detrital zircons: Implications for the provenance record of Gondwana margin terranes. Geological Society of America Bulletin 111, 1107-1119.

Cawood, P.A., Korsch, R.J., 2008. Assembling Australia: Proterozoic building of a continent. Precambrian Research 166, 1-35.

Cihan, M., Evins, P., Lisowiec, N., Blake, K., 2006. Time constraints on deformation and metamorphism from EPMA dating of monazite in the Proterozoic Robertson River Metamorphics, NE Australia. Precambrian Research 145, 1-23.

Claoué-Long, J., Maidment, D., Hussey, K., Huston, D., 2008. The duration of the Strangways Event in central Australia: Evidence for prolonged deep crust processes. Precambrian Research 166, 246-262.

Coats, R.P., Blissett, A.H., 1971. Regional and economic geology of the Mount Painter province.South Australian Geological Survey Bulletin 43.

Clarke, G.L., Guiraud, M., Powell, R., Burg, J.P., 1987. Metamorphism in the Olary Block, South Australia: compression with cooling in a Proterozoic fold belt. Journal of Metamorphic Geology 5, 291–306.

Clarke, G.L., Powell, R., Vernon, R.H., 1995. Reaction relationships during retrograde metamorphism at Olary, South Australia. J. Metam. Geol 13, 715–726.

Collins, W.J., Shaw, R.D., 1995. Geochronological constraints on orogenic events in the Arunta Inlier: a review. Precambrian Research 71, 315-346.

Collins, W.J., Williams, I.S., 1995. SHRIMP ionprobe dating of short-lived Proterozoic tectonic cycles in the northern Arunta Inlier, central Australia. Precambrian Research 71, 69-89.

Condie, K.C., Beyer, E., Belousova, E., Griffin, W.L., O'Reilly, S.Y., 2005. U-Pb isotopic ages and Hf isotopic composition of single zircons: The search for juvenile Precambrian continental crust. Precambrian Research 139, 42-100.

Conor, C.H.H., Preiss, W.V., 2008. Understanding the 1720-1640 Ma Palaeoproterozoic Willyama Supergroup, Curnamona Province, Southeastern Australia: Implications for tectonics, basin evolution and ore genesis. Precambrian Research 166, 297-317.

Cooper, 1985. Inherited zircons in the Mundi Mundi Granite, Broken Hill, New South Wales. Australian Journal of Earth Sciences 32, 467-470.

Cowley, W.M., Fanning, C.M., 1992. Low-grade Archaean Metavolcanics in the northern Gawler Craton. The geological survey of south Australia. Q. Geol. 119, 2-17.

Cutts, K., Hand, M., Kelsey, D.E., 2011. Evidence for early Mesoproterozoic (ca. 1590Ma) ultrahigh-temperature metamorphism in southern Australia. Lithos 124, 1-16.

Daly, S.J., Fanning, C.M., Fairclough, M.C., 1998. Tectonic evolution and exploration potential of the Gawler Craton, South Australia. AGSO Journal of Australian Geology & Geophysics 17, 145-168.

Davis, B.K., 1996. Biotite porphyroblast nucleation and growth: Control by microfracture of pre-existing foliations in schists in the Robertson River Metamorphics. Geol. Mag. 133, 91 – 102.

De Jong, G., Williams, P.J., 1995. Giant metasomatic system formed during exhumation of mid-crustal Proterozoic rocks in the vicinity of the Cloncurry Fault, northwest Queensland. . Australian Journal of Earth Sciences 42, 281 – 290.

Drexel, J.F., Preiss, W., Parker, A., Australia, G.S.o.S., Meridional, A., 1995. The Geology of South Australia. Department of Mines and Energy.

Elburg, M.A., Bons, P.D., Dougherty-Page, J., Janka, C.E., Neumann, N., Schaefer, B., 2001. Age and metasomatic alteration of the Mt Neil Granite at Nooldoonooldoona waterhole, Mt Painter Inlier, South Australia. Australian Journal of Earth Sciences 48, 721-730.

Elburg, M.A., Bons, P.D., Foden, J., Brugger, J., 2003. A newly defined Late Ordovician magmatic-thermal event in the Mt Painter Province, northern Flinders Ranges, South Australia. Australian Journal of Earth Sciences 50, 611-631.

Elburg, M.A., Andersen, T., Bons, P.D., Weisheit, A., Simonsen, S.L., Smet, I., 2012. Metasomatism and metallogeny of A-type granites of the Mt Painter-Mt Babbage Inliers, South Australia. Lithos 151, 83-104.

Fairclough, M.C., Schwarz, M.P., Ferris, G.M., 2003. Interpreted crystalline basement geology of the Gawler Craton. South Australia Geological Survey: Special Map, 1:1000000.

Fanning, C.M., Flint, R.B., Parker, A.J., Ludwig, K.R., Blissett, A.H., 1988. Refined Proterozoic evolution of the Gawler Craton, South Australia, through U-Pb zircon geochronology. Precambrian Research 40-41, 363-386.

Fanning, C.M., 1997. Geochronological synthesis of Southern Australia. , Part II. The Gawler Craton. . South Australia Department of Mines and Energy.

Fanning, C.M., Ashley, P.M., Cook, M.D.J., Teale, G., Conor, C.H.H., 1998. A geochronological perspective of crustal evolution in the Curnamona Province, in: Gibson, G.M. (Ed.), Broken Hill Exploration Initiative: Abstracts of Papers Presented at the 4th Annual Meeting in Broken Hill. Australian Geological Survey Organisation, pp. 30–35.

Fanning, C.M., Reid, A.J., Teale, G.S., 2007 A geochronological framework for the Gawler Craton, South Australia. S. Aust. Geol. Survey Bull 55.

Forbes, C.J., Betts, P.G., 2004. Development of type 2 fold interference patterns in the Broken Hill Block: implications for strain partitioning across a detachment during the Olarian Orogeny. Australian Journal of Earth Sciences 51, 173-188.

Forbes, C.J., Giles, D., Jourdan, F., Sato, K., Omori, S., Bunch, M., 2012. Cooling and exhumation history of the northeastern Gawler Craton, South Australia. Precambrian Research 200-203, 209-238.

Fraser, G.L., Neumann, N.L., 2010. New SHRIMP U-Pb zircon ages from the Gawler Craton and Curnamona Province, South Australia, 2008 – 2010. Geoscience Australia.

Fraser, G., McAvaney, S., Neumann, N., Szpunar, M., Reid, A., 2010. Discovery of early Mesoarchean crust in the eastern Gawler Craton, South Australia. Precambrian Research 179, 1-21.

Gibson, G.M., Rubenach, M.J., Neumann, N.L., Southgate, P.N., Hutton, L.J., 2008. Syn- and post-extensional tectonic activity in the Palaeoproterozoic sequences of Broken Hill and Mount Isa and its bearing on reconstructions of Rodinia. Precambrian Research 166, 350-369.

Giles, D., Nutman, A.P., 2002. SHRIMP U-Pb monazite dating of 1600-1580 Ma amphibolite facies metamorphism in the southeastern Mt Isa Block, Australia. Australian Journal of Earth Sciences 49, 455-465.

Giles, D., Nutman, A.P., 2003. SHRIMP U-Pb zircon dating of the host rocks of the Cannington Ag-Pb-Zn deposit, southeastern Mt Isa Block, Australia. Australian Journal of Earth Sciences 50, 295-309.

Giles, D., Betts, P.G., Lister, G.S., 2004. 1.8-1.5-Ga links between the North and South Australian Cratons and the Early-Middle Proterozoic configuration of Australia. Tectonophysics 380, 27-41.

Giles, D., Ailleres, L., Jeffries, D., Betts, P., Lister, G., 2006a. Crustal architecture of basin inversion during the Proterozoic Isan Orogeny, Eastern Mount Isa Inlier, Australia. Precambrian Research 148, 67-84.

Giles, D., Betts, P.G., Ailleres, L., Hulscher, B., Hough, M., Lister, G.S., 2006b. Evolution of the Isan Orogeny at the southeastern margin of the Mt Isa Inlier. Australian Journal of Earth Sciences 53, 91-108.

Griffin, W.L., Wang, X., Jackson, S.E., Pearson, N.J., O’Reilly, S.Y., Xu, X., Zhou, X., 2002. Zircon chemistry and magma mixing, SE China: In-situ analysis of Hf isotopes, Tonglu and Pingtan igneous complexes. Lithos 61, 237-269.

Griffin, W.L., Belousova, E.A., Shee, S.R., Pearson, N.J., O'Reilly, S.Y., 2004. Archean crustal evolution in the northern Yilgarn Craton: U-Pb and Hf-isotope evidence from detrital zircons. Precambrian Research 131, 231-282.

Griffin, W.L., Belousova, E.A., Walters, S.G., O'Reilly, S.Y., 2006. Archaean and Proterozoic crustal evolution in the Eastern Succession of the Mt Isa district, Australia: U-Pb and Hf-isotope studies of detrital zircons. Australian Journal of Earth Sciences 53, 125-149.

Gum, J., Belousova, E., 2006. Musgrave province reconnaissance using TerraneChron. ASEG Extended Abstracts 1, 1-7.

Gutscher, M.-A., Malod, J., Rehault, J.-P., Contrucci, I., Klingelhoefer, F., Mendes-Victor, L., Spakman, W., 2002. Evidence for active subduction beneath Gibraltar. Geology 30, 1071-1074.

Halilovic, J., Cawood, P.A., Jones, J.A., Pirajno, F., Nemchin, A.A., 2004. Provenance of the Earaheedy Basin: implications for assembly of the Western Australian Craton. Precambrian Research 128, 343-366.

Hand, M., Rubatto, D., 2002. The scale of the thermal problem in the Mount Isa Inlier. Geol. Soc. Aust. Abst. 67.

Hand, M., Reid, A., Jagodzinski, L., 2007. Tectonic Framework and Evolution of the Gawler Craton, Southern Australia. Economic Geology 102, 1377-1395.

Hills, Q.G., 2004. The tectonic evolution of the Georgetown Inlier., School of Geosciences. Monash University, Melbounre.

Hollis, J.A., Beyer, E.E., Whelan, J.A., Kemp, A.I.S., Scherstén, A., Greig, A., 2010. Summary of results. NTGS laser U-Pb and Hf geochronology project: Pine Creek Orogen, Murphy Inlier, McArthur Basin and Arunta Region, July 2007–June 2008. . Northern Territory Geological Survey, Record 2010-001.

Howard, K.E., Hand, M., Barovich, K.M., Belousova, E., 2011a. Provenance of late paleoproterozoic cover sequences in the central Gawler Craton: Exploring stratigraphic correlations in eastern proterozoic Australia using detrital zircon ages, Hf and Nd isotopic data. Australian Journal of Earth Sciences 58, 475-500.

Howard, K.E., Hand, M., Barovich, K.M., Payne, J.L., Belousova, E.A., 2011b. U-Pb, Lu-Hf and Sm-Nd isotopic constraints on provenance and depositional timing of metasedimentary rocks in the western Gawler Craton: Implications for Proterozoic reconstruction models. Precambrian Research In Press, Corrected Proof, 43-62.

Howard, K.E., Hand, M., Barovich, K.M., Payne, J.L., Cutts, K.A., Belousova, E.A., 2011c. U–Pb zircon, zircon Hf and whole-rock Sm–Nd isotopic constraints on the evolution of Paleoproterozoic rocks in the northern Gawler Craton. Australian Journal of Earth Sciences 58, 615-638.

Jackson, M.J., Scott, D.L., Rawlings, D.J., 2000. Stratigraphic framework for the Leichhardt and Calvert Superbasins: review and correlations of the pre-1700 Ma successions between Mt Isa and McArthur River. Australian Journal of Earth Sciences 47, 381-403.

Jackson, S.E., Pearson, N.J., Griffin, W.L., Belousva, E.A., 2004. The application of laser ablation-inductively coupled plasma-mass spectrometry to in situ U-Pb zircon geochronology. Chemical Geology 211, 47-69.

Jagodzinski, E.A., Fricke, C.E., 2010. Compilation of new SHRIMP U-Pb geochronological data for the southern Curnamona Province, South Australia 2010., Report Book 2010/00014. Department of Primary Industries and Resources.

Kirkland, C.L., Smithies, R.H., Woodhouse, A.J., Howard, H.M., Wingate, M.l.T.D., Belousova, E.A., Cliff, J.B., Murphy, R.C., Spaggiari, C.V., In Press. Constraints and deception in the isotopic record; the crustal evolution of the west Musgrave Province, central Australia. Gondwana Research.

Korsch, R.J., Kositcin, N., 2010. South Australian Seismic and MT Workshop 2010/10. Geoscience Australia Record, 2010/10.

Korsch, R.J., Preiss, W., Blewett, R., Fabris, A., Neumann, N., Fricke, C.E., Fraser, G.L., Holzschuh, J., Jones, L.E.A., 2009. The 2008 north-south oriented, deep seismic reflection transect across the Curnamona Province, South Australia. Broken Hill Exploration Initiative: Abstracts for the 2009 Conference. 2009/28, 90-100.

Korsch, R.J., Preiss, W.V., Blewett, R.S., Fabris, A.J., Neumann, N.L., Fricke, C.E., Fraser, G.L., Holzschuh, J., Milligan, P.R., Jones, L.E.A., 2010. Geological interpretation of deep seismic reflection and magnetotelluric line 08GA-C1: Curnamona Province, South Australia. Geoscience Australia, Record. 2010 10, 42-53.

Krassay, A.A., Bradshaw, B.E., Domagala, J., Jackson, M.J., 2000. Siliciclastic shoreline to growth-faulted turbiditic sub-basins: the Proterozoic River Supersequence of the upper McNamara Group on the Lawn Hill Platform, Northern Australia. Australian Journal of Earth Sciences 47, 533 – 562.

Kromkhun, K., Foden, J., Hore, S., Baines, G., 2013. Geochronology and Hf isotopes of the bimodal mafic-felsic high heat producing igneous suite from Mt Painter Province, South Australia. Gondwana Research.

Lister, G.S., O'Dea, M.G., Somaia, I., 1999. A tale of two synclines: rifting, inversion and transpressional popouts at Lake Julius, northwestern Mt Isa terrane, Queensland. Australian Journal of Earth Sciences 46, 233-250.

MacCready, T., Goleby, B.R., Goncharov, A., Drummond, B.J., Lister, G.S., 1998. A Framework of Overprinting Orogens Based on Interpretation of the Mount Isa Deep Seismic Transect. Economic Geology 93, 1422-1434.

Maidment, D.W., Hand, M., Williams, I.S., 2005. Tectonic cycles in the Strangways Metamorphic Complex, Arunta Inlier, central Australia: Geochronological evidence for exhumation and basin formation between two high-grade metamorphic events. Australian Journal of Earth Sciences 52, 205-215.

Marjoribanks, R.W., Rutland, R.W.R., Glen, R.A., Laing, W.P., 1980. The Structure and Tectonic Evolution of the Broken-Hill Region, Australia. Precambrian Research 13, 209-240.

McLaren, S., Dunlap, W.J., Sandiford, M., McDougall, I., 2002. Thermochronology of high heat-producing crust at Mount Painter, South Australia: Implications for tectonic reactivation of continental interiors. Tectonics 21.

McLaren, S., Sandiford, M., Powell, R., Neumann, N., Woodhead, J., 2006. Palaeozoic Intraplate Crustal Anatexis in the Mount Painter Province, South Australia: Timing, Thermal Budgets and the Role of Crustal Heat Production. Journal of Petrology 47, 2281-2302.

Nelson, D.R., 2001. An assessment of the determination of depositional ages for Precambrian clastic sedimentary rocks by U-Pb dating of detrital zircons. Sedimentary Geology 141-142, 37-60.

Neumann, N., 2001. Geochemical and isotopic characteristics of South Australian Proterozoic granites: implications for the origin and evolution of high heat-producing terrains., Department of Geology and Geophysics. University of Adelaide., Adelaide.

Neumann, N., Hore, S., Fraser, G., 2009. New SHRIMP geochronology from the Mount Painter Province, South Australia, in: Korsch, R.J. (Ed.), Broken Hill Exploration Initiative: Abstracts for the 2009 Conference. Geoscience Australia.

Nowell, G.M., et al., 1998. High precision Hf isotope measurements of MORB and OIB by thermal ionisation mass spectrometry: insights into thed epleted mantle. Chemical Geology 149, 211-233.

O'Dea, M.G., Lister, G.S., 1995. The role of ductility contrast and basement architecture in the structural evolution of the Crystal Creek block, Mount Isa Inlier, NW Queensland, Australia. Journal of Structural Geology 17, 949-960.

O'Dea, M.G., Lister, G.S., Betts, P.G., Pound, K.S., 1997. A shortened intraplate rift system in the Proterozoic Mount Isa terrane, NW Queensland, Australia. Tectonics 16, 425-441.

O'Dea, M.G., Betts, P.G., MacCready, T., Aillères, L., 2006. Sequential development of a mid-crustal fold-thrust complex: evidence from the Mitakoodi Culmination the eastern Mt Isa Inlier, Australia. Australian Journal of Earth Sciences 53, 69-90.

Ogilvie, J., 2006. U-Pb detrital zircon dating of structural and stratigraphic relationships within Hidden Valley, Mount Painter Inlier: Implications for Proterozoic crustal evolution of Eastern Australia., Geosciences. Monash University p. 40.

Page, R., 1983. Timing of superposed volcanism in the Proterozoic Mount Isa inlier, Australia. Precambrian Research 21, 223-245.

Page, R.W., Sun, S.S., 1998. Aspects of geochronology and crustal evolution in the Eastern Fold Belt, Mt Isa Inlier. Australian Journal of Earth Sciences 45, 343–361.

Page, R.W., Jackson, M.J., Krassay, A.A., 2000. Constraining sequence stratigraphy in north Australian basins: SHRIMP U-Pb zircon geochronology between Mt Isa and McArthur River. Australian Journal of Earth Sciences 47, 431-459.

Page, R.W., Conor, C.H.H., Stevens, B.P.J., Gibson, G.M., Preiss, W.V., Southgate, P.N., 2005. Correlation of Olary and Broken Hill Domains, Curnamona Province; possible relationship to Mount Isa and other north Australiam Pb-Zn-Ag-bearing successions. Economic Geology and the Bulletin of the society of Economic geologists 100, 663-676.

Pankhurst, M.J., Schaefer, B.F., Betts, P.G., Phillips, N., Hand, M., 2011a. A Mesoproterozoic continental flood rhyolite province, the Gawler Ranges, Australia: The end member example of the Large Igneous Province clan. Solid Earth 2, 25-33.

Pankhurst, M.J., Schaefer, B.F., and Betts, P.G. 2011b. Geodynamics of rapid voluminous felsic magmatism through time. Lithos 123 92-101.Pankhurst, M.J., Schaefer, B.F., Turner, S.P., Argles, T., Wade, C.E., 2013. The source of A-type magmas in two contrasting settings: U–Pb, Lu–Hf and Re–Os isotopic constraints. Chemical Geology 315, 175-194.

Parker, A.J., Preiss, W.V., Rankin, L.R., 1993. Geological Framework, in: Drexal, J.F., Preiss, W.V., Parker, A.J. (Eds.), The geology of South Australia, Volume 1: The Precambrian. Geological Survey of South Australia Bulletin, pp. 9-23.

Paul, E., 1998. Geometry and controls on basement-involved deformation in the Adelaide Fold Belt, South Australia. PhD Thesis, Adelaide University.

Paul, E., Flottmann, T., Sandiford, M., 1999. Structural geometry and controls on basement-involved deformation in the northern Flinders Ranges, Adelaide Fold Belt, South Australia. Australian Journal of Earth Sciences 46, 343-354.

Payne, J.L., Barovich, K.M., Hand, M., 2006. Provenance of metasedimentary rocks in the northern Gawler Craton, Australia: Implications for Palaeoproterozoic reconstructions. Precambrian Research 148, 275-291.

Payne, J.L., Hand, M., Barovich, K.M., Wade, B.P., 2008. Temporal constraints on the timing of high-grade metamorphism in the northern Gawler Craton: implications for assembly of the Australian Proterozoic. Australian Journal of Earth Sciences 55, 623 - 640.

Payne, J.L., Ferris, G., Barovich, K., Hand, M., 2010. Pitfalls of classifying ancient magmatic suites with tectonic discrimination diagrams: An example from the Paleoproterozoic Tunkillia Suite, southern Australia. Precambrian Research 177, 227-240.

Preiss, W., Korsch, R.J., Blewett, R.S., Fomin, T., Cowley, W.M., Neumann, N.L., Meixer, A.J., 2010. Geological interpretation of deep seismic reflection line 09GA-CG1: the Curnamona Province-Gawler Craton Link Line, South Australia, Geoscience Australia, Record. 10, 66-76.

Rawlings, D.J., 1999. Stratigraphic resolution of a multiphase intracratonic basin system: the McArthur Basin, northern Australia. Australian Journal of Earth Sciences 46, 703-723.

Reid, A., Hand, M., Jagodzinski, E., Kelsey, D., Pearson, N., 2008. Paleoproterozoic orogenesis in the southeastern Gawler Craton, South Australia. Australian Journal of Earth Sciences 55, 449 - 471.

Rutherford, L., Hand, M., Barovich, K., 2007. Timing of Proterozoic metamorphism in the southern Curnamona Province: implications for tectonic models and continental reconstructions. Australian Journal of Earth Sciences 54, 65-81.

Schaefer, B.F., 1993. Isotopic and geochemical constraints on Proterozoic crustal growth from the Mount Painter Inlier. Adelaide University Honours Thesis.

Schaefer, B.F., 1998. Insights into Proterozoic tectonics evolution from the Southern Eyre Peninsula, South Australia. University of Adelaide.

Scherer, E., Munker, C., Mezger, K., 2001 Calibration of the lutetium–hafnium clock. Science 293, 683–687.

Scrimgeour, I.R., Kinny, P.D., Close, D.F., Edgoose, C.J., 2005. High-T granulites and polymetamorphism in the southern Arunta Region, central Australia: Evidence for a 1.64 Ga accretional event. Precambrian Research 142, 1-27.

Shafton, R.A., 2006. A metamorphic and geochemical analysis of the Hidden Valley Region, Mount Painter Inlier, South Australia: implications for stratigraphy and orogenic evolution. School of Geosciences. Monash University, Melbourne.

Skirrow, R.G., Bastrakov, E., Barovich, K., Fraser, G.L., Creaser, R.A., Fanning, C.M., Raymond, O.L., Davidson, G.J., 2007. Timing of iron oxide Cu–Au–(U) hydrothermal activity and Nd isotope constraints on metal sources in the Gawler Craton, South Australia. Economic Geology 102, 1441-1470

Soderlund, U., Patchett, J.P., Vervoort, J.D., Isachsen, C.E., 2004. The Lu-176 decay constant determined by Lu–Hf and U–Pb isotope systematics of Precambrian mafic intrusions. Earth and Planetary Science Letters 219, 311-324.

Stevens, B.P.J., Burton, G.R., 1998. The early to late Proterozoic Broken Hill Province, New South Wales. Journal of Australian Geology and Geophysics 17, 75-86.

Stewart, J.R., Betts, P.G., 2010. Late Paleo-Mesoproterozoic plate margin deformation in the southern Gawler Craton: Insights from structural and aeromagnetic analysis. Precambrian Research 177, 55-72.

Stewart, K., Foden, J., 2001. Mesoproterozoic granites of South Australia. Department of Geology & Geophysics, University of Adelaide, Adelaide.

Swain, G., Woodhouse, A., Hand, M., Barovich, K., Schwarz, M., Fanning, C.M., 2005a. Provenance and tectonic development of the late Archaean Gawler Craton, Australia; U-Pb zircon, geochemical and Sm-Nd isotopic implications. Precambrian Research 141, 106-136.

Swain, G.M., Hand, M., Teasdale, J., Rutherford, L., Clark, C., 2005b. Age constraints on terrane-scale shear zones in the Gawler Craton, southern Australia. Precambrian Research 139, 164-180.

Swain, G., Barovich, K., Hand, M., Ferris, G., Schwarz, M., 2008. Petrogenesis of the St Peter Suite, southern Australia: Arc magmatism and Proterozoic crustal growth of the South Australian Craton. Precambrian Research 166, 283-296.

Szpunar, M., Hand, M., Barovich, K., Jagodzinski, E., Belousova, E., 2011. Isotopic and geochemical constraints on the Paleoproterozoic Hutchison Group, southern Australia: Implications for Paleoproterozoic continental reconstructions. Precambrian Research 187, 99-126.

Teale, G.S., Flint, R.B., 1993. Curnamona Craton and Mount Painter Province, in: Drexal, J.F., Preiss, W.V., Parker, A.J. (Eds.), The geology of South Australia, Volume 1; The Precambrian. Geological Survey of South Australia Bulletin, pp. 147-149.

Teale, G.S., 1993. Geology of the Mount Painter and Mount Babbage Inliers, in: Drexal, J.F., Preiss, W.V., Parker, A.J. (Eds.), The geology of South Australia, Volume 1; the Precambrian. Geological Survey of South Australia Bulletin, pp. 149-156.

Teasdale, J., 1993. Proterozoic tectonic models with application to the Mount Painter Inlier. Adelaide University Honours Thesis.

Thomas, J.L., Direen, N.G., Hand, M., 2008. Blind orogen: Integrated appraisal of multiple episodes of Mesoproterozoic deformation and reworking in the Fowler Domain, western Gawler Craton, Australia. Precambrian Research 166, 263-282.

Van Archerbergh, E., Ryan, C.G., Griffin, W.L., 1999. GLITTER: on-line interactive data reduction for the laser ablation ICP –MS microprobe. In: Proceedings of the 9th V. M. Goldschmidt Conference, 305.

Wade, B.P., Barovich, K.M., Hand, M., Scrimgeour, I.R., Close, D.F., 2006. Evidence for Early Mesoproterozoic Arc Magmatism in the Musgrave Block, Central Australia: Implications for Proterozoic Crustal Growth and Tectonic Reconstructions of Australia. The Journal of Geology 114, 43-63.

Wade, C.E., 2011. Definition of the Mesoproterozoic Ninnerie Supersuite, Curnamona Province, South Australia. MESA Journal 62, 35-52.

Wade, C.E., Reid, A.J., Wingate, M.T.D., Jagodzinski, E.A., Barovich, K., 2012. Geochemistry and geochronology of the c. 1585 Ma Benagerie Volcanic Suite, southern Australia: Relationship to the

Gawler Range Volcanics and implications for the petrogenesis of a Mesoproterozoic silicic large igneous province. Precambrian Research 206–207, 17-35.
Webb, A.W., Thomson, B.P., Blissett, A.H., Daly, S.J., Flint, R.B., Parker, A.J., 1986. Geochronology of the Gawler Craton, South Australia. Australian Journal of Earth Sciences: 33, 119 - 143.
Wiedenbeck, M., Allé, P., Corfu, F., Griffin, W.L., Meier, M., Oberli, F., Von Quadt, A., Roddick, J.C., Spiegel, W., 1995. Three natural zircon standards for U–Th–Pb, Lu–Hf, trace element and REE analyses. Geostandards Newsletter 19, 1–23.
Wilson, C.J.L., Powell, R., 2001. Strain localisation and high-grade metamorphism at Broken Hill, Australia: a view from the Southern Cross area. Tectonophysics 335, 193-210.
Withnall, I.W., Bain, J.H.C., Draper, J.J., MacKenzie, D.E., Oversby, B.S., 1988. Proterozoic stratigraphy and tectonic history of the Georgetown Inlier, northeastern Queensland. Precambrian Research 40-41, 429-446.
Withnall, I.W., Golding, S.D., Rees, I.D., Dobos, S.K., 1996. K-Ar dating of the Anakie Metamorphic Group: evidence for an extension of the Delamerian Orogeny into central Queensland. Australian Journal of Earth Sciences 43, 567-572.
Withnall, I.W., MacKenzie, D.E., Denaro, T.J., Bain, J.H.C., Oversby, B.S., Knutson, J., Donchak, P.J.T., Champion, D.C., Wellman, P., Cruikshank, B.I., Sun, S.S., Pain, C.F., 1997. Georgetown Region, in: Bain, J.H.C., Draper, J.J. (Eds.), North Queensland Geology. Australian Geological Survey Organisation Bulletin/Queensland Department of Mines and Energy Qld pp. 19-116.
Wulser, P.A., 2009. Uranium metallogeny in the North Flinders Ranges region of South Australia School of Earth and Environmental Sciences. University of Adelaide, Adelaide, p. 179.
Zhao, J.-X., 1994. Geochemical and Sm-Nd isotopic study of amphibolites in the southern Arunta Inlier, central Australia: evidence for subduction at a Proterozoic continental margin. Precambrian Research 65, 71-94.
Zhao, J.X., Bennett, V.C., 1995. SHRIMP U-Pb zircon geochronology of granites in the Arunta Inlier, central Australia: implications for Proterozoic crustal evolution. Precambrian Research 71, 17-43.
Zhao, J.-X., McCulloch, M.T., 1995. Geochemical and Nd isotopic systematics of granites from the Arunta Inlier, central Australia: implications for Proterozoic crustal evolution. Precambrian Research 71, 265-299.

Provenance of the Early Mesoproterozoic Radium Creek Group in the Northern Mount Painter Inlier: Correlating isotopic signatures to inform tectonic reconstructions.

R.J. Armit[1,*], P.J. Betts[1], B.F. Schaefer[2], M.J. Pankhurst[3], D. Giles[4]

[1]School of Geosciences, Monash University, Clayton, VIC 3800, Australia

[2]GEMOC, Department of Earth and Planetary Sciences, Macquarie University, NSW 2109, Australia

[3]School of Earth and Environment, University of Leeds, Leeds, LS2 9JT, United Kingdom

[4]School of Earth and Environmental Sciences, University of Adelaide, SA 5005, Australia

*Corresponding Author: robin.armit@monash.edu

New in-situ zircon LA-ICPMS geochronologic and Hf-isotope data from the Radium Creek Group within the Mount Painter Inlier provide important temporal constraints on the Early Mesoproterozoic palaeogeography of eastern Proterozoic Australia. The entire Radium Creek Group was deposited in a single basin forming phase, and has a maximum depositional age of 1595 ± 3.7 Ma. Detrital zircon from these metasedimentary rocks have U-Pb age populations at ca. 1595 Ma, ~~1650~~1660-1680 Ma, 1710-~~1760~~1780 Ma, ca. 1850 Ma and ca. 2500 Ma. These grains are characterised by isotopically diverse and evolved sources, and have crystallised within predominantly felsic igneous host-rocks. The relative age spectra and isotopic character has more similarity with the Gawler Craton than the Arunta Block, Curnamona Province or the Mount Isa Inlier. These observations suggest that the Mount Painter Province was adjacent to the Gawler Craton in the Early Mesoproterozoic~~, and can therefore be interpreted as a marginal terrane of the Gawler Craton. ~~. Our data supports a coherent South Australian Craton at ca. 1595 Ma and a contiguous continental mass that included the North and South Australian cratons. The Mount Painter Inlier occupied a complex plate tectonic setting in the overriding plate of two convergent margins.

Keywords: Radium Creek Group, Mount Painter Inlier, U-Pb maximum depositional ages, Hf isotopes, isotopic fingerprinting, ~~Gawler Craton~~Palaeogeographical reconstructions

1. Introduction

~~Geochronology coupled with isotopic fingerprinting of ancient rock packages is a powerful tool for constraining reconstructions of Proterozoic terranes. This is because information can be resolved in greater detail than other methods traditionally used for palaeogeographic reconstructions (e.g. Cawood et al. 1999; Halilovic et al. 2004; Nelson, 2001). This allows us to reconstruct links between~~

~~cratonic elements with greater confidence, which improves our global reconstructions of ancient supercontinents.~~

Tectonic reconstruction models of Proterozoic Australia have been enthusiastically debated in the literature (c.f. Betts and Giles, 2006; Gibson et al., 2008; Giles et al., 2004; Korsch et al., 2009; Swain et al., 2008; Wade et al., 2006). This is because understanding the Proterozoic record of Australia underpins ~~our~~the knowledge of how this continent has evolved~~ for the majority of its existence, and~~, which informs ~~our~~the view of global tectonics through time. ~~Central to most of these various Proterozoic Australia models is the important link between the South Australian Craton and the Northern Australian Craton, particularly at the nexus between the Palaeo- and Mesoproterozoic.~~

~~Current geologic/tectonic understanding of~~ Proterozoic Australia can be considered following the ~~Palaeo-~~geography-based nomenclature of Myer et al. (1996) in which the continent is divided into three major cratonic units, called the North, West and South Australian cratons (Fig. 1a). The South Australian Craton comprises the Gawler Craton and the Curnamona Province (Fig.1b-c). The South Australian Craton has a shared history with the North Australian Craton between ca. 1800 and 1550 Ma, suggesting that were contiguous during this interval. The South Australian Craton likely separated from the North Australian Craton during the Mesoproterozoic to form a discrete cratonic element (Giles et al., 2004). Consequently, the link between the South Australian Craton and the Northern Australian Craton, particularly at the boundary between the Palaeoproterozoic and Mesoproterozoic times is significant for determining the evolution of the Australian continent at this time.

Giles et al. ~~eastern Australia suggests it~~(2004) interpreted a configuration of the Palaeoproterozoic Australia where the South Australian Craton was ~~positioned in a complex palaeogeographic environment. It was~~ rotated 52^0 counter clockwise around an Euler pole in the North Australian Craton. This configuration aligned contemporaneous orogenic belts across the Gawler Craton, Arunta Inlier, Mount Isa Inlier and the Curnamona Province (Fig. 2a). Using the configuration of Giles et al. (2004), Betts and Giles (2006) suggested that between ca. 1700 and 1500 Ma, the contiguous North and South Australia cratons (Fig 2a) were situated adjacent to, and were affected by, two convergent margins~~ (Betts and Giles, 2006), which had a~~. A plume-related continental hotspot track was also superimposed upon ~~them~~these cratons (Betts et al., 2007; 2009). ~~This complex geodynamic setting has contributed to difficulties in reconciling the palaeogeography of Mesoproterozoic eastern Australia.~~ In this model, the southern margin of the Australian continent evolved in the overriding plate of a north-dipping subduction, and the eastern margin of the continent sequentially evolved from a passive margin, to a convergent margin with west-dipping subduction.

Wade et al. (2006) presented ~~a~~an alternative model in which the South Australian Craton collided with the North Australian Craton between ca. 1590 Ma and 1560 Ma~~,~~ (Fig. 2b), chiefly supported by the identification of the ca. 1590 Ma continental-arc affinity rocks in the Musgrave Block~~.~~ of central Australia. In this model the continental arc rocks formed above a south-dipping subduction zone and the Gawler Craton evolved in a continental back-arc basin. Gibson et al. (2008) proposed a model whereby eastern Proterozoic Australia evolved between ca. 1730 and 1640 Ma ~~within one~~by a series of large intra-continental ~~back-arc~~ rift ~~system~~systems along the margins of the South Australian and North Australian cratons. This system was subsequently inverted between ca. 1640~~-~~ and 1600 Ma during accretion of the Georgetown-Mojave Block. ~~A rotational model was presented by~~ These latter models consider~~Giles et al. (2004) whereby~~ the ~~Gawler Craton is rotated 52° clockwise, based on~~present-day distribution of Australia Palaeoproterozoic terranes to be representative of their distribution at the ~~alignment of orogenic belts correlated across the Gawler Craton, Arunta Inlier, Mount Isa Inlier and the Curnamona Province.~~time of tectonism.

The key points of debate are~~;~~:

1) the location and polarity of subduction systems,
2) the timing of major depositional and collisional events,
3) the interpretation of the spatial positions of the North Australian and South Australian Cratons through time with respect to one another (as a result of 1 and 2).

Increasing our knowledge of these ~~tectonics~~tectonic settings will improve our understanding of the Palaeo-Mesoproterozoic evolution of Australia. Moreover, the knowledge will provide important constraints to larger-scale Nuna-Columbia supercontinent reconstructions.

1.2 A key terrane

The Mount Painter Inlier is situated within the northern, South Australian Craton margin (Fig. ~~1~~1b-c), which makes it an ideal location to explore the links between the North and South Australian cratons. In addition, this inlier helps us investigate the interface between the Gawler Craton and northern Curnamona Province, which is currently poorly understood.

Recently, Armit et al. (2012) suggested that the Early Mesoproterozoic deformation events recorded in the Mount Painter Inlier appear to be more similar to those observed in the northern Gawler Craton and Mount Isa Inlier, rather than the southern Gawler Craton and Curnamona Province.

According to that study, the Mount Painter region would be predicted to record an evolution more similar to that of the North Australian Craton rather than the South Australian Craton. If this is indeed the case, our interpretations of the relationships between these crustal elements~~,~~ and the reconstructions to place the Mount Painter Inlier in its correct location through time, require a substantial re-appraisal.

~~The implications of~~ We~~Armit et al.~~~~'s (2012) study highlights the need to better understand the depositional and tectonic history of the Mount Painter Inlier. In this communication we have chosen to~~ investigate the provenance and depositional environment of ~~sediments~~sedimentary rocks deposited ~~at~~in the ~~nexus between the Palaeo- to~~Early Mesoproterozoic within the Mount Painter Inlier~~. We then use these data to improve our interpretation of the tectonic setting for this inlier, which in turn~~ as they may provide constraints on the palaeogeography of both the Mount Painter Province and ~~the~~ eastern Proterozoic Australia.

~~*Insert Figure 1 here*~~

1.3 **Geological Background**

1.3.1 Crustal architecture

The Radium Creek Group (Preiss et al., 2010; a nomenclature revised from the Radium Creek Metamorphics) outcrops within the Mount Painter and Mount Babbage ~~Inliers~~inliers, which are located at the northern tip of the Flinders Ranges in South Australia (see Fig. ~~1~~1c). These Inliers have been ~~traditionally~~ interpreted as part of the Moolawatana Domain (Fig. 1c) that defines the north-western extent of the Curnamona Province (Conor and Preiss, 2008; Parker et al., 1993; Teale and Flint, 1993). ~~However, a recent deep Seismic reflection and magnetotelluric survey (08GA-C1) across the area has been interpreted by Korsch et al., (2010), who demonstrate a major crustal-scale south-dipping discontinuity between this Moolawatana Domain and the Curnamona Province to the south. This interpretation suggests that a different basement (Gawler Craton) lies below the Mount Painter Province. This basement is similar to that which underlies the western flanks of the Adelaide Fold Belt (Preiss et al., 2010), and is distinct from that which underlies the rest of the Curnamona Province.~~

A major crustal-scale south-east-dipping discontinuity between the Moolawatana Domain and the Curnamona Province has been interpreted from the deep seismic reflection and magnetotelluric survey (08GA-C1) by Korsch et al. (2010). This discontinuity has been interpreted as separating distinct basement blocks. The basement below the Moolawatana Domain on the north-western side of the discontinuity is termed the Warrakimbo Seismic Block by Korsch et al. (2010). This seismic block is characterised by markedly lower reflectivity than the Yarramba Seismic Province which is interpreted to be basement to the Curnamona Province south-east of the major discontinuity (Korsch et al., 2010).

1.3.2 Stratigraphy

Within the northern Mount Painter Inlier, the Radium Creek Group is ~~comprised~~composed of micaceous psammites, psammopelites, pelitic schists, phyllites, feldspathic quartzites and quartzofeldspathic gneisses~~.~~ (Fig. 3). These rocks have yielded~~ Late Palaeoproterozoic to~~ Early Mesoproterozoic (1600-1580 Ma) maximum depositional U-Pb zircon ages (Elburg et al., 2012; Fanning et al., 2003; Fraser and Neumann, 2010). These ages appear to be significantly younger than the ca. 1720-1640 Ma Willyama Supergroup ca. 1720-1640 Ma (Conor and Preiss, 2008) from the southern part of the Curnamona Province and therefore previous correlations with the Radium Creek Group are considered erroneous (e.g. Teale, 1993).

The Radium Creek Group has undergone ~~multi-phased~~polyphase metamorphism (Elburg et al., 2003; McLaren et al., 2002) and poly-deformation in the Early Mesoproterozoic and Palaeozoic (Armit et al., ~~2012). Due to this complexity, a number of different plausible geological frameworks have been suggested for the sedimentary stratigraphy of the Radium Creek Group. These include two phase depositional models (Fanning et al., 2003; Paul, 1998; Teale, 1993) and single phase models (Coats and Blissett, 1971; Elburg et al., 2001~~2012).

~~The two phase models describe either; Palaeoproterozoic quartzofeldspathic sequences i.e. suites 4 and 5 of Teale (1993) and separate Mesoproterozoic sequences i.e. suites 1 and 2 of Teale (1993). Alternatively, two Mesoproterozoic phases are separated by a deformation event (Paul et al., 1999; Fanning et al., 2003). The single phase model suggests that basal phyllites (Yagdlin Phyllite) are overlain by the Mount Adams Quartzite, Brindana Schist and Freeling Heights Quartzite (Coats and Blissett, 1971; Elburg et al., 2001).~~

1.3.3 Igneous suites

~~The metasediments~~The metasedimentary rocks of the Mount Painter Province are intruded by a series of Early Mesoproterozoic igneous suites with A-type geochemical affinities (Elburg et al., 2012; Kromkhun et al., 2013). ~~This includes the ca. 1585-1557 Ma~~ The Mount Neill Suite was emplaced at ca. 1585-1557 Ma along the south-east margin of the inlier (Fig. ~~2) which~~3). This suite incorporates the Box Bore and Mount Neill Granite (Elburg et al., 2012; Elburg et al., 2001; Fraser and Neumann, 2010~~) and the~~). The slightly younger ~~ca. 1560-1555 Ma~~ Moolawatana Suite was emplaced between ca. 1560 Ma and 1555 Ma (Stewart and Foden, 2001) on the northern side of the Inlier~~.~~ (Fig. 3). The ca. 1552 Ma Hodgkinson Granodiorite (Fraser and Neumann, 2010) also intrudes the central part of the Inlier and outcrops as a linear NE-SW belt. Numerous metabasic bodies intrude the Radium

Creek Group and are considered to be late Mesoproterozoic to Neoproterozoic in age (Wulser, 2009). Minor pegmatite lenses throughout the Radium Creek Group in the northern Mount Painter Inlier are most likely syn- to post- the Cambro-Ordovician Delamerian Orogeny (Elburg et al., 2003). Within the central part of the inlier, the peraluminous British Empire Granite and metaluminous Paralana Granodiorite are interpreted to have been emplaced during the Palaeozoic ca. 460-440 Ma (Elburg et al., 2003; McLaren et al., 2006).

1.3.4 Metasomatism

Lenses of peraluminous to hyperaluminous rock, composed of phlogopite-corrundum-kyanite bearing~~ mineral~~ assemblages are present within the Radium Creek Group in the Mount Adams area proximal to the Mount Neill Granite (Shafton, 2006). This lithology is correlated with the Corundum Creek Schist Member (Shafton, 2006) originally mapped as part of the Radium Creek Metamorphics (Coats and Blissett, 1971). Elburg et al. (2011) interpreted these bodies as metasomatised igneous rocks ~~and most~~which likely reflect intense alteration of the Mount Neill Suite.

1.3.5 Structure

The Inlier is bisected by the Paralana Fault Zone (Fig. ~~2~~3) which~~ also~~ separates sequences of the Radium Creek Group. This fault system is a major crustal-scale feature and has a predominantly steep, northwest-dipping geometry as interpreted from the 08GA-C1 deep seismic reflection survey (Korsch and Kositcin, 2010). Field observations indicate that the fault zone is defined by a corridor of high strain, which record demonstrable reactivations since the Early Mesoproterozoic (Armit et al., 2012) through to the Cenozoic (Elburg et al., 2012; Teasdale, 1993).

1.4 Approach of this study

Geochronology coupled with isotopic fingerprinting of ancient rock packages is a powerful tool for constraining reconstructions of Proterozoic terranes (e.g. Cawood et al. 1999; Halilovic et al. 2004; Nelson, 2001). This allows us to reconstruct links between cratonic elements with greater confidence, which improves global reconstructions.

This study aims to provide constraints on the timing and provenance of deposition of the Radium Creek Group. To achieve this we compare the isotopic and geochronological signatures of detrital zircon populations from these metasediments with that of neighbouring tectonic elements. Direct comparison of our new zircon age data with Precambrian terranes across eastern Australia can then be used to identify the most likely crustal element(s) those zircons, and thus sediments, are derived from.

In addition, the employment of trace element and Lu-Hf isotope system fingerprinting allows us to also compare the source (i.e. relative contemporary crust/mantle contribution) that different zircon populations have crystallised from (Blichert-Toft and Albarede, 1997). These data have the potential to discriminate between terranes that have similar chronology, but different magmatic source chemistry and antiquity, allowing a further level of discrimination between potential sources of detritus. Our approach is to assess the U-Pb-Hf-trace element signature of samples throughout the Radium Creek Group ~~samples~~ and compare them to that of zircon populations from ~~other~~ potential source lithologies across a number of terranes, using both new data presented herein and published datasets from the Gawler Craton, Mount Isa Inlier, Curnamona Province and Arunta Block (Belousova et al., 2006b; Condie et al., 2005; Griffin et al., 2006; Hollis et al., 2010; Howard et al., 2009; Howard et al., 2011a; Howard et al., 2011b; Howard et al., 2011c; Szpunar et al., 2011).

Available whole rock Nd isotope datasets from across the region (Neumann, 2001; Schaefer, 1993; Wade et al., 2012) are also examined in order to further test observed temporal and spatial patterns with respect to relative inputs of juvenile material, which can provide insights into the provenance of the Radium Creek Group.

~~*Insert Figure 2 here*~~

1.5 Samples

Four samples from the Mount Painter Inlier were investigated~~ in extensive detail.~~. Three of which (Z3, F and 123) are from the hanging wall (western side) of the Paralana Fault~~, with the remainder~~ and one from the eastern (foot-wall) side (see Fig. ~~2).~~3). Sample Z3 is a sample of a fine-grained, mica rich, garnet + quartz psammopelitic horizon within the Brindana Schist (Fig. ~~3a,~~4a-b). This horizon is located ~100 m to the west of the Paralana Fault and Mount Neill Granite Suite. Sample F is a medium-grained quartz + muscovite ± garnet layer within the Freeling Heights Quartzite ~6 km to the south-west of sample Z3 (Fig. ~~2,3c,~~4c-d). 123 is a course grained quartz + muscovite layer of the Freeling Heights Quartzite (Fig. ~~3e,~~4e-f). This sample location is ~2 kilometres south-west of sample F. 36 is a medium grained quartz + muscovite ± biotite ± garnet layer of the Mount Adams Quartzite (Fig. ~~3g,~~4g-h), from the eastern side of both the Paralana Fault and the Mount Neill Granite Suite. ~~Thus good coverage of the Radium Creek Groups is achieved, incorporating both sides of the major defining structure.~~

Additionally, we ~~included~~studied one sample from the Central Gawler Craton. Sample YD23A is a black, course-grained porphyritic (plagioclase + k-feldspar + iron oxide) sample (Fig. ~~3i,~~4i-j) of the Pondanna member of the Upper Gawler Range Volcanics~~-~~ (uGRV; Allen et al., 2003; Blissett et al., 1993). The uGRV is a major capping sequence of the Gawler Felsic Large Igneous Province (Allen et al. 2012), ~~comprised~~and is composed of widespread and homogeneous felsic lava (due to high magmatic temperature and halogen enrichment, promoting efficient mixing via low magmatic viscosity: see Pankhurst et al. 2011a) that outcrops as monotonous sheets across the Central Gawler Craton. The emplacement of this voluminous felsic large igneous province (FLIP) was rapid (Pankhurst et al. ~~2011a~~2011b), and occurred at ca. 1592 ± 3 Ma (Fanning et al., 1988). As such, this sample represents both a snapshot of Gawler Craton evolution as well as the principle source of Gawler Craton-derived detritus, at the apparent time of Radium Creek Group deposition.

Finally, two samples are taken from drillholes ~150 ~~Kilometres~~kilometres to the south of the Mount Painter Inlier, within the Curnamona Province (Fig. ~~1~~1b-c). They have previously been dated using in-situ zircon U-Pb techniques by Jagodzinski & Fricke (2010). Sample R1707876 is ~~of~~from the Frome 12 Granite, ~~Ninnerie Supersuite~~Bimbowrie Suite, intersected in drillhole DDH Frome 12 (385176E, 6503512N). Sample R1709059 is ~~of a~~from rhyolite assigned to the Benagerie ~~Volcanics~~Volcanic Suite, intersected in DDH Frome 13 (393612E, 66528251N). Both of these samples are ~~of~~from igneous rocks emplaced within the Curnamona Province at ca. 1594-1587 Ma (Jagodzinski and Fricke, 2010). They therefore contain information regarding the Early Mesoproterozoic evolution of ~~this tectonic element at this time, which is key to understanding~~ the ~~Mount Painter Inlier~~Curnamona Province, as well as representing a potential contemporary source for detritus contributing to the Radium Creek Group.

~~*Insert Figure 3 here*~~

2 Methods

2.1 Sampling for whole rock geochemistry and zircon extraction

Several kilograms of representative material were collected from each site (see Fig. ~~2, 3)~~ 3-4). Weathered rinds and any obvious zones of alteration were discarded. These samples were then pulverised using a ceramic disc mill and sieved to collect the resulting fragments within an 18 to 250 µm size range. Magnetite within this fraction was removed using a hand magnet. Tetrabromoethane (TBE ~~(~~; 2.96g/ml) and Di-iodomethane (DIM ~~(~~; 3.3g/ml) heavy liquids were then used to separate minerals with high specific gravity (including zircon) from the predominantly lighter medium. A further magnetic separation step followed using the heavy fraction. We used a Frantz magnetic separator set at 1.4 Amps, 15° forward and 25° side tilt.

2.2 Zircon mounting, imaging and in-situ targeting

Zircons were hand-picked from the non-magnetic fraction using a binocular microscope and suspended in an epoxy resin mount for grinding, polishing and carbon coating. The mounts were imaged using a JEOL JSM 6300 SEM at Ballarat University (both back scatter electron and cathode luminescence images) on the Brindana Schist sample (sample Z3), and a JEOL JSM-840A SEM (back scatter electron images only) at the Centre for Electron Microscopy, Monash University on the uGRV sample (YD23a). A Cameca SX100 electron microprobe (back scatter electron and cathodoluminescence images) was used to image zircons from the Freeling Heights Quartzite (sample F, 123), Brindana Schist (sample Z3) and Mount Adams Quartzite (sample 36) at GEMOC, Macquarie University. These images (BSE and/or CL) were used to choose analysis spots for each grain. The most appropriate sites were those that best fit the criteria of adequate size, internal consistency and tractable petrographic context of crystal zonation domains.

2.3 Analytical methods

2.3.1 In-situ major and trace element chemistry

Electron microprobe (EMP) analysis for in-situ zircon major and trace-element (HfO_2, SiO_2, ZrO_2, Y_2O_3) geochemistry was conducted on samples from the Freeling Heights Quartzite (samples F) and Mount Adams Quartzite (sample 36) using a Cameca SX100 Electron Microprobe fitted with 5 wavelength dispersive spectrometers (WDS) and Princeton Gamma-Tech (PGT) energy dispersive system (EDS). The microprobe was operated at an accelerating voltage of 15 kV with a beam current of 20 nA, a 1-2 µm beam diameter, and a dwell time of 60 seconds acquisition after 60 seconds background. The analyses were conducted at the same site within each zircon grain chosen for both the U-Th-Pb-trace and Hf-isotope analyses.

2.3.2 U-Th-Pb

In-situ zircon U-Th-Pb isotope analysis was conducted at Macquarie University using a HP 4500 quadrupole ~~ICPMS~~inductively coupled plasma mass spectrometer (ICPMS) attached to a New Wave UV213 Laser system for samples Z3, F, 123 and 36. Analysis of zircon from sample YD23a was undertaken at Monash University by laser ablation (LA~~–~~) -ICPMS attached to a Thermo X-series quadrupole coupled with a New Wave ~~213nm~~213 nm, Nd: YAG laser. A laser spot size between 30-~~40µm~~40 µm was used depending on the size and morphological complexity of each zircon. Ablation sites were chosen to best represent populations from each of the distinct zircon morphologies that could be characterised from BSE and CL images of the zircon grains (see Fig. ~~4~~5). The lasers at both Macquarie University and Monash University were operated using a ~~5Hz~~5 Hz repetition rate with 11-~~13mJcm~~13 $mJcm^{-2}$ laser energy at the sample with a 60-~~120s~~120 s acquisition period including ~~15ms~~15 ms dwell for Pb^{206}, U^{238}; 10ms for Pb^{204}, Pb^{208}, Th^{232} and ~~30ms~~30 ms for Pb^{207}. The dwell times for sample YD23a (undertaken on the Monash University LA-ICPMS) differed slightly with a shorter ~~10ms~~10 ms dwell for Pb^{204} and ~~25ms~~25 ms for Pb^{206}, Pb^{207}, Th^{232} and U^{238}.

2.3.3 In-situ Lu-Hf

We targeted zircons for Hf isotope analysis that represented each distinct U-Pb age population within each sample. Hf isotopes were only measured from grains with U-Pb ages that were <10% discordant. The specific sites were chosen to be adjacent to the same pit and within the same internal domain, ablated for U-Pb isotopic analysis (identified by BSE and CL images: Fig. ~~4~~5).

The in-situ zircon Lu-Hf isotope analytical technique used in this study follows that described by Griffin et al., (2004); Griffin et al., (2006); Griffin et al., (2002). Analysis was conducted at GEMOC, Macquarie University using a New Wave/Merchantek LUV213 (Nd: YAG) laser-ablation system attached to a Nu Plasma multicollector ICPMS via Ar/He gas delivery. The ICPMS was tuned using a 1 ppm solution of the JMC475Hf standard spiked with 80 ppb Yb, which yielded a typical total Hf beam of 10-14 x 10^{-11} Å (Jackson et al., 2004).

The analyses in this study were carried out using a 40 to 55 µm beam diameter with a 5Hz repetition rate and ~0.6 mJ/pulse which produced a total Hf signal of 1-6 x 10^{-11} Å. Following 60 s of background measurement, 80-120 s of acquisition time per analysis produced ≤ ~~50um~~50 um deep pits.

~~*Insert Table 1 here*~~

During the analytical run, Mud Tank Zircon standard was analysed as an internal monitor (Table 1). These measurements yielded an average corrected $^{176}Hf/^{177}Hf$ ratio of 0.282527 ± 0.000029 (~~2σ,~~ n=14, 2σ), which is within the error of the long term average 0.282532 ± 0.000033 (~~2σ~~ n=984, 2σ) and 0.282523 ± 0.000043 (n=2190, 2σ) (Pearson, N.J. Pers comms, 2010). In addition, the 91500 zircon standard was analysed, and yielded a corrected average $^{176}Hf/^{177}Hf$ ratio of 0.282322 ± 0.000059 (n=4, ~~2 σ~~2σ) which is within error of the long term average of 0.282307 ± 0.000058 (n=632, 2σ) (from Pankhurst et al., 2013). In addition and where possible, multiple ablations of the same domain in our unknown samples (quasi repeat analyses) returned ε Hf values that were indistinguishable from the original analyses (1σ <0.05 ε Hf).

2.3.4 Whole-rock geochemistry

Splits (~250 g) of ~~samples~~sample Z3 and sample F were crushed using a hydraulic press and then further in an agate mill to produce a powder of each sample. A portion (~~15g~~15 g) of each powder was analysed for major~~,~~ elements using a Bruker-AXS S4 Pioneer XRF Spectrometer and processed through Bruker-AXS Spectra-plus ~~Software~~software, at the Advanced Analytical Centre at James Cook University. This is the same method and laboratory that determined the whole rock data from sample Y23a (see Pankhurst et al. 2011a). Trace (including rare-earth element) data were acquired from high-pressure digestions using HF. This step was followed by ~~a~~an HCl digestion at one atmosphere before drying down and converting to nitric complexes using HNO_3. These samples were then taken up in dilute HNO_3, spiked with a Li, In and Bi internal standard before analysing the solutions using a quadrupole ICPMS at Monash University.

2.4 Data treatment

2.4.1 U-Th-Pb isotope ratios

U-Th-Pb isotopic ratios were calculated using GLITTER software (e.g. Van Archerbergh et al., 1999) and the U-Pb ages were calculated using Isoplot 4.15. The procedure for data reduction procedure ~~used~~ follows that of Griffin (2004) and Jackson et al. (2004) and in each case GEMOC GJ-1 zircon (TIMS normalisation values of Jackson et al. (2004) are: ^{207}Pb/^{206}Pb 608.3 Ma, ^{206}Pb/^{238}U 600.7 Ma and ^{207}Pb/^{235}U 602.2 Ma) was used to correct for U-Pb fractionation. In addition, the 91500 zircon standard was analysed within each run as a monitor of the reproducibility and accuracy for both LAM-ICPMS instruments used (Table 2). A correction for ^{204}Pb was applied following the method described in Anderson (2002). This correction had a negligible effect on the majority of the ~~analysis~~analyses. Absolute ages and their individual errors were calculated using Isoplot 4.15 (Ludwig, 2008), and age populations were assessed with the unmix function (to unmix superimposed Gaussian distributions) as appropriate.

~~*Insert Table 2 here*~~

2.4.2 Zircon trace element data

A cameca Φpz correction procedure was applied to the EMP dataset to calculate oxide percentages from raw counts. The trace element concentration data (Y, Hf) were combined with U, Th, Lu, Yb concentration data acquired during the LAM-ICPMS analysis, and used to model potential magmatic source rock type (c.f. Belousova et al., 2002) for each grain, and by extension, on age populations. These data were collated for selected grains from ~~samples~~sample F (n=16) and sample 36 (n=18) that satisfy our selection criteria: ~~-~~grains were chosen to represent each of the U-Pb detrital age populations brackets, and were ~~checked that this~~ limited ~~the cut~~ to igneous crystals only, by using geochemical data as a filter (Th/U ratios of >0.5 normally indicate an igneous origin; Cowley and Fanning, 1992).

2.4.3 Lu-Hf isotope ratios

Measured masses 172, 175, 176, 177, 178, 179 and 180 were normalised to ^{179}Hf/^{177}Hf = 0.7325 using an exponential correction for mass bias. Interference of ^{176}Lu on ^{176}Hf was corrected using a ^{176}Lu/^{175}Lu ratio = 0.02669 (Claoué-Long et al., 2008) and measuring the interference-free ^{175}Lu value to calculate ^{176}Lu/^{177}Hf. Interference of ^{176}Yb on ^{176}Hf was corrected using a ^{176}Yb/^{172}Yb ratio of 0.5865 (see Griffin et al., 2000), determined by spiking the JMC475 Hf standard with Yb, and measuring the interference-free ^{172}Yb (Jackson et al., 2004). Repeated analysis of standard zircons (see 3.2.3 above) with a variety of ^{176}Lu/^{177}Hf and ^{176}Yb/^{177}Hf ratios (see Griffin et al., 2004) establishes the accuracy and precision of the Lu and Yb corrections.

The measured ^{176}Lu/^{177}Hf ratios for each of the zircons analysed were used to calculate initial ^{176}Hf/^{177}Hf ratios. Numerous proposed decay constants exist for ^{176}Lu (e.g. Bizzarro et al., 2003; Blichert-Toft et al., 1997; Scherer et al., 2001 ; Soderlund et al., 2004). We have used a value of 1.865E^{-11}/yr for all Hf isotope calculations (Scherer et al., 2001; Soderlund et al., 2004). Chondritic values of ^{176}Lu/^{177}Hf = 0.282772 and ^{176}Hf/^{177}Hf = 0.0332 (Blichert-Toft and Albarede, 1997) are used for calculating ε Hf and model ages.

The mean 2se precision of ^{176}Hf/^{177}Hf ratios presented in this study is ± 0.00002 which equates to ±0.7 ε Hf). The majority of the analyses returned a 2se uncertainty range between <1-5% contributing an uncertainty of between 0.05 and 0.25 ε Hf. This uncertainty reflects the within-grain variation in Lu/Hf observed in zircons and the analytical uncertainties (Belousova et al., 2006a). Further discussion on the precision and accuracy of this method are expanded upon in ~~(~~Griffin et al~~.,~~. (2002; 2004~~; Griffin et al., 2002~~).

Calculation of depleted mantle model ages (T_{DM}) for each zircon analysis were made using the measured ^{176}Lu/^{177}Hf and modelled values for ^{176}Hf/^{177}Hf$_i$ = 0.279718 at 4560 Ma and ^{176}Lu/^{177}Hf = 0.0384 (~~Kromkhun~~Griffin et al., ~~2013~~2000). These values produce a depleted mantle model with ^{176}Hf/^{177}Hf$_{(present\text{-}day)}$ = 0.~~283251~~28325, comparable to average MORB (~~Gum and Belousova, 2006).~~Nowell et al., 1998). These single~~-~~ stage model ages provide a minimum age on the source material from which the zircon crystallised. In addition, two stage model ages or crustal model ages (T_{DM}^c) were calculated. These models assume that a zircon's parental magma was formed from average continental crust and therefore use a ^{176}Lu/^{177}Hf ratio of 0.015 (Griffin et al., 2004) (Geochemical Earth Reference Model database) that was initially derived from the depleted mantle.

3 Results

3.1 Zircon descriptions

The zircon grains (n=57) from sample Z3 are rounded and reddish-brown. Typical diameters range from 30~~-~~ to 100 µm. In ~90% of these zircons, morphologies are ~~characterise~~characterised by oscillatory zoned cores (Fig. ~~4~~5a-b) with isometric overgrowths and rims (6 rims >30 µm in thickness). The additional 10% zircons have isometric morphologies with <15 µm overgrowths.

Formatted: No Spacing

~~*Insert Figure 4 here*~~

Zircons from sample F (n=138) are predominantly brown, subhedral grains and are slightly larger than those in sample Z3 (~80% >70µm). The morphology of these zircons is predominantly characterised by oscillatory zoned cores (~75% of grains) with variable, weak to strongly zoned rims and isometric overgrowths (Fig. ~~4~~5c-d).

Grains of zircon separated from sample 36 (n=32) are reddish-brown in colour and have a typical diameter range from 40-110 µm. The grains are subhedral and ~80% have oscillatory zoned cores (Fig. 5e-f). The remainder have isometric cores. ~10% of the grains have very thin overgrowths (<10 µm).

The zircons separated from sample 123 (n=33) are indistinct in terms of colour, shape and size from the grains in sample F. ~~~~~Approximately 90% of the grains have oscillatory zoned cores. Very thin (<10 µm) rims/overgrowths are apparent on ~30% of the grains (Fig. ~~4~~5g-h).

~~Grains of zircon separated from sample 36 (n=32) are reddish-brown in colour and have typical diameter range from 40-110 µm. The grains are subhedral and ~80% have oscillatory zoned cores (Fig. 4). The remained have isometric cores. ~10% of the grains have very thin overgrowths (<10 µm).~~

Formatted: No Spacing

The zircon grains from sample YD23a (n=29) are brown in colour, subhedral in shape, exhibit blunt pyramidal terminations, and vary in size between 100-300 µm. All of the zircon grains from this sample display oscillatory zonation and do not ~~have any~~ show any evidence for any metamorphic overgrowths (Fig. ~~4~~5i-j).

Description of the Curnamona Province zircons from R1707876 (Frome Granite) and R1709059 (Benagerie ~~Volcanics~~Volcanic Suite) can be found in Jagodzinski & Fricke (2010).

3.2 U-Th-Pb zircon geochronology

Results from LA-ICPMS U-Pb dating of ~~zircons presented in this study is~~zircon are presented in Table 3. The complete dataset is provided in Supplementary Appendix A. Probability density plots and concordia plots for each of the samples analysed in this study are shown in Fig. ~~5~~6-7.

~~*Insert Table 3 here*~~

3.2.1 Z3 (Radium Creek Group - Brindana Schist)

A total of 78 zircon U-Pb analyses were conducted on 60 separate zircon grains. Data were gathered from both the cores and regions with clear oscillatory zoning for completeness (Fig. ~~4~~6a-b). Six analyses from this total dataset were interpreted as metamorphic zircon growth (see Armit et al., 2012). Armit et al.~~Those authors~~ (2012) described these zircons as exhibiting isometric rims and overgrowths, yet only 3 of these analyses returned Th/U ratios <0.3 (an order of magnitude lower than the detrital igneous zircon cores presented here) and were less than 10% discordant. These metamorphic overgrowths have weighted mean $^{207}Pb/^{206}Pb$ age of 1552 ± 32 Ma (2σ).

Fifty-four analyses from the remaining 72 are within 10% concordancy. The probability density plot for this sample has two major zircon population peaks (Fig. ~~5~~6). The younger population consists of a group of 19 zircons which have a weighted mean $^{207}Pb/^{206}Pb$ age of 1595.7 ± 9.2Ma (n = 19, MSWD = 0.38, 2σ). An older population of 21 zircons has a weighted mean $^{207}Pb/^{206}Pb$ age of 1708 ± 17 Ma (n = 21, MSWD = 1.9, 2σ). This peak consists of two separate populations ~~(Isoplot unmix function relative misfit = 0.967 based on 2 components),~~ at ~~1687.8 ± 8.8~~ca. 1680 Ma ~~(1σ, 0.51 fraction)~~ and at ~~1737 ± 11~~ca. 1740 Ma~~ (1σ, 0.49 fraction).~~. Three zircons with an age range of between ~~1765-~~ca. 1790 and ca. 1850 Ma were present in the sample. Archaean to earliest Palaeoproterozoic aged detrital zircons were also present in the sample and exhibit an age range of between ca. 2370 and ca. 2900 Ma.

3.2.2 F (Radium Creek Group – Freeling Heights Quartzite)

A total of 148 U-Pb zircon analyses were conducted for this sample across 138 grains. Four of these analyses were located on zircon overgrowths/rims with isometric and/or 'fir-tree' and/or sector zoned morphology that were >30μm wide, and therefore could return signals uncontaminated by neighbouring domains, these are discussed in Armit et al. (2012). One hundred of the analyses from the remaining 144 igneous detrital zircon fraction were within 10% concordancy. The probability density plot of concordant analyses (<10% discordant) for this sample has 3 major peaks (Fig. ~~5~~6c-d). The youngest population consists of 17 zircon grains and has a weighted mean $^{207}Pb/^{206}Pb$ age of 1591.7 ± 7.8 Ma (n =17, MSWD = 1.9, 2σ). An older peak is ~~comprised~~composed of two distinct populations (Isoplot unmix ~~function relative misfit = 0.687 based on 2 components~~routine) at ~~1674.6 ± 2.8~~ca. 1680 Ma ~~(1σ, 0.56 fraction, n = 21)~~ and ~~a 1732.8 ± 2.9~~at ca. 1730 Ma~~ (1σ, 0.44 fraction, n = 18).~~. A single grain from this sample returned a ca. 1841 Ma age. Eighteen analyses returned an age plateau between 2240 Ma and 2600 Ma. ~~A three component unmixing calculation (Isoplot unmix~~

~~function relative misfit = 0.249), resolves these data into 3 populations aged at a 2295 ± 7.1 Ma (1σ, 0.11 fraction), 2449 ± 4 Ma (1σ, 0.53 fraction) and 2552 ± 4.5 Ma (1σ, 0.36 fraction).~~

3.2.3 123 (Radium Creek Group - Freeling Heights Quartzite)

U-Pb analysis was conducted on 40 separate detrital igneous-sourced zircons. Nine analyses were more than 10% discordant. Probability plots for the 31 remaining analyses are displayed in figure ~~5~~6e-f. A tight cluster of late Mesoproterozoic zircon ages (n=8) have a weighted mean ^{207}Pb/^{206}Pb age of 1590 ± 6 Ma (n = 8, MSWD = 0.95, 2σ). ~~A three component unmixing calculation of the~~The remaining, older ages ~~(Isoplot unmix function relative misfit = 0.410) resolves~~are characterised by Palaeoproterozoic populations at ~~1656 ± 4~~ca. 1660 Ma~~ (1σ, 0.38 fraction, n=6), 1704.4 ± 3.4~~, ca. 1710 Ma ~~(1σ, 0.5 fraction, n=7)~~ and ~~1771.1 ± 6.7~~1770 Ma~~ (1σ, 0.13 fraction, n=2).~~. An Earliest Palaeoproterozoic population is also present and returns a weighted mean ^{207}Pb/^{206}Pb age of 2490.1 ± 9.9 Ma (n=4, MSWD = 0.41, 2σ).

3.2.4 36 (Radium Creek Group – Mount Adams Quartzite)

Thirty-nine analyses were conducted on 38 zircon grains for U-Pb ages from this sample of the Mount Adams Quartzite~~.~~ (Fig. 6g-h). One analysis is >10% discordant. The youngest ~~population~~ distinguishable population from the remaining 38 analyses is a cluster at 1592 ± 10 Ma (n = 8, MSWD = 1.4, 2σ). ~~A three component unmixing calculation of the remaining, older ages resolves (Isoplot unmix function relative misfit = 0.549)~~Other population peaks are evident at ~~1677.7 ± 3.3~~ca. 1680 Ma~~ (1σ, 0.42 fraction), 1709.9 ± 4.1~~, ca. 1710 Ma ~~(1σ, 0.30 fraction)~~ and ~~1743.8 ± 3.3~~ca. 1740 Ma ~~(1σ, 0.27 fraction).~~. An older, Earliest Palaeoproterozoic population has a weighted mean ^{207}Pb/^{206}Pb age of 2477.1 ± 11 Ma (n=3, MSWD = 2.2, 2σ).

~~*Insert Figure 5 here*~~

3.2.5 YD23a (upper Gawler Range Volcanics)

A total of 33 analyses were conducted on 29 separate zircons grains. 26 of these are ≤10% discordant. No concordia age or intercept age could be satisfactorily determined using the entire population. In addition, the weighted mean ^{207}Pb/^{206}Pb age for the entire group (Fig. ~~6~~7) produced an MSWD >8. The very high MSWD implies the presence of inherited zircon populations. These are calculated using probability plots and unmixing models to have ages of ca. 1680 ~~± 24~~ Ma and ca. ~~1762 ± 22~~1760 Ma. These analyses correlate with dark core regions in CL images, which independently ~~suggests~~suggest that they should not be included in a weighted crystallisation age calculation. Instead we prefer the weighted mean ^{207}Pb/^{206}Pb age of 1595 ± 19 Ma (n = 17, MSWD = 0.046, 2σ), which is consistent with the previously published age of the Yardea Dacite (upper Gawler

Range Volcanics: 1592 ± 3 Ma; Fanning et al., 1988) as well as the lower units of the Gawler Range Volcanics 1591± 3 Ma (Fanning et al., 1988).

~~*Insert Figure 6 here*~~

3.3 In-situ Lu-Hf

A total of 74 zircon grains were analysed from the Radium Creek Group. This included 37 grains from the pelitic Brindana Schist, 18 from the overlying Freeling Heights Quartzite and 19 from the Mount Adams Quartzite~~.~~ (Fig. 8a-b). Twenty-five grains were analysed from the upper Gawler Range Volcanics (Central Gawler Craton; YD23a) ~~were conducted.~~(Fig. 8c). Twenty-two grains with 2 repeats [from the same domain] were analysed from the Frome Granite (Fig. 8c), and 13 zircon grains from the rhyolitic Benagerie ~~Volcanics~~Volcanic Suite (Fig. 8c) (Curnamona Province; R1707876 and R1709059 respectively). These results are presented in Table 3 and summarised in ~~Fig. 7~~Figure 8a-d (the full dataset is presented in Appendix A).

~~*Insert Figure 7 here*~~

3.3.1 Z3 (Radium Creek Group - Brindana Schist)

Hf isotope ratios measured from the ca. 2900 Ma (Archaean) zircon grain has a ε $Hf_{(t)}$ value of +7.27 and a crustal model age (T_{DM}^{c}) of 2880 Ma~~.~~ (Fig 8a-b). Early Palaeoproterozoic zircon grains that are dated at 2300 and 2500 Ma have ε $Hf_{(t)}$ of -4.89 and -1.11, and T_{DM}^{c} at ~~3.11~~3110 Ma to 3240 Ma respectively~~.~~ (Fig. 8a-b). Zircon grains with ages between 1765 Ma and 1850 Ma (n=3) possess an ε $Hf_{(t)}$ range from -4.9 to -2.89 and T_{DM}^{c} ages between 2660 and 2800 Ma. Zircon grains with ca. 1710-1760 Ma dates have initial ε Hf values that are scattered between -6.58 and +2.74 (n=6). T_{DM}^{c} ages for these ca. 1710-1760 Ma zircons range from 2280 to 2840 ~~Ga~~Ma. A continuum of initial ε $Hf_{(t)}$ values from -4.21 to +5.8 characterise zircon grains with ages ca. 1630-1690 Ma (n=11) and correspond to T_{DM}^{c} ages between 2000 and 2630 Ma. The youngest population ca. 1595 Ma has a ε $Hf_{(t)}$ range between -6.7 and +2.77 (n=14) (Fig. 8a) and T_{DM}^{c} from 2150 to 2750 Ma~~.~~ (Fig. 8b).

3.3.2 F (Radium Creek Group – Freeling Heights Quartzite)

The ca. 2500 Ma zircon grains (n=2) have ε $Hf_{(t)}$ values of -5.15 and +1.29 (T_{DM}^{c} values of 3.38 and ~~2.97 Ga~~2970 Ma respectively) (Fig. 8a-b). A single grain with an age of ca. 1841 Ma has a ε $Hf_{(t)}$ of -2.56 and a T_{DM}^{c} of 2680 Ma. A ca. 1730 Ma population s (n=8) records ε $Hf_{(t)}$ values ranging from -9.4 to -0.53, T_{DM}^{c} for this group are 2480 to 3030 ~~Ga~~Ma. Zircons with U-Pb ages of ca. ~~1670~~1680 Ma (n=3) have a range of ε $Hf_{(t)}$ values from -9.91 to 0 and T_{DM}^{c} from 2390 to 3000 Ma. An early Mesoproterozoic population ca. 1595 Ma (n=4) have ε $Hf_{(t)}$ values ranging from -6.11 to +2.44 (Fig. 8a) and T_{DM}^{c} between 2170 and 2720 Ma~~.~~ (Fig. 8b).

3.3.3 36 (Radium Creek Group – Freeling Heights Quartzite)

This sample includes grains from 5 discrete age populations. All but the youngest (the early Mesoproterozoic population) have negative ε $Hf_{(t)}$ values~~.~~ (Fig. 8a). The oldest grain ca. 2948 Ma has a ε $Hf_{(t)}$ value of -9.46 and a T_{DM}^{c} of ~~3.97~~3970 Ma. A ca. 2500 Ma population (n=2) has initial ε Hf values of -2.77 and -0.93 (T_{DM}^{c} values of 3220 and 3070 Ma respectively). Ca. 1850 Ma (n=2) zircon grains have ε $Hf_{(t)}$ values of -6.32 and -3.24 (Fig. 8a) with T_{DM}^{c} of 2730 and 2940 Ma respectively~~.~~ (Fig 8b). Grains at ca. ~~1700~~1710-1740 Ma (n=4) return a tight cluster of initial ε $Hf_{(t)}$ values that range between -3.63 and -2.07. This group have T_{DM}^{c} from 2540 to 2670 Ma. A ca. 1677 Ma (n=3) population have a ε $Hf_{(t)}$ value range of -3.82 to -1.07 and T_{DM}^{c} between ~~2.45~~2450 and 2630 Ma. A ca. 1595 Ma (n=7) population have a spread of ε $Hf_{(t)}$ values ranging from -5.37 to +2.79 (Fig 8a) and corresponding T_{DM}^{c} of 2130 to 2690 Ma~~.~~ (Fig 8b).

3.3.4 YD23a (upper Gawler Range Volcanics)

This sample has 4 U-Pb age clusters. The principle age population (ca. 1595 Ma, n=20) ranges between -4.51 and -0.82, T_{DM}^{c} range of 2380-2620 Ma with an outlier that returned a ε $Hf_{(t)}$ value of +3.01 and 2250 Ma T_{DM}^{c}~~.~~ (Fig. 8c). ε $Hf_{(t)}$ of grains older than ca. ~~1700~~1710 Ma (n=4) range between +1.61 and +2.81, T_{DM}^{c} ranges from 2300-2430 Ma. ε $Hf_{(t)}$ values of ca. ~~1655~~1680 Ma (n=2) zircon grains are -1.14 and -0.98,T_{DM}^{c} ~~range are~~ages of 2440 and 2450 Ma~~.~~ (Fig. 8c).

3.3.5 R1707876 (Curnamona Province: Frome Granite~~)~~ – Bimbowrie Suite)

The dominant population at 1594 ± 8 Ma (n=22; Jagodzinski and Fricke, 2010) have ε $Hf_{(t)}$ values ranging from -5.29 to +1.02 and T_{DM}^{c} between 2260 and 2670 Ma~~.~~ (Fig 8c). A single older grain ca. 1640 Ma has an ε $Hf_{(t)}$ value of -2.7 and T_{DM}^{c} of 2.53 Ga. A young grain ca. 1557 Ma has a distinctly positive ε $Hf_{(t)}$ value of +5.96 and T_{DM}^{c} of 1920 Ma.

3.3.6. R1709059 (Curnamona Province: Benagerie ~~Volcanics) - 1587 ± 6 Ma~~Volcanic Suite)

The single population ca. 1587 Ma calculated for this rhyolite (Jagodzinski and Fricke, 2010) recorded a range of ε $Hf_{(t)}$ values from -1.7 to +4.0 and T_{DM}^{c} between 2070 and 2440 Ma~~.~~ (Fig. 8c).

3.4 In-situ trace element chemistry

The modelled rock type for each zircon analysed using the classification scheme of Belousova et al. (2002) are shown in Table 4 and are shown graphically in ~~Fig. 8~~Figure 9. In both samples modelled (F and 36), three modelled rock types for all of the zircons analysed were distinguished. These were low SiO_2 granitoids, granitoids (70-75 wt% SiO_2) and dolerites.

~~*Insert Table 4 here*~~

The ca. 1595 Ma zircons in sample F (Freeling Heights Quartzite) were modelled as originating from low SiO_2 granitoids (n=2) and from moderate SiO_2 content (70-75 wt%) granitoids (n=1). The ca. 1650-1680 Ma population was modelled as dolerite and 70-75 wt% granitoid (n=2). A subset of 8 zircons from the ca. 1700-1740 Ma zircon population indicates a predominantly granitoid source rock (n=5), although two zircons modelled as being sourced from dolerite (n=2) and 1 from a low SiO_2 granitoid. The ca. 1800-1850 Ma and ~~Earliest~~earliest Palaeoproterozoic populations were modelled as wholly 70-75 wt% SiO_2 granitoid derived. The overall modelled rock type source distributions for this sample ~~was~~are 62.5~~-~~% granitoid (70-75 wt% SiO_2 content) derived (n=10/16) and 18.75% from both dolerite and low SiO_2 (<65 wt%) granitoids.

The ca. 1595 Ma zircons in sample 36 (Mount Adams Quartzite) model as being derived from both low (n=2) and moderate (n=3) SiO_2 content granitoids. The ca. 1650-1680 Ma grains in this sample are evenly sourced from dolerite and 70-75 wt% SiO_2 granitoid rock types, which is identical to sample F. The ca. 1700-1740 Ma grains in this sample (n=3) are similar to those from that in ~~the Sample~~sample F, as two are modelled as granitoid (70-75 wt% SiO_2), and the third as dolerite sourced zircon, but lack zircons derived from low SiO_2 granitoids. It is possible this is due to sample size. One zircon in the 1800-1850 Ma population is derived from a low silica granitoid, and the other to a moderate SiO_2 content granitoid. The Archaean portion of the zircons analysed from this sample are sourced from a granitoid with 70-75 wt% SiO_2 content (n=3) or from a dolerite (n=1). The total modelled rock type source distributions for this sample was 61.1% granitoid (70-75 wt% silica content) derived (n=11/18), 22.2% dolerite derived (n=4/18) and 16.67% from low silica granitoids (n=3/18).

~~*Insert Figure 8 here*~~

3.5 Whole rock geochemistry

Complete major and trace element data is presented in supplementary appendix B. Major element data ~~define~~defines sample Z3 as shale and sample F as subarkose according to the classification of Herron (1998). Th/Sc ratios for each of ~~samples~~sample Z3 and sample F are 2.506 and 2.23 respectively. The samples display negative Eu/Eu* anomalies (Taylor & McLennan, 1985) of 0.41 for sample Z3 and 0.575 for sample F. Sample Z3 has a La/Yb_n value of 6.05 and sample F has a value (La/Yb_n) value of 1.08.

4 Discussion

4.1 Implications of new Radium Creek Group U-Pb zircon ages

In-situ U-Pb zircon dating of the Radium Creek Group units yielded a distinct Early Mesoproterozoic population within analytical uncertainty of each other. The 4 samples in this study yield a weighted mean average $^{207}Pb/^{206}Pb$ age of 1595.5 ± 3.7 Ma (n=41), which can be interpreted as the maximum depositional age of the Radium Creek Group. This robust age is within error of the SHRIMP IIe U-Pb maximum depositional ages of 1600 ± 8 Ma (Palaeoproterozoic suite 4; Teale, 1993) and 1591 ± 6 Ma (Palaeoproterozoic suite 5; Teale, 1993) for quartzofeldspathic gneisses sampled in the Paralana Creek ~10 kilometres to the south of the current study (Fraser and Neumann, 2010). Since we find these early Mesoproterozoic depositional ages to be prominent throughout the Radium Creek Group, we ~~regard~~interpret a geological framework involving a single phase of deposition for the entire package (Coats and Blissett, 1971; Elburg et al., 2001) at ca. 1595 Ma rather involving two distinct phases as previously interpreted (Paul, 1998; Teale 1993~~) to be most appealing.~~). This single depositional episode model is consistent with the structural framework interpreted by Armit et al. (2012) who described an upwards coarsening sequence from basal pelitic units (Brindana Schist) conformably overlain by quartzites and conglomerates of the Freeling Heights Quartzite (Fig. ~~9~~10).

~~*Insert Figure 9 here*~~

The overall detrital zircon U-Pb population distributions (Fig. ~~5~~6) for all 4 Radium Creek Group samples in this study, are very similar to each other; with significant U-Pb age contributions at ca. 1595 Ma, ca. ~~1650~~1660-1680 Ma, ca. 1710-~~1760~~1780 Ma and ca. 2500 Ma. Moreover, the in-situ zircon geochemistry of zircons from both the hanging wall (Freeling Heights Quartzite; sample F) and the footwall (Mount Adams Quartzite; sample 36) of the Paralana Fault is remarkably similar (Fig. ~~8~~9). Modelling of these zircon grain's geochemistry classifies the population as predominantly derived from felsic magmatism, but both units also have a small component of more mafic derived magmatic zircons of ca. ~~1650~~1660-1680 Ma and ca. ~~1700-1760~~1710-1780 Ma age.

Our data support the suggestion of comparable provenance for these units, and by extension, the Radium Creek Group across the fault. The most straightforward explanation is that entire group shares the same provenance. On this basis we interpret a source terrane for the Radium Creek Group that contains ca. 1595 Ma intermediate to felsic magmatic rocks and reworked older Archaean to Palaeoproterozoic mafic to felsic magmatic material.

In addition, a subordinate U-Pb population at ca. 1850 was discovered in both the Freeling Heights Quartzite (Sample F) and the Mount Adams Quartzite (sample 36). These quartzites have been previously interpreted as distinct units; the Mount Adams Quartzite forming an older unit in the stratigraphy (Coats and Blissett, 1971). The lower Freeling Heights Quartzite has also been interpreted to be significantly older than the upper Freeling Heights Quartzite and Mount Adams Quartzite on the basis of stronger deformation recorded in these lower horizons (Paul et al., 1999).

Our data suggest these differences in deformation intensity may be due to factors other than a time break, as the indistinguishable maximum depositional ages for these two units and the similarities in both the dominant and subordinate U-Pb detrital populations (i.e. ca. 1850 Ma) would suggest that these quartzites are likely to be lateral correlatives to each other. The greater deformation intensity observed within the lower parts of the Freeling Heights Quartzite could instead be explained by the location of the Freeling Heights Quartzite in the ~~hanging-wall~~hangingwall of the Paralana Fault, whilst the Mount Adams Quartzite is restricted to the footwall (Fig. ~~2~~3). Strain partitioning related to protracted shearing along the Paralana Fault is suggested to result in the development of more intense deformation in the proximal parts of hangingwall to the fault.

The lower horizons of the Freeling Heights Quartzite are slightly more micaceous than the upper part of the unit and to the Mount Adams Quartzite (Armit, 2007). In particular, proximal to the contact with the underlying Brindana Schist, the Freeling Heights Quartzite contains large micaceous pods in which strain has been localised during Mesoproterozoic and Palaeozoic deformation (Armit et al~~.~~., 2012) producing a stronger structural fabric than is evident at the meso-scale in the upper horizons of the Freeling Heights Quartzite and in the Mount Adams Quartzite. According to this single deposition framework the entire ca. 1595 Ma Radium Creek Group is deformed by ca. 1591-1585 Ma deformation~~ (D_1-D_2)~~ and is not sub-divided into pre- and post-deformational sequences (c.f. Fanning et al., 2003; Paul, 1998; Paul et al., 1999).

4.2 Whole rock geochemistry

Th/Sc ratios for ~~each of samples~~sample Z3 and sample F are higher than Post Archaean Australian Shale~~-~~ (PAAS, The/Sc = 0.91; Taylor & McLennan, 1985) which supports the interpretation from the in-situ zircon geochemistry that both of these samples were most likely sourced from a region dominated by felsic material (Bhatia & Cook 1986; Cullers & Berendsen 1998). The samples display moderately negative Eu/Eu* anomalies (0.41 for sample Z3 and 0.575 for sample F) when compared to PAAS (0.65; Taylor & McLennan, 1985). This indicates their source was also characterised by negative Eu anomalies, a ubiquitous ~~feature~~affinity of A-type magmatic suites. La/Yb_n ratios of 6.05 for sample Z3 indicate it is slightly LREE enriched. Sample F ~~(La/Yb_n value of 1.08) ~~displays significant HREE enrichment~~,~~ (La/Yb_n value of 1.08), which is most likely due to accumulation of previously mobile HREE in garnets that grew as a result of regional metamorphism at ca. 1591-~~155Ma~~1552Ma (Armit et al. 2012).

4.3 In-situ Hf Isotopes

Hf isotope signatures of the Radium Creek Group samples are fairly diverse and most likely reflect both ~~crustally ~~less evolved and substantially more evolved signatures (Fig. ~~7~~8a-b). Within each U-Pb age population, considerable overlap in the Hf isotope ratios is present across the ~~3~~three Mount

Painter samples (Table 3). ~~Our~~These data strengthens the argument that both the pelitic and more quartz-rich units of the Radium Creek Group are of the same provenance.

The ca. 1595 Ma U-Pb population within the Radium Creek Group samples (n=25, this study) in the northern Mount Painter Inlier is consistent with the spread in Hf isotope ratios of the Early Mesoproterozoic aged grains (n=4) in sample ARK661 ~~which is~~(Fig. 8c-d), from the southern Mount Painter Inlier (Elburg et al. 2012). This strengthens ~~support~~ for the interpretation of a similar provenance for all of the Early Mesoproterozoic metasediments in the Mount Painter Inlier. Our larger dataset both confirms the maximum depositional age for the Radium Creek Group, and demonstrates for the first time a clear bimodal ε Hf$_{(t)}$ signature for this population. Mixing between an evolved component (ε Hf$_{(1595)}$ -6.7 to -1.17, n=16) and a more juvenile component (ε Hf$_{(1595)}$ 0 to +2.79, n=9) is consistent with this pattern~~.~~ (Fig. 8d).

~~Due to the overwhelming preponderance of igneous derived detrital zircons, we are able to focus on magmatic packages. This allows robust comparison with neighbouring tectonic elements, which we now turn our attention to.~~

The magmatic pulse that generated the detrital source material of the Radium Creek Group must have contained a juvenile component, but also recrystallised more evolved material. Contemporaneous melting of various mantle and crust is consistent with the bimodal Hf isotope data in the resultant sedimentary packages. The Early Mesoproterozoic U-Pb age population peak (ca. 1595 Ma) within the age spectra of neighbouring felsic-dominated magmatic rocks; the upper Gawler Range Volcanics (sample YD23a), Frome Granite and Benagerie ~~Volcanics~~Volcanic Suite, therefore invite ε Hf$_{(t)}$ comparison with the Radium Creek Group~~.~~ (Fig. 8c).

The predominantly negative ε Hf$_{(1595Ma)}$ values (-4.51 to -0.82) of the upper Gawler Range Volcanics ~~zircon~~zircons (Fig. 8c) would suggest (prima facie) that it was formed from moderately evolved crustal material. However the single, positive ε Hf$_{(1595Ma)}$ value implies more juvenile material was also involved to a degree. Pankhurst et al. (2013) report whole-rock Hf data for the small volume mafic components of the Gawler Range Volcanics which record a more primitive signal ~~that~~than we observe within our zircon population. This demonstrates that a juvenile component of the Gawler Range Volcanics can be detected, and that its weak contribution to subsequent basin detritus may be muted by lack of mafic outcrop in the hinterland.

The Hf isotope signature of the upper Gawler Range Volcanics is ~~not dissimilar~~similar to that of the ca. 1595 Ma detrital zircons from the Radium Creek Group, as their absolute range of ε Hf$_{(1595Ma)}$ values overlap~~.~~ (Fig. 8c). However, the Radium Creek Group data extends to both more evolved and strongly negative ε $Hf_{(1595Ma)}$ values. This might reflect a sampling bias (e.g. Andersen et al. 2005) or that the source terrane of the Radium Creek Group ca. 1595 Ma zircon peak has a greater isotopic heterogeneity than the preserved Gawler Range Volcanics alone.

Zircon grains with ca. 1595 Ma ages from the Frome Granite (Bimbowrie Suite) indicate that this magma formed at least in part from reworked crust of ca. 2260-2670 Ma~~.~~ (Fig. 8c). The signature is similar to the range of ε $Hf_{(1595Ma)}$ values from the upper Gawler Range Volcanics grains, as they also record predominantly negative values to weakly positive (-5.29 to +1.02) (Fig. 8c). Similarly, this range of values falls within that of the Radium Creek Group. Importantly, >1650 Ma U-Pb populations are absent from our data. Moreover the Frome Granite intrusive age of 1594 ± 8 Ma (Jagodzinski and Fricke, 2010) would suggest that it would have been located within the crustal pile during the earliest Mesoproterozoic and hence unlikely to be actively eroding to provide the required detritus into a nascent ca. 1595 Ma basin now preserved in the Mount Painter Inlier.

The Hf isotope signature of the ca. 1595 Ma zircon populations in the Benagerie ~~Volcanics~~Volcanic Suite sample is defined by a relatively tightly clustered group of ε $Hf_{(1595Ma)}$ values (-1.73 to +4.0). This group is appreciably more juvenile than the ~~ranges~~values for the upper Gawler Range Volcanics and Frome Granite~~. Importantly, the range extends~~ (Fig. 8c). It is important to ~~more juvenile values than those recorded in zircon grains within~~note that unlike the Radium Creek Group~~.~~, we did not detect a more evolved and negative Hf component (-6 to -2) in this sample of Benagerie Volcanic Suite (Fig. 8c).

~~-~~The lack of a good match between the Benagerie ~~Volcanics~~Volcanic Suite and Radium Creek Groups zircon Hf isotope signature (Fig. 8c) implies that provenance of the metasediment within the Mount Painter Inlier is unlikely to include the Benagerie ~~Volcanics.~~Volcanic Suite. The ca. 1587 Ma crystallisation age calculated for this sample (Jagodzinski and Fricke, 2010) is also slightly younger ~~of~~than the maximum deposition age (ca. 1595 Ma) of the Radium Creek Group (although within analytical uncertainty). Rather, this age has greater similarity with the age of the Mount Neill Suite magmatism in the Mount Painter Inlier (ca. 1585 Ma). This suite intrudes the metasediments following an episode of burial and deformation at ca. 1595-1585 Ma (Armit et al., 2012). Thus if the Benagerie ~~Volcanics~~Volcanic Suite are extrusive equivalents of the magmatic pulse that generated the Mount Neill Suite, it would not be feasible for these rocks to contribute to the source of the Radium Creek Group.

Thus a combination of Hf isotope data and geologic evidence, effectively remove the Curnamona Province felsic magmatic rocks with ca. 1595 ages (Frome Granite and Benagerie ~~Volcanics~~Volcanic

Suite) from consideration as potential sources of the Radium Creek Group. The remaining sample is the Gawler Range Volcanics sample. The following discussion aims to explore this hypothesis.

The prominent ca. 1680-~~1650~~1660 Ma detrital zircon U-Pb population within the Radium Creek Group has a grouped ε $Hf_{(t)}$ value range of -9.91 to +5.8 (n=17). A similar spread of values is evident in ARK661 (Elburg et al., 2012) with ε $Hf_{(t)}$ values of between -7 to +6.7 (n=9) (Fig. 8c-d). A source terrane for this scattered and highly variable Hf isotope signature is likely to be ~~comprised~~composed of reworked, refractory ca. 3000-2400 Ma Archaean to Palaeoproterozoic crust which has mixed with significantly more isotopically primitive material ca. 1680-~~1650Ma~~1660Ma.

Two zircons from the upper Gawler Range Volcanics have U-Pb ages ca. 1655 Ma and therefore match the age peak within the Radium Creek Group. These two grains record slightly negative ε $Hf_{(t)}$ values. While these are within the ε $Hf_{(t)}$ range for the corresponding Radium Creek Group age peak; it is difficult to ascribe much significance given the size of the data subset.

No pre-1650 Ma U-Pb population was identified from either the Frome Granite or Benagerie Volcanic samples (Jagodzinski and Fricke, 2010). ~~The~~It is worth noting that the absence of a ca. ~~1650-80~~1660-1680 age peak in these samples ~~may also imply~~strengthens the argument that the pre-1650 Ma zircons in the Radium Creek Group cannot have been sourced from these magmatic suites.

Detrital zircons that define a U-Pb population at ca. 1710-~~1760~~1780 Ma in the Radium Creek Group have a relatively evolved Hf isotopic signature, although an appreciably juvenile signal is also present (ε $Hf_{(t)}$ ranges between -9.4 to +2.74; n=18). Any potential sources for this detritus are interpreted to be ~~comprised~~composed of predominantly reworked and refractory ca. 3030-2680 Ma Archaean to Palaeoproterozoic crust that has mixed with slightly more isotopically juvenile material (T_{DM}^{c} of 2280 Ma) at ca. 1710-~~1760 Ma. In all of the Radium Creek Group samples in this study, zircons analyses from this ca. 1710-1760 Ma U-Pb age bracket are spread between ca. 1711 Ma and ca. 1783 Ma (Fig. 5). Only a single analysis from the metasediment sample ARK661 (661-40) of Elburg et al. (2012) has a U-Pb age within this range (ca. 1711 Ma). This grain has a similar, distinctly evolved Hf signature (ε Hf = -10.4). The lack of other grains of similar age in this sample could be an artefact of small sample size (Andersen, 2005).~~1780 Ma.

~~Zircons from the ca. 1650-1680 and ca. 1710-1760 Ma populations in the Radium Creek Group which modelled as having mafic derived in-situ geochemistry affinities did not exhibit positive (more primitive) ε $Hf_{(t)}$ values. This would suggest that in terms of their isotope ratios, these mafic derived zircon grains reflect crustal contamination processes, or metasomatised mantle, rather than derivation from the depleted mantle.~~

The three zircons ca. 1710-~~1790~~1780 Ma from the upper Gawler Range Volcanics all record positive ε $Hf_{(t)}$ (+1.61 to +2.73), which is similar to the small (n=2; +0.08, +2.73) juvenile component within the ca. 1710-~~1760~~1780 Ma Brindana Schist of the Radium Creek Group~~.~~ (Fig. 8c). Unlike the Radium Creek Group however, we ~~were unable to find an~~did not detect a more evolved Hf component of ca. 1710-~~1760~~1780 Ma age in sample YD23a. Larger U-Pb-Hf ~~in~~ zircon datasets for the upper Gawler Range Volcanics may resolve this Hf isotope mis-match. ~~The complete lack of similar aged ca. 1710-1760 Ma inherited zircon populations in either the Frome Granite or Benagerie Volcanics further supports that they are unlikely to be the sole source of detrital zircons in the Radium Creek Group.~~

All of the ca. 1850 Ma zircons analysed (n=4) from the Radium Creek Group in this study have isotopically evolved Hf signatures, interpreted as reworked ca. 2680-2940 Ma Archaean material~~. A slightly older ca. 1904 Ma U-Pb population (n=2) from ARK661 have appreciably juvenile ε $Hf_{(t)}$ values (+3.02 & +4.53; Elburg et al. 2012), and reflect reworking of ca. 2280-2370 Ma Early Palaeoproterozoic crust.~~ (Fig. 8a). The ~~6~~six Hf isotope analyses ~~on~~from ca. 2500 Ma ~~zircons~~zircon grains have a ε $Hf_{(t)}$ value range between -5.15 and +1.29 reflecting reworked >2970 Ma Archaean crust. Archaean zircon in sample ARK661 (n=5) have overlapping to moderately more juvenile Hf isotopic signatures with respect to the other sample of Radium Creek Group and are characterised by ε $Hf_{(t)}$ values ranging between -0.35 and +4.12 (Fig. 8d) ($T_{DM}{}^{c}$ range of 2820-3110 Ma). This most likely reflects a large isotopic heterogeneity in the Archaean component of the source terrane for the metasediments in the Mount Painter Inlier.

It is important to note the small sample populations of zircon grains (n <4) representing the ca. 1710-1780 Ma and ca. 1850 Ma ages. It is therefore possible that the Hf isotopic signatures of these populations may not be truly representative.

4.4 Whole rock Nd isotopes

Whole rock Nd isotope ratios of the Freeling Heights Quartzite and Yaglin Phyllite units of the Radium Creek Group (Neumann, 2001; Schaefer, 1993) have been recalculated to 1595 Ma to reflect the maximum depositional age of these units determined in this study. The result is negative $\varepsilon Nd_{(1595)}$ values of -5.19 to -3.25 (Freeling Heights Quartzite) and -4.36 (Yaglin Phyllite). This is consistent with the predominantly negative in-situ Hf isotopic signature presented in this study for the ca. 1595 Ma Radium Creek Group.

The $\varepsilon Nd_{(1585)}$ values of the felsic upper Gawler Range Volcanics range from -4.3 to -1.8, and as such are indistinguishable from those of the Benagerie ~~Volcanics~~Volcanic Suite (Wade et al., 2012). The felsic rocks of the lower Gawler Range Volcanics contain more variable values of $\varepsilon Nd_{(1585)}$, and range from evolved ($\varepsilon Nd_{(1585)}$ of -7) to less evolved ($\varepsilon Nd_{(1585)}$ of -0.2) signals (Wade et al., 2012). The

Radium Creek Group contains slightly more evolved εNd$_{(1595)}$ (e.g. -5.19 for the Freeling Heights Quartzite) and disperse ε Hf$_{(1595)}$ values than the upper Gawler Range or Benagerie ~~Volcanics.~~Volcanic Suite. We suggest that isotopic correlation between the Radium Creek Group and the more diverse negative εNd$_{(1585)}$ values for the lower Gawler Range Volcanics is more consistent.

The in-situ zircon age spectra and contained ε Hf$_{(t)}$ coupled with geologic context and whole-rock εNd support a Gawler Craton dominated provenance for the Radium Creek Group. The Curnamona Province contains appropriate felsic magmatic rocks of a similar age to that of the maximum Radium Creek Group deposition age, however, several lines of evidence preclude a Curnamona Province provenance for the Radium Creek Group.

~~4.5 Proterozoic tectonic implications~~

4.5 Comparison with regional datasets

The present location of the Mount Painter Inlier within the northern South Australia Craton (Fig. 1a-b) and relative proximity to both the Curnamona Province and the Gawler Craton (Fig. 1c) merits isotopic comparison between these terranes and with the North Australian Craton. Disperse U-Pb-Hf isotopic signatures from the detrital zircons in the Radium Creek Group supports a more complex provenance than from any one of the proximal magmatic suites (e.g. upper Gawler Range Volcanics, Frome Granite and Benagerie ~~Volcanics~~Volcanic Suite) analysed in this study (Fig. ~~7c~~8c).

The combined detrital zircon patterns of the Radium Creek Group strongly argue for provenance from a terrane that includes ca. 1595 Ma, ca. ~~1650~~1660-1680 Ma, ca. 1710-~~1760~~1780 Ma, 1850 Ma and Earliest Palaeoproterozoic to Archaean magmatic rocks or significant inherited populations. Major magmatic events in eastern Early Mesoproterozoic Australia ca. 1595 Ma are also recorded in the Arunta Inlier with the ca. 1603-1615 Ma Burt-Rungutjirba Suite (Zhao and McCulloch, 1995; Zhao and Bennett, 1995), in the Musgrave Block with the Musgravian Gneiss (Gum and Belousova, 2006; Kirkland et al., In Press; Wade et al., 2006), and in the Curnamona Province with the ca. ~~1591-1596~~1600-1570 Ma Mundi Mundi, Cusin Creek plutons, Benagerie Volcanic Suite and Ninnerie Supersuite (Fanning et al., 1998; Jagodzinski and Fricke, 2010; Wade et al., ~~2012) which was accompanied by localised clastic deposition e.g. white sandstone in Bumbarlow 1 drillhole (Fraser and Neumann,~~ 2011;2012).~~2010).~~ The Gawler Craton magmatism ca. 1604-1583 Ma is dominated by the voluminous felsic Gawler Range Volcanics and Hiltaba Suite (Fanning et al., 1988; Fanning et al., 2007) and localised deposition of clastic sediments (e.g. the upper Corunna Conglomerate) (Daly et al., 1998). Sedimentation in the Early Mesoproterozoic is also recorded across the North Australian Craton including the Upper McNamara Group in the Mount Isa Inlier (Andrews, 1998; Krassay et al., 2000), the Favenc Package in the McArthur River area (Rawlings, 1999) and the Dargalong Metamorphics in the Georgetown Inlier (Withnall et al., 1997) (Fig. ~~1~~1b).

Palaeoproterozoic basin evolution is widespread and broadly comparable across eastern Australia characterised by the Leichhardt, Calvert and Isa Superbasins in the Mount Isa Inlier (Jackson et al., 2000), the Etheridge Group in the Georgetown Inlier (Withnall et al., 1988), Willyama Supergroup in the Curnamona Province (Conor and Preiss, 2008), and the metasediments preserved in the central and northern Gawler Craton (Hand et al., 2007; Payne et al., 2006; Szpunar et al., 2011). The basins in the Curnamona and Gawler Craton have been interpreted to have a predominantly evolved, felsic magmatic ca. 1710-~~1760~~1780 Ma Arunta (Barovich and Hand, 2008; Payne et al., 2006) or northern Gawler Craton provenance (Howard et al., 2011c). Hf isotope datasets that include these 1710-~~1760~~1780 Ma metasediments and felsic intrusives from the Fowler, Spencer, Olympic domains (Fig. 1c) of the Gawler Craton (Fig. 11a-b) (Belousova et al., ~~2006a; Belousova et al., 2009; Belousova et al., 2006c~~2009; Howard et al., 2011a; Howard et al., 2011b; Howard et al., 2011c~~) (Fig. 7e~~; Szpunar et al., 2011) closely correlate with the felsic derived 1710-~~1760~~1780 Ma zircons in the Radium Creek Group. This would suggest that ca. 1710-~~1760~~1780 Ma detrital zircons in the Radium Creek Group could have been sourced from felsic intrusives in the Gawler Craton (e.g. ca. 1736 Ma Middle Camp Granite and ca. 1755 Ma Wertigo Granite; Fanning et al. 2007; see Fig. 1c), re-worked ca. 1710-~~1760~~1780 Ma metasediments (e.g. Wallaroo Group and Moonabie Formation; see Fig. 1c) in the Gawler Craton, or from their protoliths in the northern Gawler Craton or Arunta Block.

However, potential ca. 1595 Ma felsic magmatic protoliths in the Arunta Block, such as the Burt-Rungutjirba Suite (Zhao, 1994) which has $\varepsilon Nd_{(1603-1615)}$ values of +0.91 to +2.49 is interpreted to be too juvenile to be a likely source of more evolved ca. 1595 Ma detritus in the Radium Creek Group. Moreover, comparison of the Hf isotopes of the Radium Creek Group detrital zircons with those of the Meso-Palaeoproterozoic Arunta Inlier (Hollis et al., 2010) shows little correlation between the disperse and generally negative, evolved ~~Hf~~$\varepsilon Hf_{(t)}$ in zircon characteristics ~~in~~of the Radium Creek Group ~~(Fig. 7a-d)~~ and the predominantly juvenile $\varepsilon Hf_{(t)}$ values for zircons from the Arunta region (Fig. ~~7h~~12a). This would imply that the direct ca. 1595 Ma source of the detritus in the Mount Painter Province is unlikely to be the Arunta Block but does not preclude the incorporation and assimilation of ca. 1710-1760 Ma Arunta derived material with more refractory Archaean to Palaeoproterozoic crust, in the potential source terrane for the Radium Creek Group.

Correlation of the Radium Creek Group with the available Hf isotopic datasets (modern drainage samples) for the Curnamona Province (Condie et al., 2005) (Fig. 12b) and Mount Isa Inlier (Griffin et al., 2006) (Fig. ~~7f~~12c) is plausible. The dataset for the Broken Hill Block of the Curnamona Province however, does not include any analysis ~~on~~of older Early Palaeoproterozoic or Archaean zircon grains~~.~~ (Fig. 12b). A number of authors (e.g. Cooper, 1985; Page et al., 2005) have indicated the existence of ~~older~~ Archaean to Palaeoproterozoic zircon populations in the Curnamona Province, but further Hf isotope work is required to provide robust comparison with the pre-1700 Ma zircons in the Radium Creek Group. The Late Palaeoproterozoic to Early Mesoproterozoic zircon grains that constitute this Broken Hill dataset (Fig. ~~7g~~12b) are characterised by predominantly more juvenile Hf isotopic values than the Radium Creek Group. This more isotopically juvenile Hf range is consistent with the primitive $\varepsilon Nd_{(1650)}$ values of -3 to 0 reported by Barovich et al. (2008) for the upper Willyama Supergroup for which a distinct south-western Laurentia (Barovich et al., 2008) or ~~south west~~southwest Baltica (Howard et al. 2011a) provenance has been proposed.

The U-Pb ages and Hf isotopic compositions from Mount Isa Inlier (Griffin et al., 2006) and Mount Painter Province metasediments reflect both Archaean and Palaeoproterozoic phases of crustal reworking~~.~~ (Fig. 11c). Mesoproterozoic magmatism in the Mount Isa Inlier did not initiate until ca. 1550 Ma with the emplacement of the Williams and Naraku Batholiths (Page and Sun, 1998). It is therefore problematic to consider any major magmatic suites in the Mount Isa Inlier as the ~~likely~~ source of the dominant ca. 1595 Ma magmatic derived zircon population in the Radium Creek Group.

Instead, it is plausible that the ca. 1595 Ma zircons in the Radium Creek Group could have been derived from 1595 ± 6 Ma, 1589 ± 3 Ma minor tuffaceous horizons in the Lawn Hill Formation and Balbirini Dolomite of the McArthur Basin (Page et al., 2000). However they would most likely represent volumetrically insignificant contributions if the Mount Isa Inlier or McArthur ~~Block~~Basin were actively eroding ca. 1595 Ma and shedding material into the Mount Painter Province. The zircon budget from these tuffs would likely be swamped by competing sources.

~~An increase in isotopically juvenile input ca. 1625 Ma in the Mount Isa dataset reflecting the emplacement of the mafic Toole Creek Volcanics (Griffin et al., 2006) is similar to the increasingly positive ε Hf$_{(t)}$ values in the Radium Creek Group ca. 1650-1680 Ma zircon population. In the Mount Painter Province, this increase in more isotopically juvenile material reflects a more felsic magmatic source based on the zircon geochemistry.~~ A paucity of isotopically juvenile felsic magmatism ca. ~~1650~~1660-1680 Ma in eastern Proterozoic Australia ~~telescopes~~reduces potential source correlations for the Radium Creek Group. The ca. 1680 Ma felsic Tunkilla Suite in the Gawler Craton (Fig. 1c) (Payne et al., 2010) which exhibits a large isotopic variation ($\varepsilon Nd_{(1680)}$ -6.3 to +2.6) is one possible exception. Erosion ca. 1595 Ma of a crustal pile that included this ca. 1680 Ma felsic material as well as more refractory Archaean to Palaeoproterozoic precursors is considered to be consistent with the isotopic fingerprint of the Radium Creek Group.

The ca. 1600-1540 Ma Musgravian Gneiss in the Musgrave Block, is characterised by juvenile Nd and Hf isotopic compositions that are too juvenile (Gum and Belousova, 2006; Kirkland et al., 2012; Wade et al., 2006) that are too juvenile to be considered as viable correlatives with the ca. 1595 Ma Radium Creek Group. Therefore, it is unlikely that the Radium Creek Group represents derivation from a proposed ca. 1600-1540 Ma magmatic arc in the Musgrave Block.

Correlation of the felsic magmatic-derived ca. 1850 Ma zircon grains in the Radium Creek Group is permissible with Hf datasets from the Gawler Hf datasetOlympic (Belousova et al.., 2009).) and Spencer domains (Szpunar et al., 2011) (Fig. 11a) of the Gawler Craton (Fig. 1c). These grains reflect the emplacement of the felsic Donington Suite (Fig. 1c) in the Gawler Craton (Drexel et al., 1995) which has ε Hf$_{(1850)}$ value range between -3.53 and +4.3 (using the Lu-Hf decay constant of 1.865E^{-11}/yr (Scherer et al. 2001) for values from- and +5 (Reid et al., 2008; Szpunar et al. 2011). These data indicate both reworking of the ca. 2500 Ma material as well as some juvenile input ca. 1850 Ma.

These data are not dissimilar fromsimilar to the ca. 1850 Ma Mount Isa Inlier Hf dataset (Fig. 12c) (Griffin et al. 2006) which- corresponds to the emplacement of the ca. 1856 Ma Kalkadoon Batholith and co-magmatic Leichardt Volcanics (Page, 1983), and reflects remelting of Late Archaean material ca. 2500 Ma. The ca. 1850 Ma event in the Mount Isa Inlier does, however, comprise a far greater degree of mafic rocks with very positive ε Hf$_{(1850)}$ and are isotopically similar to the depleted mantle at ca. 1850 Ma. No such mafic (Fig. 9) and primitive isotopic signature (Fig. 8a,d) was recordeddetected for zircons from the Radium Creek Group.

The Neoarchaean to Earliest Palaeoproterozoic zircon grains in the Radium Creek Group return a broad range of ε Hf$_{(t)}$ values (-5.15 to +4.12), consistent with derivation from a complex Archaean source terrane that comprises both reworked and juvenile components. Whilst this is largely similar to the Archaean Mount Isa Inlier (Fig. 12c; Griffin et al. 2006) and Gawler datasets (Griffin et al. 2006; Belousova et al., 2006,2009; Howard et al., 2011a,b;2011b), both the more evolved ε Hf$_{(t)}$ values and > ca. 2600 Ma U-Pb populations evident in sample ARK661 (Elburg et al., 2012)), are more consistent with derivation from average Archaean Gawler Craton crust. (Fig. 11a-b). This crustincludescrust includes the Meso-Neoarchaean Middleback Group (Szpunar et al., 2011),) preserved in Spencer and Cleve domains, granite gneisses (Fraser et al., 2010), and the Sleaford and Mulgathing complexes preserved in the Coulta and Christie domains of the Gawler Craton (Fig. 1c) (Cowley and Fanning, 1992; Fanning, 1997; Schaefer, 1998; Swain et al., 2005a).

Collectively the detrital zircon isotopic pattern of the Radium Creek Group requires a complex source terrane. This source must include a significant felsic Early Mesoproterozoic portion as well as

Neoarchaean to Palaeoproterozoic material that has undergone phases of Late Archaean to Early Mesoproterozoic re-working. This older material must itself have incorporated some juvenile components.

We consider the Gawler Craton to be the most plausible source for this composite signature of the ca. 1595 Ma Radium Creek Group. In this scenario, the Mount Painter Province is likely to be proximal to, and receiving material from, the eastern and central Gawler Craton at ca. 1595 Ma. The most probable source would be sub-aerial exposures of voluminous ca. 1595 Ma felsic material associated with the Gawler Range Volcanics ~~FLIP~~felsic large igneous province (FLIP) (Pankhurst et al., 2013), particularly zircon grains derived from the Lower Gawler Range Volcanics.

4.6 Proterozoic tectonic implications

Korsch et al. (2010) interpreted a distinctive seismic basement (termed the Warrakimbo Seismic Package) below the Mount Painter Province. We suggest that this basement is the eastern extension of the Gawler Craton and that the palaeo~~-~~-Paralana Fault represents the eastern extent of the Gawler Craton. The palaeo~~-~~-Paralana Fault is interpreted a moderately south-east-dipping, crustal-scale fault that separates the Warrakimbo and Yarramba seismic packages ~~(Korsch et al. 2010), suggesting that it represents~~and has been interpreted as a major crustal boundary~~.~~ (Korsch et al. 2010).

Since we now consider the Freeling Heights Quartzite and the Mount Adams Quartzite to be lateral equivalents and stitch the Paralana Fault, the age of the tectonic boundary (possibly a suture) between the Warrakimbo and Yarramba seismic packages must pre-date ca. 1595 Ma. ~~Given~~Further, the isotopic and geochemical similarities between the Upper Gawler Range Volcanics and the Benagerie Volcanic Suite (Wade et al., 2012~~),~~) suggests the lower crust in the footwall of the palaeo~~-~~-Paralana Fault may represent the same crustal sources (e.g. Pankhurst et al., 2013) of magmatism as the central Gawler Craton. The correlation of the upper Gawler Range Volcanics with the Benagerie ~~Volcanics~~Volcanic Suite in the Curnamona Province (Wade et al., ~~(~~2012) stitches the Gawler Craton and Curnamona Province together at ca.~~ 1587 Ma, and may suggest that the Mount Painter Province represents the eastern-most marginal terrane of the Gawler Craton prior to ca.~~ 1587 Ma.

An extensional event ca. 1595 Ma as suggested by Stewart and Betts (2010) is consistent with this scenario and supported by the interpretation by Korsch et al. (2010). In this scenario the Radium Creek Group was deposited within an extensional basin setting following the Olarian-Wartakan orogenic system~~.~~ (Page et al., 2005; Hand et al., 2007; Stewart and Betts, 2010). This ~~extensional~~tectonic system could be quite far-reaching~~ to~~, and include the Mount Woods Inlier and northern Gawler Craton (Cutts et al., 2011; Forbes et al., 2012) across southern Proterozoic Australia.

~~Rapid switching from extension to shortening and back to extension during the ca. 1595-1585 Ma interval suggests far-field plate margin influences on the tectonics of the Mount Painter Province (Armit et al. 2012).~~This extensional phase was followed by renewed crustal shortening and inversion of the Radium Creek Metamorphics (Armit et al., 2012), and may have affected the northern Gawler Craton (Kararan Orogeny: Hand et al., 2007), southern Curnamona Province (Rutherford et al., 2007), and the Mount Isa Inlier (e.g., Betts et al., 2006). Repeated rapid switching from extension to shortening at convergent plate margins is common during transient episodes of flat subduction (Gutscher et al., 2002) or when subduction roll-back is interrupted by accretion of buoyant material such as an ocean plateau (Rosenbaum et al., 2005; Mason et al., 2010), plume-head (Murphy et al., 1998; Betts et al., 2009; 2012), arc terrane (Boutelier et al., 2003) or continental micro-continent (Moresi et al., in review), which are all characterised by local trench advance and shortening in the overriding plate. We propose that during the ca. 1595-1555 Ma interval, the Mount Painter Inlier was located in the overriding plate of one or more subduction zones and was subjected to tectonic mode switches caused by disruption of a convergent margin.

~~The reconstructions of Betts & Giles (2006); Betts et al. (2002; 2009) and Wade et al. (2006) are consistent with a proximal plate margin. However, the stitching of the Gawler Craton and the Curnamona Province is inconsistent with the craton configuration of Wade et al. (2006). Data presented here does not conclusively support or preclude configurations proposed by Betts & Giles (2006); Betts et al. (2002; 2009); Cawood & Korsch (2008).~~

The palaeogeographic reconstructions of Betts & Giles (2006) (Fig. 2a); Betts et al. (2002; 2009), Cawood and Korsch et al. (2008) and Wade et al. (2006) (Fig. 2b) are consistent the Mount Painter Inlier being positioned proximal to one or more plate margins at ca. 1595 Ma. The configuration of Wade et al. (2006) does not have the Gawler Craton and the Curnamona Province co-located between ca. 1600-1580 Ma (Fig. 2b). The model of Wade et al. (2006) proposes that the Gawler Craton was positioned in the overriding plate of the south-dipping subduction zone prior to collision with the North Australian Craton at ca. 1590 Ma (Fig. 2b). In our reconstruction, the Curnamona Province is also required to be co-located with the Gawler Craton and therefore must have evolved in a back-arc setting on the overriding plate of a south dipping subduction zone and separated from the Mount Isa Inlier before ca. 1580 Ma (Fig. 2b). In this model, the Radium Creek Group would have been deposited in a back-arc setting and subsequent shortening resulted from collision between North and South Australian cratons at ca. 1560 Ma. However, separation between the North and South Australian cratons seems unlikely because of the well-established correlation of the ca.1720 to 1640 Ma basin systems between the Curnamona Province and North Australian Craton (Giles et al., 2002; Page et al., 2005; Conor and Priess, 2008; Gibson et al., 2008). We therefore consider a south-dipping subduction zone along the northern edge of the South Australian Craton highly unlikely at the beginning of the Mesoproterozoic.

The palaeogeographic reconstructions of Betts et al. (2002) and Betts and Giles (2006) consider that North and South Australian cratons to be contiguous at ca. 1600 Ma. The South Australian Craton was positioned between a long-lived accretionary convergent margin along the southern edge of the Australian continent (Betts et al., 2011), and a convergent margin along the eastern edge of the continent (Betts et al., 2002). Both these subduction zones are interpreted to dip towards the interior of the Australian continent (Betts et al., 2009). Superimposed on this complex tectonic setting is a major plume-related magmatic event (Betts et al., 2007; 2009). Tectonic interpretation of the evolution of the North Australian and South Australian cratons suggest that protracted episodes of high temperature metamorphism and continental basin systems formed in a back-arc setting (Giles et al., 2002; Cutts et al., 2013), which were interrupted by transient accretion events (Betts et al., 2011) at the plate margin. Betts et al., (2009) proposed that the Olarian-Wartaken orogenic event was driven by the accretion of a plume-head with the Australian continent, which was followed by an episode of crustal extension after the transfer of the plume to the overriding plate (see Betts et al., 2013), producing a voluminous FLIP (Pankhurst et al., 2013) and a hotspot track defined by dominantly A-type magmatism after ca. 1600 Ma (Betts et al., 2007). We suggest that the deposition of the Radium Creek Group occurred in an extensional basin sourced from the FLIP preserved on the Gawler Craton (Fig. 13a). The Radium Creek Group were buried to mid crustal levels and then exhumed to the upper crust between ca. 1592 and ca. 1585 Ma requiring rapid switches to crustal shortening (Fig. 13b) to renewed extension (Armit et al., 2012). This was followed by renewed crustal shortening at ca. 1570-1555 Ma (Rutherford et al., 2007; Armit et al., 2012) (Fig. 13c). We interpret the tectonic switching is driven by perturbations in the convergent margin. We are unable to assess the relative role of these convergent margins but may speculate that the earlier shortening events (ca. 1585 Ma) is related to accretion along the southern margin of the continent (Fig.13a-b), whereas ca. 1570-1555 Ma shortening is related to subduction along the eastern margin of the continent (Fig. 13c).

5 Conclusions

- The Radium Creek Group consists of a single stratigraphic package deposited in the Early Mesoproterozoic with a maximum deposition $^{207}Pb/^{206}Pb$ age of 1595.5 ± 3.7 Ma (n=41).
- The detrital zircon patterns in the Radium Creek Group are characterised by peaks at ca. 2500 Ma, ca. 1850 Ma, 1710-1760 Ma and 1650-1680 Ma. These are consistent with

~~major zircon forming episodes within the Gawler Craton (Belousova et al., 2009; Howard et al., 2011a; Howard et al., 2011b; Reid et al., 2008; Swain et al., 2005b).~~

The isotopic fingerprint of the Radium Creek Group requires a source with diverse but predominantly felsic character and evolved isotopic sources reflecting poly-phased crustal reworking from the Archaean to the Early Mesoproterozoic. Detrital zircon patterns in the Radium Creek Group that contains peaks at ca. 2500 Ma, ca. ~~This fingerprint is most~~1850 Ma, 1710-1780 Ma and 1660-1680 Ma. These ages are consistent with derivation from the Gawler Craton as opposed to other tectonic elements of eastern Proterozoic Australia~~.~~, suggesting the Curnamona Province and Gawler Craton were co-located at ca. 1595 Ma. The implication of this interpretation is that the North and South Australian cratons were contiguous at ca. 1595 Ma placing the Mount Painter Inlier at the nexus of two convergent margins characterised by subduction zones that dip towards the continent interior. Perturbations in the dynamics of these convergent margins resulted in rapid tectonic switches following deposition of the Radium Creek Group. Our data provides a critical constraint for palaeogeographic reconstruction for eastern Australia at the Palaeo- to Mesoproterozoic transition.

Formatted: Normal, No bullets or numbering

- ~~On the basis of its Early Mesoproterozoic Gawler provenance (this study), Mesoproterozoic architecture (Armit et al. 2012), and seismically distinctive basement (Korsch et al. 2010), we now consider the Mount Painter Province to be more consistent as an eastern marginal terrane of the Gawler Craton rather than as a north-eastern extension of the Curnamona Province.~~

6 Acknowledgements

We would like to thank the reviewers of this paper for providing constructive feedback. We are grateful to Heathgate Resources Pty Ltd for accommodation, access and company in the field. Marge and Doug Sprigg (Arkaroola station) are thanked for access and accommodation. Also thanks to Steve Hore and Wolfgang Preiss (Primary Industry and Resources, South Australia) for advice and base maps. We would also like to thank Caroline Venn, Massimo Raveggi, Kirsty Sheerin, Jerram Adams, Ahmed Saleem, Laurent Ailleres and Andy Tomkins (Monash University) for field support, ideas and discussions. Norm Pearson, Elenor Belousova and Rosanna Murphy (GEMOC) are thanked for their invaluable technical assistance. This work was supported in part by ARC LP0882000.

Figure Captions

~~Fig. 1: Map highlighting the location of the Mount Painter Inlier~~Fig. 1: a) Map of Australia showing the geography-based nomenclature after Myer et al. (1996) in which the continent is divided into three major cratonic units, called the North, West and South Australian cratons draped over a composite of the bouguer gravity and first vertical derivative of the total magnetic intensity (TMI) map of Australia (geophysical data provided by Geoscience Australia); b) Map highlighting the location of the Mount Painter Block and other eastern Australian Proterozoic terranes in relation to the major geological provinces of Australia. These are draped across a composite total magnetic intensity (TMI) anomaly and first vertical derivative of the TMI map of Australia. This magnetic image was produced using a two kilometre grid spacing and by applying a low pass filter (upward continued six kilometres), which highlights the longer wavelengths/major structural elements of eastern Australia. Data provided by Geoscience Australia~~.~~; c). Map showing the position of the Mount Painter Province (grey box) in respect to the major domains and Archaean to Mesoproterozoic geology of the Curnamona Province after Conor and Preiss (2008) and the Gawler Craton modified after Fairclough et al. (2003) and Hand et al. (2007).

~~Fig. 2~~Fig 2: a) Palaeogeographical reconfiguration model after Giles et al. (2004); Betts and Giles (2006) supporting a shared history for the South Australian Craton and the North Australian Craton between ca. 1800 and 1550 Ma. This configuration aligns contemporaneous orogenic belts across the Gawler Craton, Arunta Inlier, Mount Isa Inlier and the Curnamona Province.; b) Palaeogeographical reconfiguration model after Wade et al. (2006) in which the Gawler Craton and Curnamona Province are separated by a south-dipping subduction zone between ca.1600-1580 Ma with the Gawler Craton positioned in the overriding plate.

Fig. 3: Map of the Mount Painter Inlier showing sample locations and regional geology after Armit et al. (2012).

Fig. ~~3~~4: a) Photograph of the steeply dipping, foliated psammopelites of the Brindana Schist unit at the base of Radium Creek Group, geo-pick shown for scale (~~Sample~~sample Z3 363800E 6675681N); b) Photo-micrograph of a thin section of ~~Sample~~sample Z3 from the Brindana Schist in cross-polarised light ~~(363800E 6675681N) from the Brindana Schist~~, cut normal to the S_3 foliation. This view demonstrates overprinting, spaced foliations defined by muscovite ± biotite fabrics (sub-horizontal in photo-micrograph) and recrystallised polygonal quartz aggregate (microlithons); c) Photograph of the intensely crenulated, micaceous quartzite outcrop of the Freeling Heights Quartzite (~~Sample~~sample F 357632E 6673138N); d) Photo-micrograph of a thin section of the Freeling Heights Quartzite in cross-polarised light ~~(Sample F 357632E 6673138N).~~. The section, taken normal to the S_3 foliation, highlights a spaced schistosity defined by muscovite with elongate relic quartz grains which display undulose extinction. A discrete crenulation cleavage overprints the existing schistosity; e) Photograph of quartzite ~~unitof~~unit of the Freeling Heights Quartzite (~~Sample~~sample 123 355996E, 6672099N). Cross-beds defined by heavy ~~mineral assemblages~~minerals and distinct compositional layering (compare with bottom right of picture) record reverse grading. This indicates that younging is upwards and towards the west (head of the geo-pick is orientated E-W); f) Photo-micrograph of ~~Sample~~sample 123 in cross-polarised light ~~(355996E, 6672099N).~~. The section was cut normal to the S_3 foliation and highlights two spaced and overprinting foliations defined by biotite ± muscovite and polygonal quartz-rich microlithons; g) Photograph of the fine-grained pinky-grey micaceous quartzite outcrop of the Mount Adams Quartzite (Sample 36; 357161E, 6668472N). Cross beds defined by heavy ~~mineral assemblages~~minerals indicate upward younging; h) Photo-micrograph of ~~Sample~~sample 36 in cross-polarised light shows fine grained muscovite, sercite and quartz-rich assemblage. A sub-horizontal spaced foliation, defined by fine-grained micaceous material, overprints an earlier mica fabric with polygonal undulose quartz and

Formatted: Subscript

Formatted: Subscript

biotite microlithons; i) Photograph of a hand specimen from the Pondanna member of the upper Gawler Range Volcanics (573593E, 6405524N) showing porphyritic texture with phenocrysts of quartz and feldspar within a dark, aphanitic groundmass; j) Photo-micrograph of Sample YD23a from the Pondanna member of the upper Gawler Range Volcanics (573593E, 6405524N), section shows phenocrysts of k-feldspar, quartz, and ~~clinopyroxene~~pyroxene within a fine grained matrix .

Fig. ~~4~~5: Cathodoluminescence and ~~Back~~back scatter electron images (a-d & e-j respectively of ~~example~~representive zircon grains from each sample analysed in this study. The region ablated during analysis is indicated; a) ~~Cathodoluminescence image of~~ Z1-29a,b zircon grains from sample Z3 (Brindana Schist). Z1-29a grain has a U-Pb age 1659 ±15 Ma and an εHf value of+5.80, Z1-29b grain has a U-Pb age of 1604 ± 16 Ma and a εHf value of -6.1; b) ~~Cathodoluminescence image of~~ Z3-24 zircon grain from sample Z3 (Brindana Schist). This grain has a U-Pb age of 2369 ± 28 Ma and an εHf value of-4.89; c) ~~Cathodoluminescence image of~~ F6 zircon grain from sample F (Freeling Heights Quartzite). This grain has a U-Pb age of 1670 ± 10 Ma and an εHf value of +0.01; d) ~~Cathodoluminescence image of~~ F9 zircon grain from sample F (Freeling Heights Quartzite). This grain has a U-Pb age of 2539 ± 28 Ma and an εHf value of +1.29; e) ~~Back scatter electron image of~~ 36-13 zircon grain from sample 36 (Mount Adams Quartzite). This grain has a U-Pb age of 1596 ± 8 Ma and an εHf value of -1.79; f) Back scatter electron image of 36-10 zircon grain from sample 36 (Mount Adams Quartzite). This grain has a U-Pb age of 1678 ± 29 Ma and an εHf value of -1.64; g) ~~Back scatter electron image of~~ 123-17 zircon grain from sample 123 (Freeling Heights Quartzite). This ~~grainhas~~grain has a U-Pb age of 1589 ± 9 Ma; h)~~ Back scatter electron image of~~ 123-1 zircon grain from sample 123 (Freeling Heights Quartzite). This grain has a U-Pb age of 1712 ± 8 Ma; i) ~~Back scatter electron image of~~ YD23a-7 zircon grain from sample YD23a (uGRV). This grain has a U-Pb age of 1596.2 ± 36 Ma and an εHf value of -2.74; j) ~~Back scatter electron image of~~ YD23a-27 zircon grain from sample YD23a (uGRV). This grain has a U-Pb age of 1597.6 ± 47 Ma and ~~an~~a εHf value of -4.5.

Fig. ~~5~~6: a) Probability plot of detrital zircons analysed from sample Z3. Inset: weighted mean $^{207}Pb/^{206}Pb$ (2σ) age plot for the youngest population in this sample, interpreted as the maximum depositional age.; b) Concordia plot for zircons analysed from sample Z3 ;c) Probability plot of detrital zircons analysed from sample F. Inset: weighted mean $^{207}Pb/^{206}Pb$ (2σ) age plot for the maximum depositional age of this sample; c) ~~Zircons~~Zircon grains from sample F plotted on a U-Pb concordia plot; d) Concordia plot for zircons analysed from sample F; e) Detrital zircon probability plot from sample 123. Inset: weighted mean age $^{207}Pb/^{206}Pb$ ages (2σ) for the maximum depositional age ; ~~e~~f) Concordia diagram for zircons analysed from sample 123; ~~f~~g) Probability plots for zircon analysed from sample 36. Inset: weighted mean $^{207}Pb/^{206}Pb$ ages (2σ) for the maximum depositional age for this sample; ~~g~~h) U-Pb concordia plot for ~~zircons~~zircon analysed from sample 36.

Fig. ~~6:~~7: Weighted mean $^{207}Pb/^{206}Pb$ ages plot for sample YD23a showing the dominant population and older inherited grains. Inset: Tera-Wasserburg concordia plot shows the concordant (<10% discordant) analyses, as well as all data >10% discordant from this sample. Data error ellipses and error bars used are 1σ.

Fig. ~~7: Plots~~8: a) Plot of ε $Hf_{(t)}$ versus $^{207}Pb/^{206}Pb$ ages for the Radium Creek Group samples; b) Plot of T_{DM}^{c} versus $^{207}Pb/^{206}Pb$ ages for the Radium Creek Group samples; c) Plot of ε $Hf_{(t)}$ versus $^{207}Pb/^{206}Pb$ ages for the Radium Creek Group samples including values for ARK661 sample from Elburg et al. (2012~~). Fields~~) compared with the values for the upper Gawler ~~(Belousova et al. 2009), Isa (Griffin et al. 2006), Broken Hill (Condie et al. 2005~~Range Volcanics, uGRV from the Gawler Craton (sample YD23a), and ~~Arunta (Hollis et al. 2010) terranes are~~the Frome Granite of the Bimbowrie Suite (sample FG12) and Benagerie Volcanic Suite (sample BV) from the Curnamona Province (see Fig. 1c-d for sample locations). Insert shows a plot of T_{DM}^{c} versus $^{207}Pb/^{206}Pb$ ages for these samples; d) Field for the Radium Creek Group ε $Hf_{(t)}$ values plotted as gridded density and data points for comparison.
~~All U-Pb dates shown as $^{207}Pb/^{206}Pb$ ages, Hf isotope values recalculated using a decay constant of~~

Formatted: Font: +Body

Formatted: Font: +Body

~~$1.865E10^{-11}$/yr.~~ Density ~~grids for the Radium Creek Group, Gawler, Isa and Broken Hill are~~grid constructed using cell size of 20 ~~Myrs~~Myr in the X direction and 0.5 ε Hf units in the Y direction, a threshold level of 0.05 and a smoothing level of 3.

Fig. ~~8~~9: Comparison of zircon crystallisation rock type, modelled from in-situ trace chemistry after Belousova et al. (2002) to determine the source rock type of zircon grains across the Paralana Fault. Sample F (357632E 6673138N) is from the Freeling Heights Quartzite to the west (Hangingwall) of the Paralana Fault. Sample 36 (357161E, 6668472N) is from the Mount Adams Quartzite to the east (Footwall) of the Paralana Fault. The modelled source rock type is predominantly felsic and indistinguishable across the Paralana Fault.

Fig. ~~9~~10: Stratigraphic and structural framework of the Mount Painter Inlier using data from this study and Armit et al. (2012). Proterozoic magmatic ages determined using U-Pb geochronology by LA-ICPMS and SHRIMP where available. Mount Neill Granite and porphyry age from Teale (1987, unpublished), Elburg et al. (2003), Neumann (2001), Neumann et al. (2009) and Fraser and Neumann (2010). Northern Gawler tectonism from Payne et al. (2008), Fanning et al. (2007), Thomas et al. (2008), Swain et al. (2005b) and Skirrow et al. (2007). Southern Gawler tectonism from Stewart and Betts (2010), Webb et al. (1986) and Parker et al. (1993). Southern Curnamona Province tectonism from Conor and Preiss (2008), Forbes et al. (2008), Betts et al. (2002), Stüwe and Ehlers (1997), Forbes and Betts (2004), Forbes et al. (2004), Stevens et al. (1988), Wilson and Powell (2001), Page et al. (2000, 2005), Rutherford et al. (2007), Marjoribanks et al. (1980) and Clarke et al. (1987, 1995). Georgetown tectonism from Black et al. (1979), Withnall et al. (1996), Hills (2004), Cihan et al. (2006), Davis (1996), Betts et al. (2009), Boger and Hansen (2004), Black and Withnall (1993), Black et al. (1998), Withnall et al. (1988), Withnall et al. (1996), Blewett et al. (1998) and Bell and Rubenach (1983). Tectonism in the Eastern Fold Belt of the Mount Isa Inlier from Betts et al. (2006), MacCready et al. (1998), Giles et al. (2006a), O'Dea et al. (2006), Page and Sun (1998), Giles and Nutman (2002), Hand and Rubatto (2002), Giles and Nutman (2003), De Jong and Williams (1995), Betts et al. (2006), Connors and Page (1995) and O'Dea et al. (1997). West Fold Belt tectonism from O'Dea and Lister (1995), O'Dea et al. (1997), Lister et al. (1999), Hand and Rubatto (2002), Connors and Page (1995), O'Dea et al. (1997), MacCready et al. (1998), Betts et al. (2006) and Blenkinsop et al. (2008). Tectonism in the Arunta Block after (Claoué-Long et al., 2008; Collins and Shaw, 1995; Collins and Williams, 1995; Maidment et al., 2005; Scrimgeour et al., 2005). Stratigraphy after Armit and Betts(2011) and references therein.

Fig. 11: a) Plot of ε $Hf_{(t)}$ versus $^{207}Pb/^{206}Pb$ ages for Archaean to Mesoproterozoic zircon populations for the major domains of the Gawler Craton from Belousova et al. (2009); Howard et al. (2009;2010;2011a;2011b); Szpunar et al. (2011), compared with the samples from the Radium Creek Group (this study); b) Field for the Gawler Craton ε $Hf_{(t)}$ values from Belousova et al. (2009); Howard et al. (2009;2010;2011a;b); Szpunar et al. (2011) plotted as gridded density and data points for comparison with the samples from the Radium Creek Group plotted as points. Density grid constructed using cell size of 20 Myr in the X direction and 0.5 ε Hf units in the Y direction, a threshold level of 0.05 and a smoothing level of 3.

Fig. 12: a) Plot of ε $Hf_{(t)}$ versus $^{207}Pb/^{206}Pb$ ages for Archaean to Mesoproterozoic zircon populations from the Arunta Block (Hollis et al. 2010) displayed as a gridded density field compared with the samples from the Radium Creek Group shown as points; b) Plot of ε $Hf_{(t)}$ versus $^{207}Pb/^{206}Pb$ ages for Archaean to Mesoproterozoic zircon populations from the Broken Hill Block of the Curnamona Province (Condie et al. 2005) displayed as a gridded density field, compared with the samples from the Radium Creek Group shown as points; c) Plot of ε $Hf_{(t)}$ versus $^{207}Pb/^{206}Pb$ ages for Archaean to Mesoproterozoic zircon populations from the Broken Hill Block of the Mount Isa Inlier (Griffin et al. 2006) displayed as a gridded density field compared with the samples from the Radium Creek Group

Formatted: Font: +Body

Formatted: Font: +Body

Formatted: Space After: 10 pt, Adjust space between Latin and Asian text, Adjust space between Asian text and numbers shown as points. All U-Pb dates shown as $^{207}Pb/^{206}Pb$ ages, Hf isotope values recalculated using a decay constant of 1.865E10^{-11}/yr. ~~Table 1~~Density grids for the Radium Creek Group, Gawler Craton, Curnamona Province and Mount Isa Inlier are constructed using cell size of 20 Myrs in the X direction and 0.5 ε Hf units in the Y direction, a threshold level of 0.05 and a smoothing level of 3.

Fig 13: a) Palaeogeographical reconstruction of eastern Proterozoic Australia at ca. 1595 Ma adapted after Giles et al. (2004); Betts and Giles (2006); Betts et al. (2006;2007;2009). In this model the Radium Creek Group are deposited in an extensional back-arc basin and sourced from the Felsic large igneous province (FLIP) preserved on the Gawler Craton; b) Rapid tectonic switching to shortening ca. 1585 Ma and back to extension is driven by perturbations in the convergent margins along the southern margin of Australia; c) Renewed crustal shortening at ca. 1555 Ma is related to subduction along the eastern margin of the continent.

Table 1: Lu-Hf values for standards run to determine instrumentation precision and accuracy.

Table 2: U-Pb values for standards run during the study acquisition period and longer-term averages indicating the level of reproducibility and instrument stability obtained.

~~Table 2: Lu-Hf values for standards run for to determine instrumentation precision and accuracy.~~

Table 3: Summary of the U-Pb dating and Hf isotope analysis.

Table 4: ~~Modelled~~Zircon crystallisation rock type, modelled rock type from in-situ trace element chemistry~~.~~ after Belousova et al. (2002).

Formatted: Line spacing: single

References

Allen, S.R., Simpson, C.J., McPhie, J., Daly, S.J., 2003. Stratigraphy, distribution and geochemistry of widespread felsic volcanic units in the Mesoproterozoic Gawler Range Volcanics, South Australia. Australian Journal of Earth Sciences 50, 97-112.

Anderson, T., 2002. Correction of common Pb in U– Pb analyses that do not report 204Pb.Chemical Geology 192, 59-79.

Andersen, T., 2005. Detrital zircons as tracers of sedimentary provenance: limiting conditions from statistics and numerical simulation. Chemical Geology 216, 249-270.

Andrews, S.J., 1998. Stratigraphy and depositional setting of the upper McNamara Group, Lawn Hills region, Northwest Queensland. Economic Geology 93, 1132 – 1152.

Armit, R.J., Betts, P.G., 2011. Proterozoic Eastern Australia Time-Space Plot, in: Beeston, J.W. (Ed.), Geological Survey of Queensland, North-West Queensland Mineral and Energy Province Report. Queensland Department of Employment, Economic Development and Innovation, Brisbane, pp. 1-123.

Armit, R.J., Betts, P.G., Schaefer, B.F., Ailleres, L., 2012. Mesoproterozoic and Palaeozoic constraints on long-lived poly-deformation in the northern Mount Painter Inlier. Gondwana Research 22, 207-226.

Barovich, K., Hand, M., 2008. Tectonic setting and provenance of the Paleoproterozoic Willyama Supergroup, Curnamona Province, Australia: Geochemical and Nd isotopic constraints on contrasting source terrain components. Precambrian Research 166, 318-337.

Bell, T.H., Rubenach, M.J., 1983. Sequential porphyroblast growth and crenulation cleavage development during progressive deformation. Tectonophysics 92, 171-194.

Belousova, E., Griffin, W., O'Reilly, S., Fisher, N., 2002. Igneous zircon: trace element composition as an indicator of source rock type. Contributions to Mineralogy and Petrology 143, 602-622.

Belousova, E.A., Preiss, W.V., Schwarz, M.P., Griffin, W.L., 2006a. Tectonic affinities of the Houghton Inlier, South Australia: U-Pb and Hf-isotope data from zircons in modern stream sediments. Australian Journal of Earth Sciences 53, 971 - 989.

Belousova, E.A., Reid, A.J., Griffin, W.L., O'Reilly, S.Y., 2006b. Proterozoic rejuvenation of the Archean Crust tracked by U-Pb and Hf-isotopes in Detrital Zircon. Geochimica et Cosmochimica Acta 70, A44-A44.

Belousova, E.A., Reid, A.J., Schwarz, M.P., Griffin, W.L., Fairclough, M.C., 2006c. Crustal evolution of the Gawler Craton, South Australia: Application of the TerraneChron technique to detrital zircon from modern stream sediments,South Australia. Department of Primary Industries and Resources, pp. 1-198.

Belousova, E.A., Reid, A.J., Griffin, W.L., O'Reilly, S.Y., 2009. Rejuvenation vs. recycling of Archean crust in the Gawler Craton, South Australia: Evidence from U-Pb and Hf isotopes in detrital zircon. Lithos 113, 570-582.

Betts, P.G., Giles, D., Lister, G.S., ~~Frick~~Fricke, L.R., 2002. Evolution of the Australian lithosphere. Australian Journal of Earth Sciences 49, 661-695.

Betts, P.G., Giles, D., 2006. The 1800-1100 Ma tectonic evolution of Australia. Precambrian Research 144, 92-125.

Betts, P.G., Giles, D., Mark, G., Lister, G.S., Goleby, B.R., Aillères, L., 2006. Synthesis of the Proterozoic evolution of the Mt Isa Inlier. Australian Journal of Earth Sciences 53, 187-211.

Betts, P.G., Giles, D., Schaefer, B.F., Mark, G., 2007. 1600-1500 Ma hotspot track in eastern Australia: Implications for Mesoproterozoic continental reconstructions. Terra Nova 19, 496-501.

Betts, P.G., Giles, D., Foden, J., Schaefer, B.F., Mark, G., Pankhurst, M.J., Forbes, C.J., Williams, H.A., Chalmers, N.C., Hills, Q., 2009. Mesoproterozoic plume-modified orogenesis in eastern Precambrian Australia. Tectonics 28.

Bizzarro, M., Baker, J.A., Haack, H., Ulfbeck, D., Rosing, M., 2003. Early history of Earth's crust–mantle system inferred from hafnium isotopes in chondrites. Nature 421, 931-933.

Black, L.P., Gulson, B.L., 1978. The age of the Mud Tank carbonatite, Strangways Range, Northern Territory. Bureau of Mineral Resources. Journal of Australian Geology and Geophysics 3, 227–232.

Black, L.P., Bell, T.H., Rubenach, M.J., Withnall, I.W., 1979. Geochronology of discrete structural-metamorphic events in a multiply deformed precambrian terrain. Tectonophysics 54, 103-137.

Black, P.M., Gregory, P., Withnall, I.W., Bain, J.H.C., 1998. U-Pb zircon age for the Etheridge Group, Georgetown region, north Queensland: implications for relationship with Broken Hill and Mt Isa sequences. Australian Journal of Earth Sciences 45, 925-935.

Blenkinsop, T.G., Huddlestone-Holmes, C.R., Foster, D.R.W., Edmiston, M.A., Lepong, P., Mark, G., Austin, J.R., Murphy, F.C., Ford, A., Rubenach, M.J., 2008. The crustal scale architecture of the Eastern Succession, Mount Isa: The influence of inversion. Precambrian Research 163, 31-49.

Blewett, R.S., Black, L.P., Sun, S.S., Knutson, J., Hutton, L.J., Bain, J.H.C., 1998. U-Pb zircon and Sm-Nd geochronology of the Mesoproterozoic of Northern Queensland: implications for a Rodinian Connection with the Belt supergroup of North America. Precambrian Research 89, 101-127.

Blichert-Toft, J., Albarede, F., 1997. The Lu–Hf isotope geochemistry of chondrites and the evolution of the mantle–crust system. Earth and Planetary Science Letters 148, 243-258.

Blichert-Toft, J., Chauvel, C., Albarède, F., 1997. Separation of Hf and Lu for high-precision isotope analysis of rock samples by magnetic sector-multiple collector ICP-MS. Contributions to Mineralogy and Petrology 127, 248-260.

Blissett, A.H., Creaser, R.A., Daly, S.J., Flint, R.B., Parker, A.J., 1993. Gawler Range Volcanics, in: Drexal, J.F., Preiss, W.V., Parker, A.J. (Eds.), The Geology of South Australia, Volume 1: The Precambrian. Geological Survey of South Australia Bulletin, pp. 107-124.

Boger, S.D., Hansen, D., 2004. Metamorphic evolution of the Georgetown Inlier, northeast Queensland, Australia; evidence for an accreted Palaeoproterozoic terrane? Journal of Metamorphic Geology 22, 511-527.

Cawood, P.A., Nemchin, A.A., Leverenz, A., Saeed, A., Balance, P.F., 1999. U/Pb dating of detrital zircons: Implications for the provenance record of Gondwana margin terranes. Geological Society of America Bulletin 111, 1107-1119.

Cawood, P.A., Korsch, R.J., 2008. Assembling Australia: Proterozoic building of a continent. Precambrian Research 166, 1-35.

Cihan, M., Evins, P., Lisowiec, N., Blake, K., 2006. Time constraints on deformation and metamorphism from EPMA dating of monazite in the Proterozoic Robertson River Metamorphics, NE Australia. Precambrian Research 145, 1-23.

Claoué-Long, J., Maidment, D., Hussey, K., Huston, D., 2008. The duration of the Strangways Event in central Australia: Evidence for prolonged deep crust processes. Precambrian Research 166, 246-262.

Coats, R.P., Blissett, A.H., 1971. Regional and economic geology of the Mount Painter province.South Australian Geological Survey Bulletin 43.

Clarke, G.L., Guiraud, M., Powell, R., Burg, J.P., 1987. Metamorphism in the Olary Block, South Australia: compression with cooling in a Proterozoic fold belt. Journal of Metamorphic Geology 5, 291–306.

Clarke, G.L., Powell, R., Vernon, R.H., 1995. Reaction relationships during retrograde metamorphism at Olary, South Australia. J. Metam. Geol 13, 715–726.

Collins, W.J., Shaw, R.D., 1995. Geochronological constraints on orogenic events in the Arunta Inlier: a review. Precambrian Research 71, 315-346.

Collins, W.J., Williams, I.S., 1995. SHRIMP ionprobe dating of short-lived Proterozoic tectonic cycles in the northern Arunta Inlier, central Australia. Precambrian Research 71, 69-89.

Condie, K.C., Beyer, E., Belousova, E., Griffin, W.L., O'Reilly, S.Y., 2005. U-Pb isotopic ages and Hf isotopic composition of single zircons: The search for juvenile Precambrian continental crust. Precambrian Research 139, 42-100.

Conor, C.H.H., Preiss, W.V., 2008. Understanding the 1720-1640 Ma Palaeoproterozoic Willyama Supergroup, Curnamona Province, Southeastern Australia: Implications for tectonics, basin evolution and ore genesis. Precambrian Research 166, 297-317.

Cooper, 1985. Inherited zircons in the Mundi Mundi Granite, Broken Hill, New South Wales. Australian Journal of Earth Sciences 32, 467-470.

Cowley, W.M., Fanning, C.M., 1992. Low-grade Archaean Metavolcanics in the northern Gawler Craton. The geological survey of south Australia. Q. Geol. 119, 2-17.

Cutts, K., Hand, M., Kelsey, D.E., 2011. Evidence for early Mesoproterozoic (ca. 1590Ma) ultrahigh-temperature metamorphism in southern Australia. Lithos 124, 1-16.

Daly, S.J., Fanning, C.M., Fairclough, M.C., 1998. Tectonic evolution and exploration potential of the Gawler Craton, South Australia. AGSO Journal of Australian Geology & Geophysics 17, 145-168.

Davis, B.K., 1996. Biotite porphyroblast nucleation and growth: Control by microfracture of pre-existing foliations in schists in the Robertson River Metamorphics. Geol. Mag. 133, 91 – 102.

De Jong, G., Williams, P.J., 1995. Giant metasomatic system formed during exhumation of mid-crustal Proterozoic rocks in the vicinity of the Cloncurry Fault, northwest Queensland. . Australian Journal of Earth Sciences 42, 281 – 290.

Drexel, J.F., Preiss, W., Parker, A., Australia, G.S.o.S., Meridional, A., 1995. The Geology of South Australia. Department of Mines and Energy.

Elburg, M.A., Bons, P.D., Dougherty-Page, J., Janka, C.E., Neumann, N., Schaefer, B., 2001. Age and metasomatic alteration of the Mt Neil Granite at Nooldoonooldoona waterhole, Mt Painter Inlier, South Australia. Australian Journal of Earth Sciences 48, 721-730.

Elburg, M.A., Bons, P.D., Foden, J., Brugger, J., 2003. A newly defined Late Ordovician magmatic-thermal event in the Mt Painter Province, northern Flinders Ranges, South Australia. Australian Journal of Earth Sciences 50, 611-631.

Elburg, M.A., Andersen, T., Bons, P.D., Weisheit, A., Simonsen, S.L., Smet, I., 2012. Metasomatism and metallogeny of A-type granites of the Mt Painter-Mt Babbage Inliers, South Australia. Lithos 151, 83-104.

Fairclough, M.C., Schwarz, M.P., Ferris, G.M., 2003. Interpreted crystalline basement geology of the Gawler Craton. South Australia Geological Survey: Special Map, 1:1000000.

Fanning, C.M., Flint, R.B., Parker, A.J., Ludwig, K.R., Blissett, A.H., 1988. Refined Proterozoic evolution of the Gawler Craton, South Australia, through U-Pb zircon geochronology. Precambrian Research 40-41, 363-386.

Fanning, C.M., 1997. Geochronological synthesis of Southern Australia. , Part II. The Gawler Craton. . South Australia Department of Mines and Energy.

Fanning, C.M., Ashley, P.M., Cook, M.D.J., Teale, G., Conor, C.H.H., 1998. A geochronological perspective of crustal evolution in the Curnamona Province, in: Gibson, G.M. (Ed.), Broken Hill Exploration Initiative: Abstracts of Papers Presented at the 4th Annual Meeting in Broken Hill. Australian Geological Survey Organisation, pp. 30–35.

Fanning, C.M., Reid, A.J., Teale, G.S., 2007 A geochronological framework for the Gawler Craton, South Australia. S. Aust. Geol. Survey Bull 55.

Forbes, C.J., Betts, P.G., 2004. Development of type 2 fold interference patterns in the Broken Hill Block: implications for strain partitioning across a detachment during the Olarian Orogeny. Australian Journal of Earth Sciences 51, 173-188.

Forbes, C.J., Giles, D., Jourdan, F., Sato, K., Omori, S., Bunch, M., 2012. Cooling and exhumation history of the northeastern Gawler Craton, South Australia. Precambrian Research 200-203, 209-238.

Fraser, G.L., Neumann, N.L., 2010. New SHRIMP U-Pb zircon ages from the Gawler Craton and Curnamona Province, South Australia, 2008 – 2010. Geoscience Australia.

Fraser, G., McAvaney, S., Neumann, N., Szpunar, M., Reid, A., 2010. Discovery of early Mesoarchean crust in the eastern Gawler Craton, South Australia. Precambrian Research 179, 1-21.

Gibson, G.M., Rubenach, M.J., Neumann, N.L., Southgate, P.N., Hutton, L.J., 2008. Syn- and post-extensional tectonic activity in the Palaeoproterozoic sequences of Broken Hill and Mount Isa and its bearing on reconstructions of Rodinia. Precambrian Research 166, 350-369.

Giles, D., Nutman, A.P., 2002. SHRIMP U-Pb monazite dating of 1600-1580 Ma amphibolite facies metamorphism in the southeastern Mt Isa Block, Australia. Australian Journal of Earth Sciences 49, 455-465.

Giles, D., Nutman, A.P., 2003. SHRIMP U-Pb zircon dating of the host rocks of the Cannington Ag-Pb-Zn deposit, southeastern Mt Isa Block, Australia. Australian Journal of Earth Sciences 50, 295-309.

Giles, D., Betts, P.G., Lister, G.S., 2004. 1.8-1.5-Ga links between the North and South Australian Cratons and the Early-Middle Proterozoic configuration of Australia. Tectonophysics 380, 27-41.

Giles, D., Ailleres, L., Jeffries, D., Betts, P., Lister, G., 2006a. Crustal architecture of basin inversion during the Proterozoic Isan Orogeny, Eastern Mount Isa Inlier, Australia. Precambrian Research 148, 67-84.

Giles, D., Betts, P.G., Ailleres, L., Hulscher, B., Hough, M., Lister, G.S., 2006b. Evolution of the Isan Orogeny at the southeastern margin of the Mt Isa Inlier. Australian Journal of Earth Sciences 53, 91-108.

Griffin, W.L., Wang, X., Jackson, S.E., Pearson, N.J., O’Reilly, S.Y., Xu, X., Zhou, X., 2002. Zircon chemistry and magma mixing, SE China: In-situ analysis of Hf isotopes, Tonglu and Pingtan igneous complexes. Lithos 61, 237-269.

Griffin, W.L., Belousova, E.A., Shee, S.R., Pearson, N.J., O'Reilly, S.Y., 2004. Archean crustal evolution in the northern Yilgarn Craton: U-Pb and Hf-isotope evidence from detrital zircons. Precambrian Research 131, 231-282.

Griffin, W.L., Belousova, E.A., Walters, S.G., O'Reilly, S.Y., 2006. Archaean and Proterozoic crustal evolution in the Eastern Succession of the Mt Isa district, Australia: U-Pb and Hf-isotope studies of detrital zircons. Australian Journal of Earth Sciences 53, 125-149.

Gum, J., Belousova, E., 2006. Musgrave province reconnaissance using TerraneChron. ASEG Extended Abstracts 1, 1-7.

Gutscher, M.-A., Malod, J., Rehault, J.-P., Contrucci, I., Klingelhoefer, F., Mendes-Victor, L., Spakman, W., 2002. Evidence for active subduction beneath Gibraltar. Geology 30, 1071-1074.

Halilovic, J., Cawood, P.A., Jones, J.A., Pirajno, F., Nemchin, A.A., 2004. Provenance of the Earaheedy Basin: implications for assembly of the Western Australian Craton. Precambrian Research 128, 343-366.

Hand, M., Rubatto, D., 2002. The scale of the thermal problem in the Mount Isa Inlier. Geol. Soc. Aust. Abst. 67.

Hand, M., Reid, A., Jagodzinski, L., 2007. Tectonic Framework and Evolution of the Gawler Craton, Southern Australia. Economic Geology 102, 1377-1395.

Hills, Q.G., 2004. The tectonic evolution of the Georgetown Inlier., School of Geosciences. Monash University, Melbounre.

Hollis, J.A., Beyer, E.E., Whelan, J.A., Kemp, A.I.S., Scherstén, A., Greig, A., 2010. Summary of results. NTGS laser U-Pb and Hf geochronology project: Pine Creek Orogen, Murphy Inlier, McArthur Basin and Arunta Region, July 2007–June 2008. . Northern Territory Geological Survey, Record 2010-001.

Howard, K.E., Hand, M., Barovich, K.M., Belousova, E., 2011a. Provenance of late paleoproterozoic cover sequences in the central Gawler Craton: Exploring stratigraphic correlations in eastern proterozoic Australia using detrital zircon ages, Hf and Nd isotopic data. Australian Journal of Earth Sciences 58, 475-500.

Howard, K.E., Hand, M., Barovich, K.M., Payne, J.L., Belousova, E.A., 2011b. U-Pb, Lu-Hf and Sm-Nd isotopic constraints on provenance and depositional timing of metasedimentary rocks in the western Gawler Craton: Implications for Proterozoic reconstruction models. Precambrian Research In Press, Corrected Proof, 43-62.

Howard, K.E., Hand, M., Barovich, K.M., Payne, J.L., Cutts, K.A., Belousova, E.A., 2011c. U–Pb zircon, zircon Hf and whole-rock Sm–Nd isotopic constraints on the evolution of Paleoproterozoic rocks in the northern Gawler Craton. Australian Journal of Earth Sciences 58, 615-638.

Jackson, M.J., Scott, D.L., Rawlings, D.J., 2000. Stratigraphic framework for the Leichhardt and Calvert Superbasins: review and correlations of the pre-1700 Ma successions between Mt Isa and McArthur River. Australian Journal of Earth Sciences 47, 381-403.

Jackson, S.E., Pearson, N.J., Griffin, W.L., Belousva, E.A., 2004. The application of laser ablation-inductively coupled plasma-mass spectrometry to in situ U-Pb zircon geochronology. Chemical Geology 211, 47-69.

Jagodzinski, E.A., Fricke, C.E., 2010. Compilation of new SHRIMP U-Pb geochronological data for the southern Curnamona Province, South Australia 2010., Report Book 2010/00014. Department of Primary Industries and Resources.

Kirkland, C.L., Smithies, R.H., Woodhouse, A.J., Howard, H.M., Wingate, M.l.T.D., Belousova, E.A., Cliff, J.B., Murphy, R.C., Spaggiari, C.V., In Press. Constraints and deception in the isotopic record; the crustal evolution of the west Musgrave Province, central Australia. Gondwana Research.

Korsch, R.J., Kositcin, N., 2010. South Australian Seismic and MT Workshop 2010/10. Geoscience Australia Record, 2010/10.

Korsch, R.J., Preiss, W., Blewett, R., Fabris, A., Neumann, N., Fricke, C.E., Fraser, G.L., Holzschuh, J., Jones, L.E.A., 2009. The 2008 north-south oriented, deep seismic reflection transect across the Curnamona Province, South Australia. Broken Hill Exploration Initiative: Abstracts for the 2009 Conference. 2009/28, 90-100.

Korsch, R.J., Preiss, W.V., Blewett, R.S., Fabris, A.J., Neumann, N.L., Fricke, C.E., Fraser, G.L., Holzschuh, J., Milligan, P.R., Jones, L.E.A., 2010. Geological interpretation of deep seismic reflection and magnetotelluric line 08GA-C1: Curnamona Province, South Australia. Geoscience Australia, Record. 2010 10, 42-53.

Krassay, A.A., Bradshaw, B.E., Domagala, J., Jackson, M.J., 2000. Siliciclastic shoreline to growth-faulted turbiditic sub-basins: the Proterozoic River Supersequence of the upper McNamara Group on the Lawn Hill Platform, Northern Australia. Australian Journal of Earth Sciences 47, 533 – 562.

Kromkhun, K., Foden, J., Hore, S., Baines, G., 2013. Geochronology and Hf isotopes of the bimodal mafic-felsic high heat producing igneous suite from Mt Painter Province, South Australia. Gondwana Research.

Formatted: German (Germany)

Lister, G.S., O'Dea, M.G., Somaia, I., 1999. A tale of two synclines: rifting, inversion and transpressional popouts at Lake Julius, northwestern Mt Isa terrane, Queensland. Australian Journal of Earth Sciences 46, 233-250.

MacCready, T., Goleby, B.R., Goncharov, A., Drummond, B.J., Lister, G.S., 1998. A Framework of Overprinting Orogens Based on Interpretation of the Mount Isa Deep Seismic Transect. Economic Geology 93, 1422-1434.

Maidment, D.W., Hand, M., Williams, I.S., 2005. Tectonic cycles in the Strangways Metamorphic Complex, Arunta Inlier, central Australia: Geochronological evidence for exhumation and basin formation between two high-grade metamorphic events. Australian Journal of Earth Sciences 52, 205-215.

Marjoribanks, R.W., Rutland, R.W.R., Glen, R.A., Laing, W.P., 1980. The Structure and Tectonic Evolution of the Broken-Hill Region, Australia. Precambrian Research 13, 209-240.

McLaren, S., Dunlap, W.J., Sandiford, M., McDougall, I., 2002. Thermochronology of high heat-producing crust at Mount Painter, South Australia: Implications for tectonic reactivation of continental interiors. Tectonics 21.

McLaren, S., Sandiford, M., Powell, R., Neumann, N., Woodhead, J., 2006. Palaeozoic Intraplate Crustal Anatexis in the Mount Painter Province, South Australia: Timing, Thermal Budgets and the Role of Crustal Heat Production. Journal of Petrology 47, 2281-2302.

Nelson, D.R., 2001. An assessment of the determination of depositional ages for ~~precambrian~~Precambrian clastic sedimentary rocks by U-Pb dating of detrital zircons. Sedimentary Geology 141-142, 37-60.

Neumann, N., 2001. Geochemical and isotopic characteristics of South Australian Proterozoic granites: implications for the origin and evolution of high heat-producing terrains., Department of Geology and Geophysics. University of Adelaide., Adelaide.

Neumann, N., Hore, S., Fraser, G., 2009. New SHRIMP geochronology from the Mount Painter Province, South Australia, in: Korsch, R.J. (Ed.), Broken Hill Exploration Initiative: Abstracts for the 2009 Conference. Geoscience Australia.

Nowell, G.M., et al., 1998. High precision Hf isotope measurements of MORB and OIB by thermal ionisation mass spectrometry: insights into thed epleted mantle. Chemical Geology 149, 211-233.

O'Dea, M.G., Lister, G.S., 1995. The role of ductility contrast and basement architecture in the structural evolution of the Crystal Creek block, Mount Isa Inlier, NW Queensland, Australia. Journal of Structural Geology 17, 949-960.

O'Dea, M.G., Lister, G.S., Betts, P.G., Pound, K.S., 1997. A shortened intraplate rift system in the Proterozoic Mount Isa terrane, NW Queensland, Australia. Tectonics 16, 425-441.

O'Dea, M.G., Betts, P.G., MacCready, T., Aillères, L., 2006. Sequential development of a mid-crustal fold-thrust complex: evidence from the Mitakoodi Culmination the eastern Mt Isa Inlier, Australia. Australian Journal of Earth Sciences 53, 69-90.

Ogilvie, J., 2006. U-Pb detrital zircon dating of structural and stratigraphic relationships within Hidden Valley, Mount Painter Inlier: Implications for Proterozoic crustal evolution of Eastern Australia., Geosciences. Monash University p. 40.

Page, R., 1983. Timing of superposed volcanism in the Proterozoic Mount Isa inlier, Australia. Precambrian Research 21, 223-245.

Page, R.W., Sun, S.S., 1998. Aspects of geochronology and crustal evolution in the Eastern Fold Belt, Mt Isa Inlier. Australian Journal of Earth Sciences 45, 343–361.

Page, R.W., Jackson, M.J., Krassay, A.A., 2000. Constraining sequence stratigraphy in north Australian basins: SHRIMP U-Pb zircon geochronology between Mt Isa and McArthur River. Australian Journal of Earth Sciences 47, 431-459.

Page, R.W., Conor, C.H.H., Stevens, B.P.J., Gibson, G.M., Preiss, W.V., Southgate, P.N., 2005. Correlation of Olary and Broken Hill Domains, Curnamona Province; possible relationship to Mount Isa and other north Australiam Pb-Zn-Ag-bearing successions. Economic Geology and the Bulletin of the society of Economic geologists 100, 663-676.

Pankhurst, M.J., Schaefer, B.F., Betts, P.G., Phillips, N., Hand, M., 2011a. A Mesoproterozoic continental flood rhyolite province, the Gawler Ranges, Australia: The end member example of the Large Igneous Province clan. Solid Earth 2, 25-33.

Pankhurst, M.J., Schaefer, B.F., and Betts, P.G. 2011b. Geodynamics of rapid voluminous felsic magmatism through time. Lithos 123 92-101.Pankhurst, M.J., Schaefer, B.F., Turner, S.P., Argles, T., Wade, C.E., 2013. The source of A-type magmas in two contrasting settings: U–Pb, Lu–Hf and Re–Os isotopic constraints. Chemical Geology 315, 175-194.

Parker, A.J., Preiss, W.V., Rankin, L.R., 1993. Geological Framework, in: Drexal, J.F., Preiss, W.V., Parker, A.J. (Eds.), The geology of South Australia, Volume 1: The Precambrian. Geological Survey of South Australia Bulletin, pp. 9-23.

Paul, E., 1998. Geometry and controls on basement-involved deformation in the Adelaide Fold Belt, South Australia. PhD Thesis, Adelaide University.

Paul, E., Flottmann, T., Sandiford, M., 1999. Structural geometry and controls on basement-involved deformation in the northern Flinders Ranges, Adelaide Fold Belt, South Australia. Australian Journal of Earth Sciences 46, 343-354.

Payne, J.L., Barovich, K.M., Hand, M., 2006. Provenance of metasedimentary rocks in the northern Gawler Craton, Australia: Implications for Palaeoproterozoic reconstructions. Precambrian Research 148, 275-291.

Payne, J.L., Hand, M., Barovich, K.M., Wade, B.P., 2008. Temporal constraints on the timing of high-grade metamorphism in the northern Gawler Craton: implications for assembly of the Australian Proterozoic. Australian Journal of Earth Sciences 55, 623 - 640.

Payne, J.L., Ferris, G., Barovich, K., Hand, M., 2010. Pitfalls of classifying ancient magmatic suites with tectonic discrimination diagrams: An example from the Paleoproterozoic Tunkillia Suite, southern Australia. Precambrian Research 177, 227-240.

Preiss, W., Korsch, R.J., Blewett, R.S., Fomin, T., Cowley, W.M., Neumann, N.L., Meixer, A.J., 2010. Geological interpretation of deep seismic reflection line 09GA-CG1: the Curnamona Province-Gawler Craton Link Line, South Australia, Geoscience Australia, Record. 10, 66-76.

Rawlings, D.J., 1999. Stratigraphic resolution of a multiphase intracratonic basin system: the McArthur Basin, northern Australia. Australian Journal of Earth Sciences 46, 703-723.

Reid, A., Hand, M., Jagodzinski, E., Kelsey, D., Pearson, N., 2008. Paleoproterozoic orogenesis in the southeastern Gawler Craton, South Australia. Australian Journal of Earth Sciences 55, 449 - 471.

Rutherford, L., Hand, M., Barovich, K., 2007. Timing of Proterozoic metamorphism in the southern Curnamona Province: implications for tectonic models and continental reconstructions. Australian Journal of Earth Sciences 54, 65-81.

Schaefer, B.F., 1993. Isotopic and geochemical constraints on Proterozoic crustal growth from the Mount Painter Inlier. Adelaide University Honours Thesis.

Schaefer, B.F., 1998. Insights into Proterozoic tectonics evolution from the Southern Eyre Peninsula, South Australia. University of Adelaide.

Scherer, E., Munker, C., Mezger, K., 2001 Calibration of the lutetium–hafnium clock. Science 293, 683–687.

Scrimgeour, I.R., Kinny, P.D., Close, D.F., Edgoose, C.J., 2005. High-T granulites and polymetamorphism in the southern Arunta Region, central Australia: Evidence for a 1.64 Ga accretional event. Precambrian Research 142, 1-27.

Shafton, R.A., 2006. A metamorphic and geochemical analysis of the Hidden Valley Region, Mount Painter Inlier, South Australia: implications for stratigraphy and orogenic evolution. ~~,~~School of Geosciences. Monash University, Melbourne.

Skirrow, R.G., Bastrakov, E., Barovich, K., Fraser, G.L., Creaser, R.A., Fanning, C.M., Raymond, O.L., Davidson, G.J., 2007. Timing of iron oxide Cu–Au–(U) hydrothermal activity and Nd isotope constraints on metal sources in the Gawler Craton, South Australia. ~~Econ. Geol.~~Economic Geology 102, 1441-1470

Soderlund, U., Patchett, J.P., Vervoort, J.D., Isachsen, C.E., 2004. The Lu-176 decay constant determined by Lu–Hf and U–Pb isotope systematics of Precambrian mafic intrusions. Earth and Planetary Science Letters 219, 311-324.
Stevens, B.P.J., Burton, G.R., 1998. The early to late Proterozoic Broken Hill Province, New South Wales. Journal of Australian Geology and Geophysics 17, 75-86.
Stewart, J.R., Betts, P.G., 2010. Late Paleo-Mesoproterozoic plate margin deformation in the southern Gawler Craton: Insights from structural and aeromagnetic analysis. Precambrian Research 177, 55-72.
Stewart, K., Foden, J., 2001. Mesoproterozoic granites of South Australia. Department of Geology & Geophysics, University of Adelaide, Adelaide.
Swain, G., Woodhouse, A., Hand, M., Barovich, K., Schwarz, M., Fanning, C.M., 2005a. Provenance and tectonic development of the late Archaean Gawler Craton, Australia; U-Pb zircon, geochemical and Sm-Nd isotopic implications. Precambrian Research 141, 106-136.
Swain, G.M., Hand, M., Teasdale, J., Rutherford, L., Clark, C., 2005b. Age constraints on terrane-scale shear zones in the Gawler Craton, southern Australia. Precambrian Research 139, 164-180.
Swain, G., Barovich, K., Hand, M., Ferris, G., Schwarz, M., 2008. Petrogenesis of the St Peter Suite, southern Australia: Arc magmatism and Proterozoic crustal growth of the South Australian Craton. Precambrian Research 166, 283-296.
Szpunar, M., Hand, M., Barovich, K., Jagodzinski, E., Belousova, E., 2011. Isotopic and geochemical constraints on the Paleoproterozoic Hutchison Group, southern Australia: Implications for Paleoproterozoic continental reconstructions. Precambrian Research 187, 99-126.
Teale, G.S., Flint, R.B., 1993. Curnamona Craton and Mount Painter Province, in: Drexal, J.F., Preiss, W.V., Parker, A.J. (Eds.), The geology of South Australia, Volume 1; The Precambrian. Geological Survey of South Australia Bulletin, pp. 147-149.
Teale, G.S., 1993. Geology of the Mount Painter and Mount Babbage Inliers, in: Drexal, J.F., Preiss, W.V., Parker, A.J. (Eds.), The geology of South Australia, Volume 1; the Precambrian. Geological Survey of South Australia Bulletin, pp. 149-156.
Teasdale, J., 1993. Proterozoic tectonic models with application to the Mount Painter Inlier. Adelaide University Honours Thesis.
Thomas, J.L., Direen, N.G., Hand, M., 2008. Blind orogen: Integrated appraisal of multiple episodes of Mesoproterozoic deformation and reworking in the Fowler Domain, western Gawler Craton, Australia. Precambrian Research 166, 263-282.
Van Archerbergh, E., Ryan, C.G., Griffin, W.L., 1999. GLITTER: on-line interactive data reduction for the laser ablation ICP –MS microprobe. In: Proceedings of the 9th V. M. Goldschmidt Conference, 305.
Wade, B.P., Barovich, K.M., Hand, M., Scrimgeour, I.R., Close, D.F., 2006. Evidence for Early Mesoproterozoic Arc Magmatism in the Musgrave Block, Central Australia: Implications for Proterozoic Crustal Growth and Tectonic Reconstructions of Australia. The Journal of Geology 114, 43-63.
Wade, C.E., 2011. Definition of the Mesoproterozoic Ninnerie Supersuite, Curnamona Province, South Australia. MESA Journal 62, 35-52.
Wade, C.E., Reid, A.J., Wingate, M.T.D., Jagodzinski, E.A., Barovich, K., 2012. Geochemistry and geochronology of the c. 1585 Ma Benagerie Volcanic Suite, southern Australia: Relationship to the Gawler Range Volcanics and implications for the petrogenesis of a Mesoproterozoic silicic large igneous province. Precambrian Research 206–207, 17-35.
Webb, A.W., Thomson, B.P., Blissett, A.H., Daly, S.J., Flint, R.B., Parker, A.J., 1986. Geochronology of the Gawler Craton, South Australia. Australian Journal of Earth Sciences:~~ An International Geoscience Journal of the Geological Society of Australia~~ 33, 119 - 143.
Wiedenbeck, M., Allé, P., Corfu, F., Griffin, W.L., Meier, M., Oberli, F., Von Quadt, A., Roddick, J.C., Spiegel, W., 1995. Three natural zircon standards for U–Th–Pb, Lu–Hf, trace element and REE analyses. Geostandards Newsletter 19, 1–23.

Wilson, C.J.L., Powell, R., 2001. Strain localisation and high-grade metamorphism at Broken Hill, Australia: a view from the Southern Cross area. Tectonophysics 335, 193-210.

Withnall, I.W., Bain, J.H.C., Draper, J.J., MacKenzie, D.E., Oversby, B.S., 1988. Proterozoic stratigraphy and tectonic history of the Georgetown Inlier, northeastern Queensland. Precambrian Research 40-41, 429-446.

Withnall, I.W., Golding, S.D., Rees, I.D., Dobos, S.K., 1996. K-Ar dating of the Anakie Metamorphic Group: evidence for an extension of the Delamerian Orogeny into central Queensland. Australian Journal of Earth Sciences 43, 567-572.

Withnall, I.W., MacKenzie, D.E., Denaro, T.J., Bain, J.H.C., Oversby, B.S., Knutson, J., Donchak, P.J.T., Champion, D.C., Wellman, P., Cruikshank, B.I., Sun, S.S., Pain, C.F., 1997. Georgetown Region, in: Bain, J.H.C., Draper, J.J. (Eds.), North Queensland Geology. Australian Geological Survey Organisation Bulletin/Queensland Department of Mines and Energy Qld pp. 19-116.

Wulser, P.A., 2009. Uranium metallogeny in the North Flinders Ranges region of South Australia School of Earth and Environmental Sciences. University of Adelaide, Adelaide, p. 179.

Zhao, J.-X., 1994. Geochemical and Sm-Nd isotopic study of amphibolites in the southern Arunta Inlier, central Australia: evidence for subduction at a Proterozoic continental margin. Precambrian Research 65, 71-94.

Zhao, J.X., Bennett, V.C., 1995. SHRIMP U-Pb zircon geochronology of granites in the Arunta Inlier, central Australia: implications for Proterozoic crustal evolution. Precambrian Research 71, 17-43.

Zhao, J.-X., McCulloch, M.T., 1995. Geochemical and Nd isotopic systematics of granites from the Arunta Inlier, central Australia: implications for Proterozoic crustal evolution. Precambrian Research 71, 265-299.

Table 1

Table 1

Analysis No.	$^{176}Lu/^{177}Hf$	$^{176}Yb/^{177}Hf$
91500-263	0.00031	0.010689
91500-10-28	0.000334	0.015847
91500-10-28	0.000334	0.015847
91500-262	0.000312	0.011659
91500 average	0.000322	0.01351
MT8	0.000129	0.006351
MT3	0.000061	0.002555
MT-10-141	0.000023	0.001197
MT-10-147	0.000023	0.001014
MT9	0.000151	0.006771
MT2	0.000141	0.006
MT4	0.000114	0.004514
MT-10-1045	0.000058	0.002614
MT-10-1046	0.000134	0.007539
MT-10-1047	0.000134	0.007145
MT-10-746	0.000128	0.00598
MT-10-745	0.000119	0.005629
MT-10-727	0.000102	0.005138
MT-10-744	0.000149	0.008101
Mudtank average	0.000105	0.005039

Table 2

Table 2

Sample	Method	207Pb/206Pb	± 2 σ
Mud Tank a)	TIMS		
Jackson et al. 2004 (73 values) b)	LAM-ICPMS	736	7
This study (17 values)	LAM-ICPMS	749	13
91500 c)	TIMS	1065.4	0.3
Jackson et al. 2004 (83 values) b)	LAM-ICPMS	1068	6
This study (18 values)	LAM-ICPMS	1072	12
This study (5 values)	LAM-ICPMS	1067	17

Weighted mean ages in Ma and reported with 2 σ error.

a)Mud Tank TIMS age from Black and Gulson (1978).

b)Long term ages from LAM-ICPMS at GEMOC (Jackson et al., 2004).

c)91500 TIMS age from Wiedenbeck et al. (1995).

Table 3

Table 3

Sample	$^{207}Pb/^{206}Pb$ population	Age type	$\varepsilon Hf_{(t)}$ range
Z3	ca. 1595 Ma	Max dep	-6.7 to +2.77
Z3	1630-1690 Ma	Detrital population	-4.21 to +5.8
Z3	1710-1760 Ma	Detrital population	-6.58 to +2.74
Z3	1790-1850 Ma	Detrital population	-4.9 to -2.89
Z3	2300-2500 Ma	Detrital population	-4.89 to -1.11
Z3	ca. 2900 Ma	Detrital population	+7.27
F	ca.1595 Ma	Max dep	-6.11 to +2.44
F	ca. 1680 Ma	Detrital population	-9.91 to 0
F	ca. 1730 Ma	Detrital population	-9.4 to -0.53
F	ca. 1841 Ma	Detrital population	-2.56
F	ca. 2500 Ma	Detrital population	-5.15 to +1.29
36	ca. 1595 Ma	Max dep	-5.37 to +2.79
36	ca. 1680 Ma	Detrital population	-3.82 to -1.07
36	1710-1740 Ma	Detrital population	-3.63 to -2.07
36	ca. 1850 Ma	Detrital population	-6.32 to -3.24
36	ca. 2500 Ma	Detrital population	-2.77 to -0.93
36	ca. 2948 Ma	Detrital population	-9.46
RCG grouped			
	ca. 1595 Ma	Max dep	-6.7 to +2.79
	ca. 1660-1680 Ma	Detrital population	-9.91 to +5.8
	ca. 1710-1780 Ma	Detrital population	-9.4 to +2.74
	ca. 1850 Ma	Detrital population	-6.32 to -2.56
	ca. 2500 Ma	Detrital population	-5.15 to +1.29
YD23a	ca. 1595 Ma	Crystallisation	-4.51 to +3.01
YD23a	ca. 1680 Ma	Inherited	-1.14 to -0.98
YD23a	ca. 1760 Ma	Inherited	+1.61 to+ 2.43
YD23a	ca. 1793 Ma	Inherited	+2.73
YD23a	ca. 1955 Ma	Inherited	+2.81
FG12	ca. 1557 Ma	?	+5.96
FG12	ca. 1594 Ma	Crystallisation	-5.29 to +1.02
FG12	ca. 1640 Ma	Inherited	-2.7
BV	ca. 1587 Ma	Crystallisation	-1.73 to +4.0

Table 4

Table 4

Analysis No.	$^{207}Pb/^{206}Pb$ age (Ma)	$\varepsilon Hf_{(t)}$	Lu (ppm)	Hf (wt%)
Freeling Heights Quartzite				
F217	1596	2.440156	52.7089	1.148022
F218	1571	-7.83882	73.74621	1.089765
F5	1652	-9.90644	91.14652	1.284635
F6	1670	0.002682	96.96011	1.212131
F212	1679	-0.57732	114.0913	1.004032
F7	1703	-5.12109	41.04014	1.258517
F220	1717	-6.0367	75.11273	0.863858
F213	1727	-9.48304	110.8835	1.178974
F4	1732	-4.64357	42.17228	0.886923
F214	1736	-5.67648	152.9471	1.179822
F219	1739	-5.77617	70.22908	1.107149
F2	1743	-0.52651	168.4766	1.214675
F223	1755	-7.28026	86.62932	1.06424
F215	1841	-2.5559	86.25845	1.515122
F8	2532	-5.15289	57.69946	1.242744
F9	2539	1.294357	87.61727	1.105029
Mount Adams Quartzite				
36_10	1678	-1.64	97.6505	1.014038
36_11	1873	-6.32115	121.7584	1.17643
36_35	2948	-9.45523	115.2526	0.906342
36_13	1596	-1.79517	69.46603	1.056693
36_12	1624	-5.37101	80.68111	1.180331
36_15	2466	3.401276	102.6962	1.37571
36_16	1680	-3.8181	90.38005	0.970706
36_17	1671	-1.07311	111.0748	1.677768
36_18	1711	-3.3586	96.14368	0.983765
36_14	1714	-3.42383	122.0813	1.106979
36_2	2519	-2.7661	143.2733	1.416838
36_6	2479	-0.93406	91.94859	1.283618
36_19	1697	-2.06505	146.4794	1.243507
36_7	1739	-3.62661	137.8884	1.155739
36_20R	1585	0.906116	101.2873	1.483322
36_3	1575	2.791108	96.43351	1.211707
36_4	1850	-3.23558	59.27636	1.049909
36_5	1586	-1.36469	221.7525	1.266997

Figure 1

Click here to download high resolution image

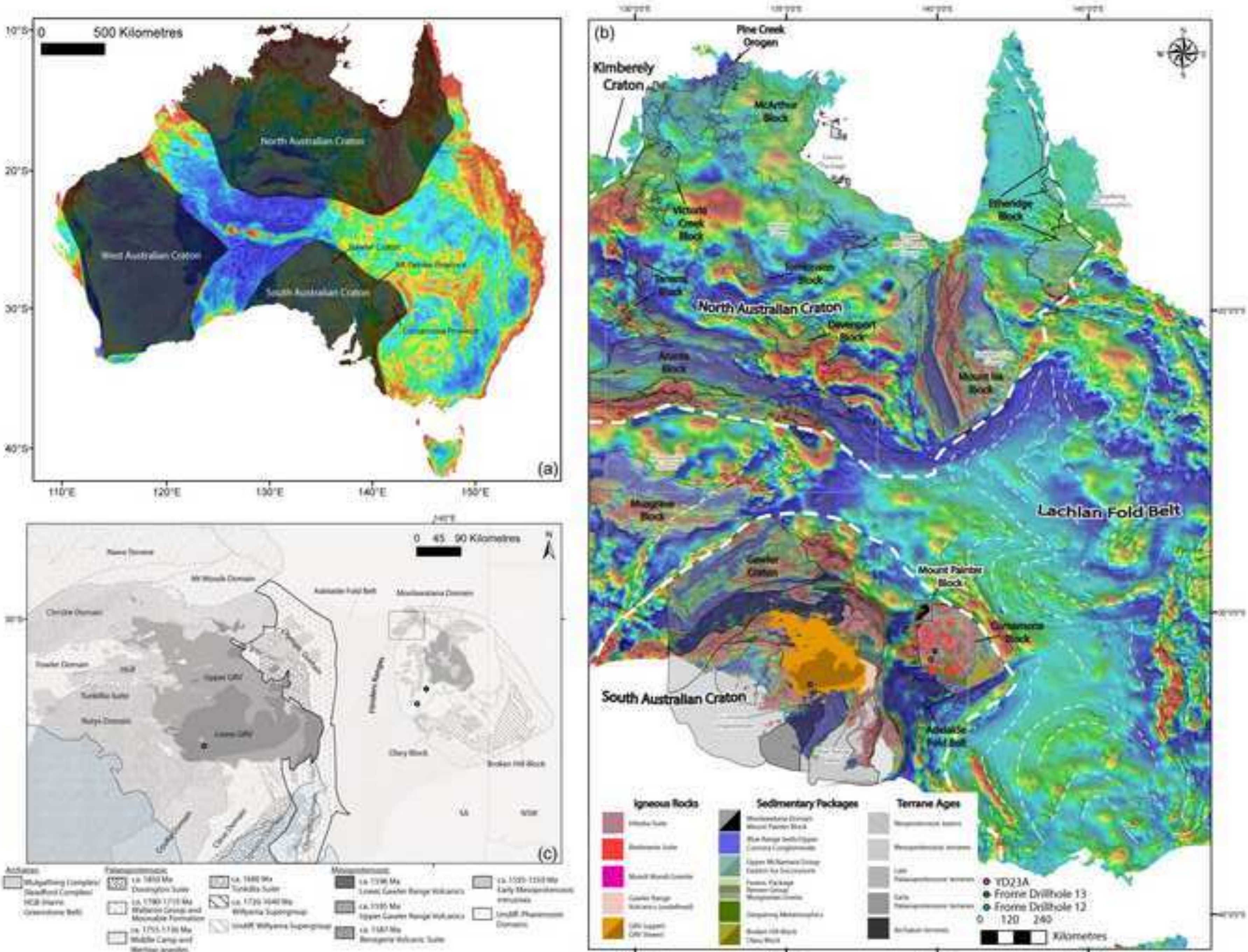

Figure 2
Click here to download high resolution image

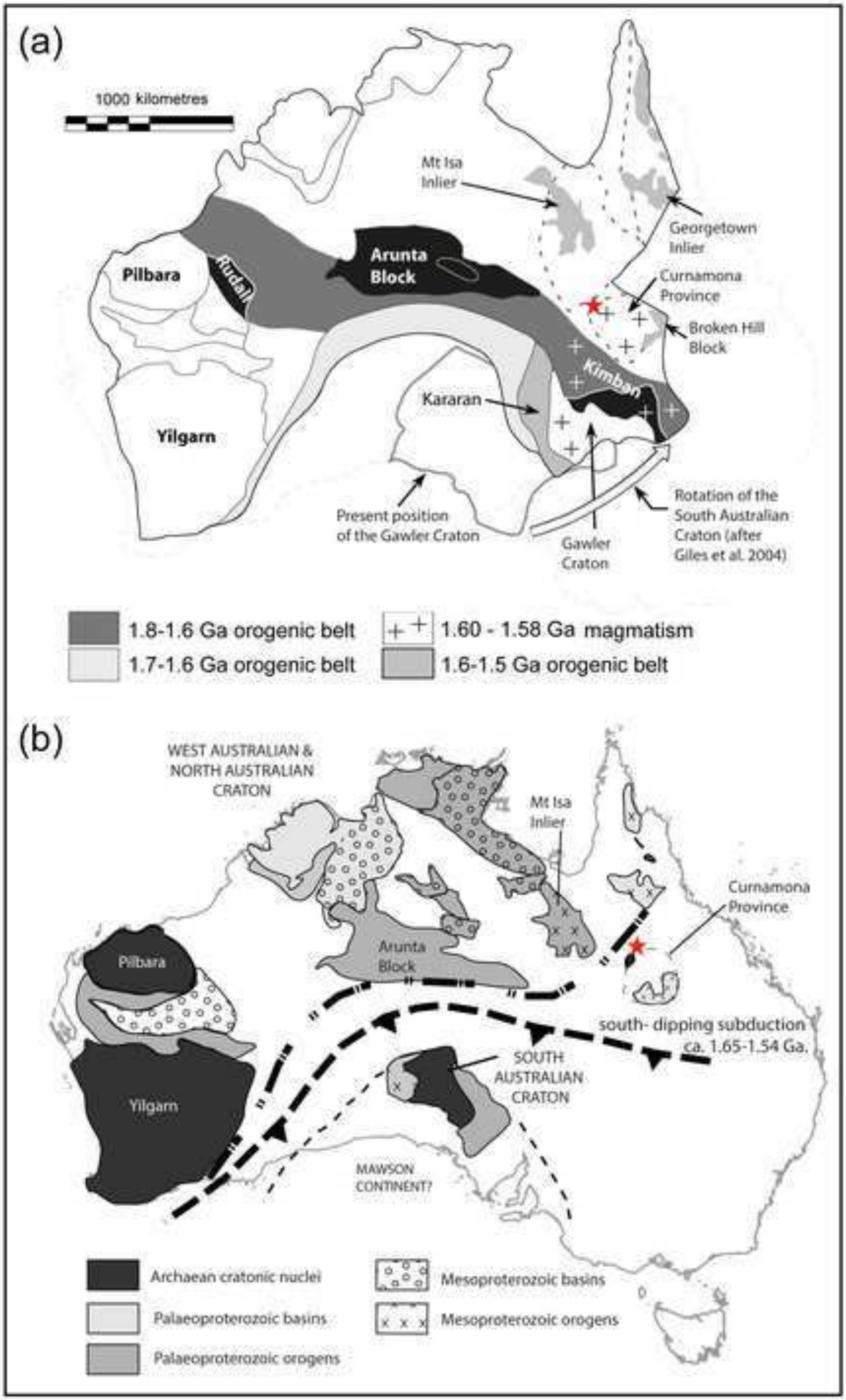

Figure 3
Click here to download high resolution image

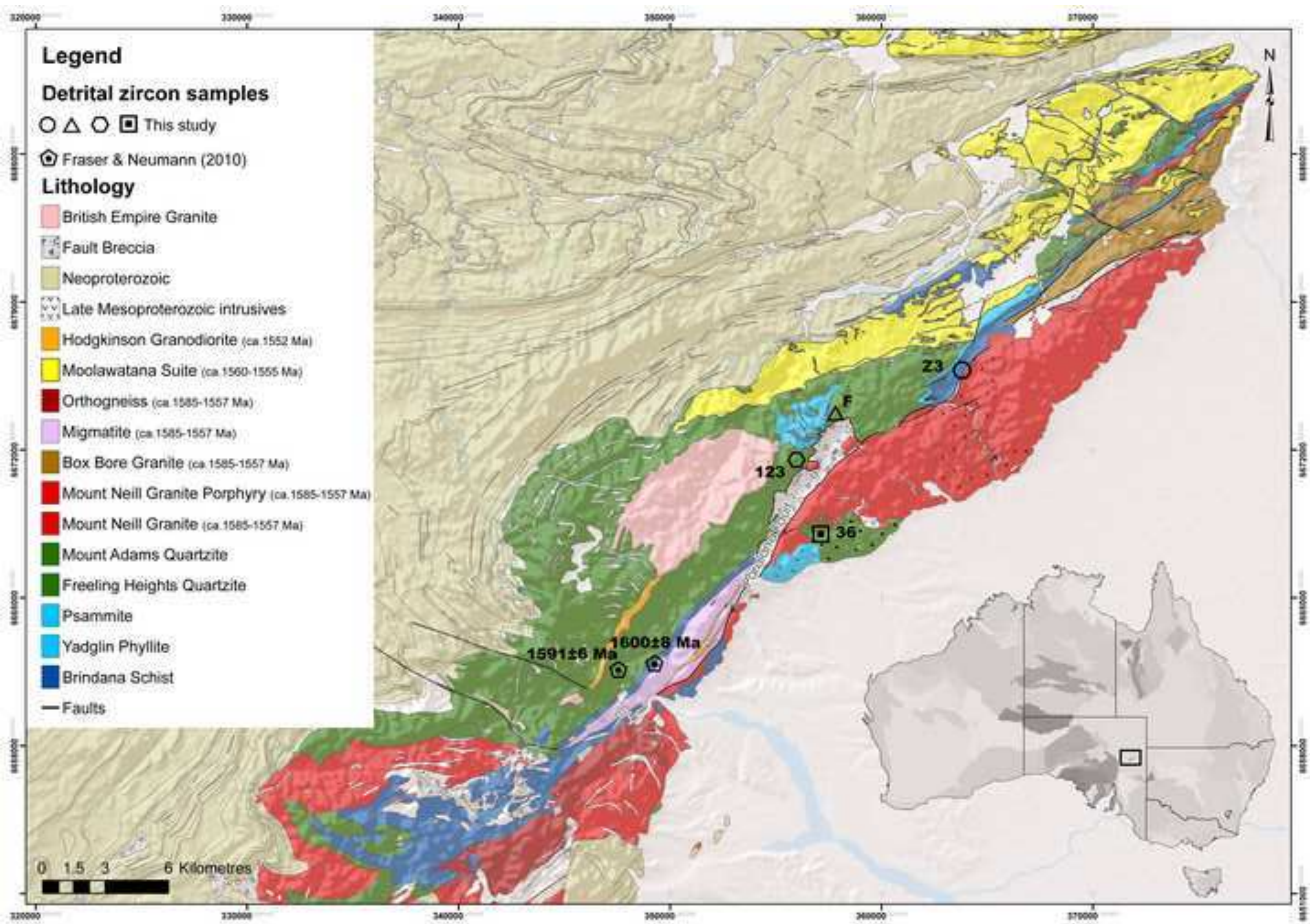

Figure 4
Click here to download high resolution image

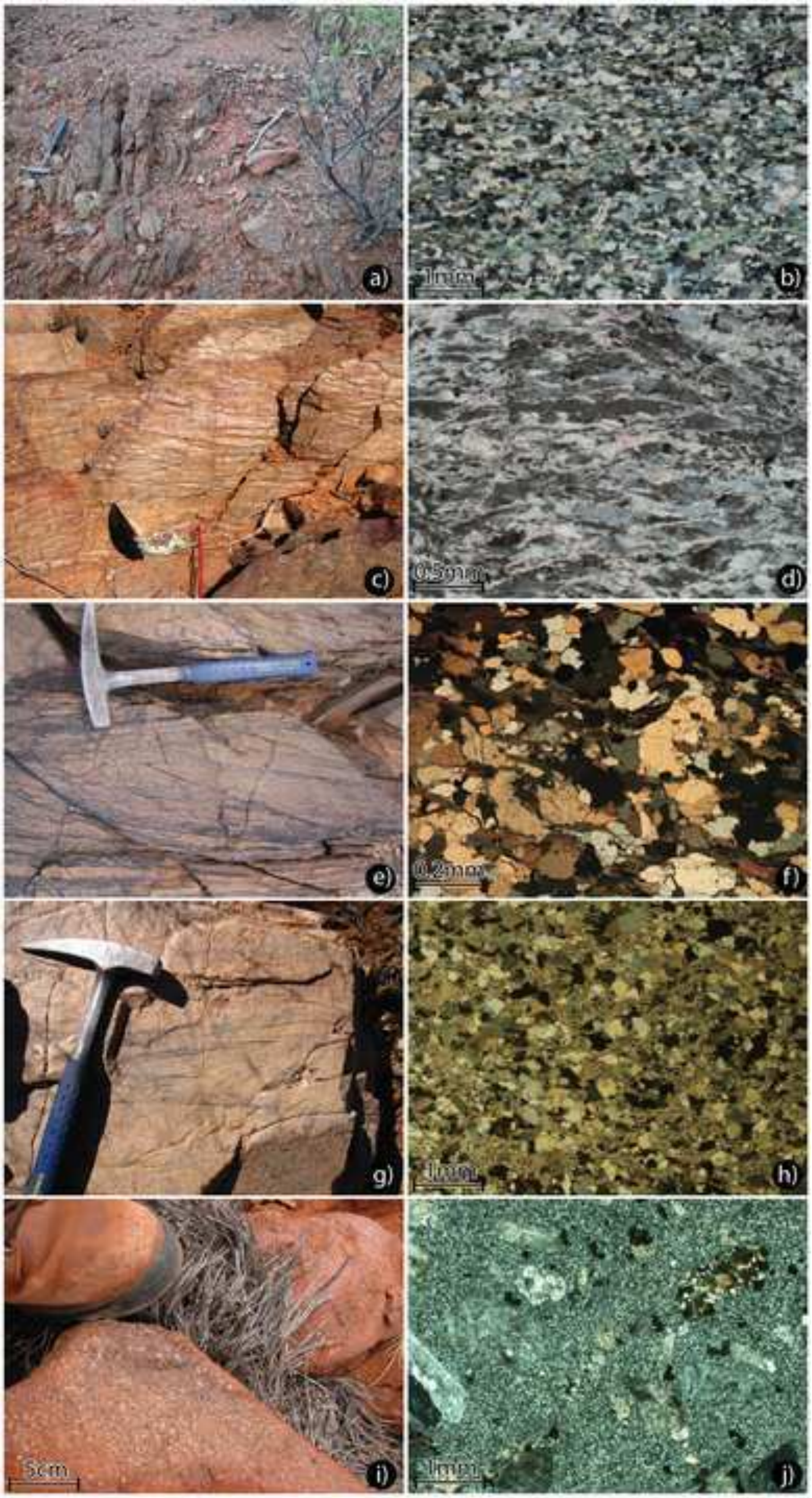

Figure 5

Click here to download high resolution image

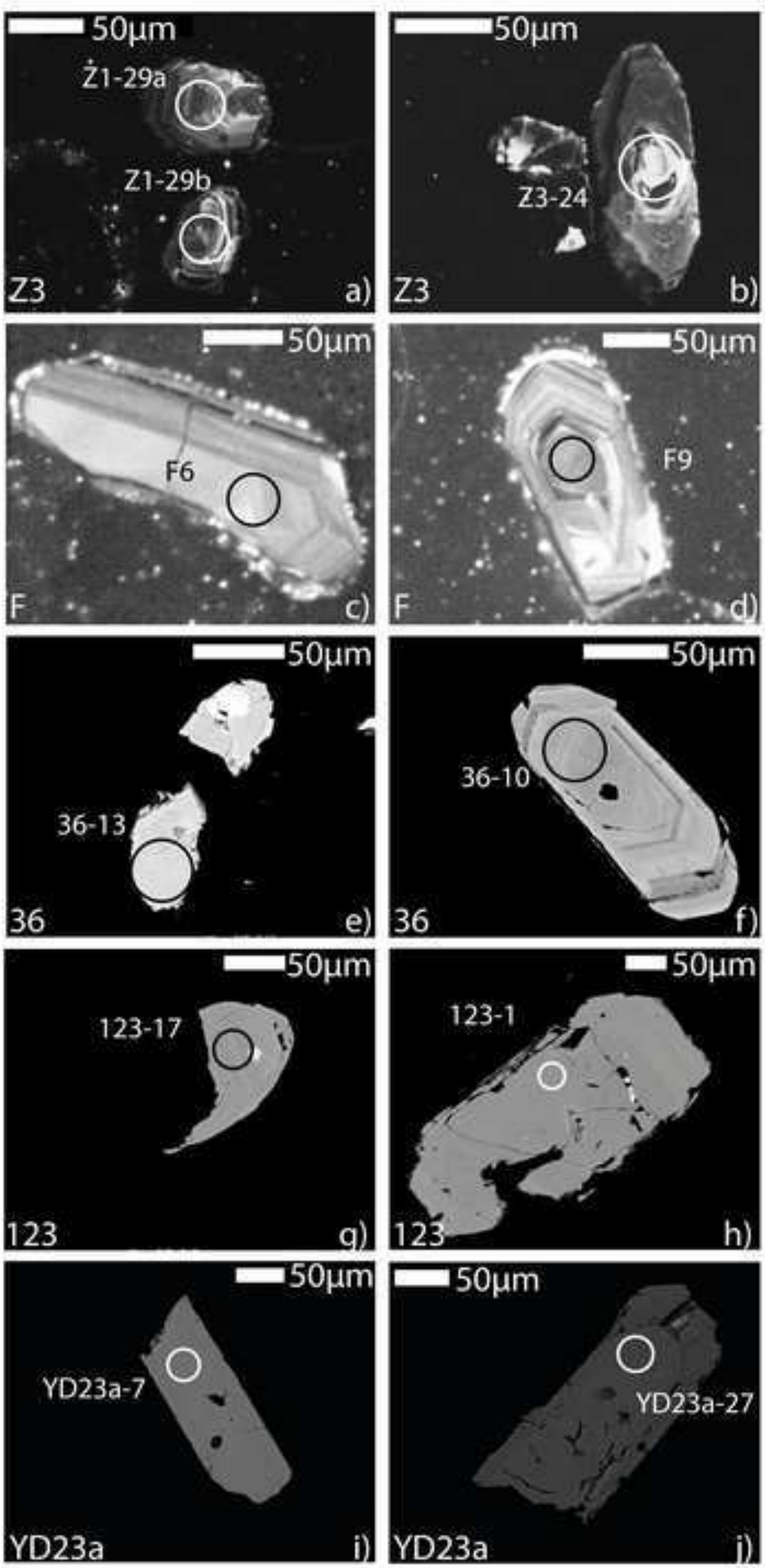

Figure 6

Click here to download high resolution image

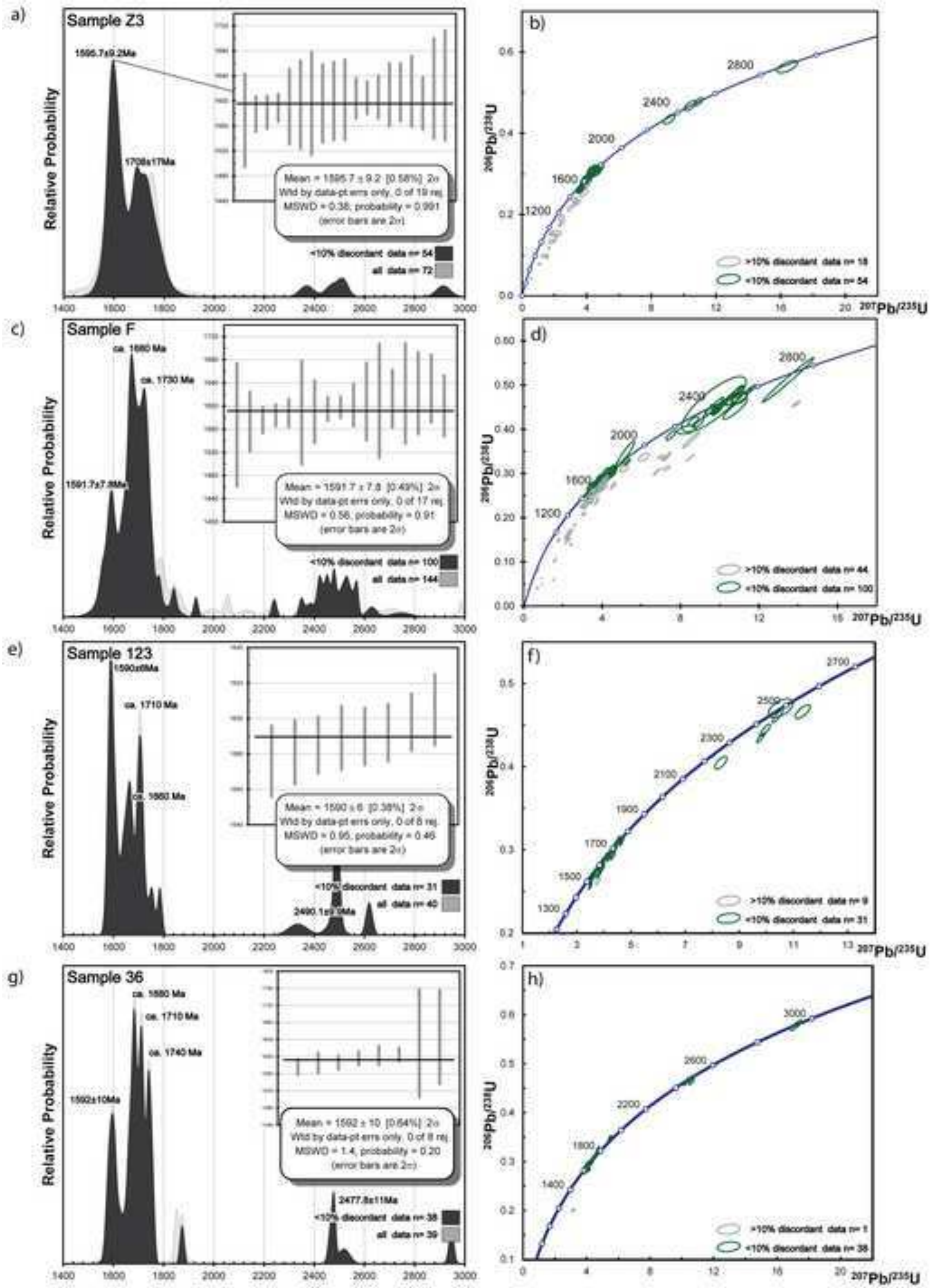

Figure 7

Click here to download high resolution image

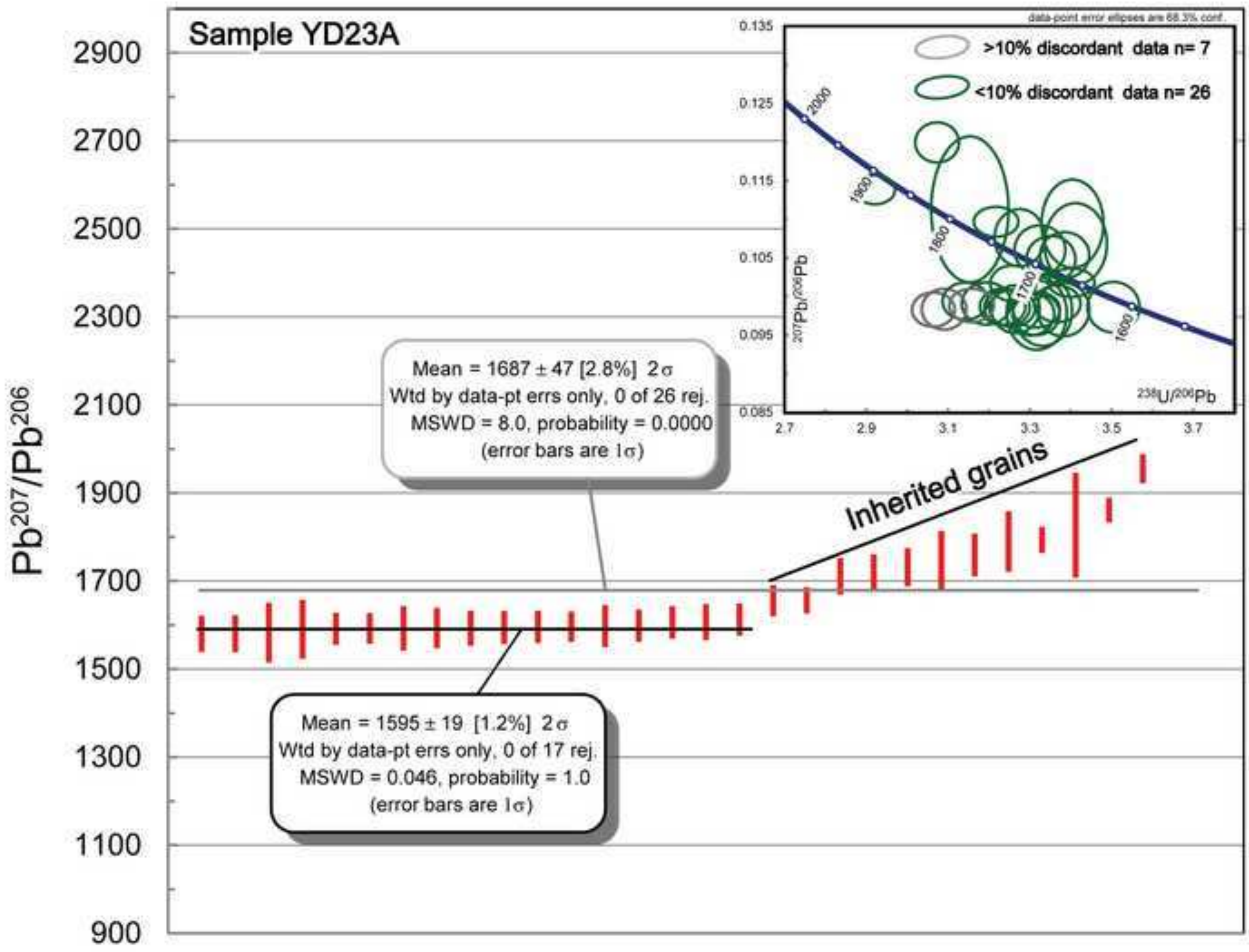

Figure 8

Click here to download high resolution image

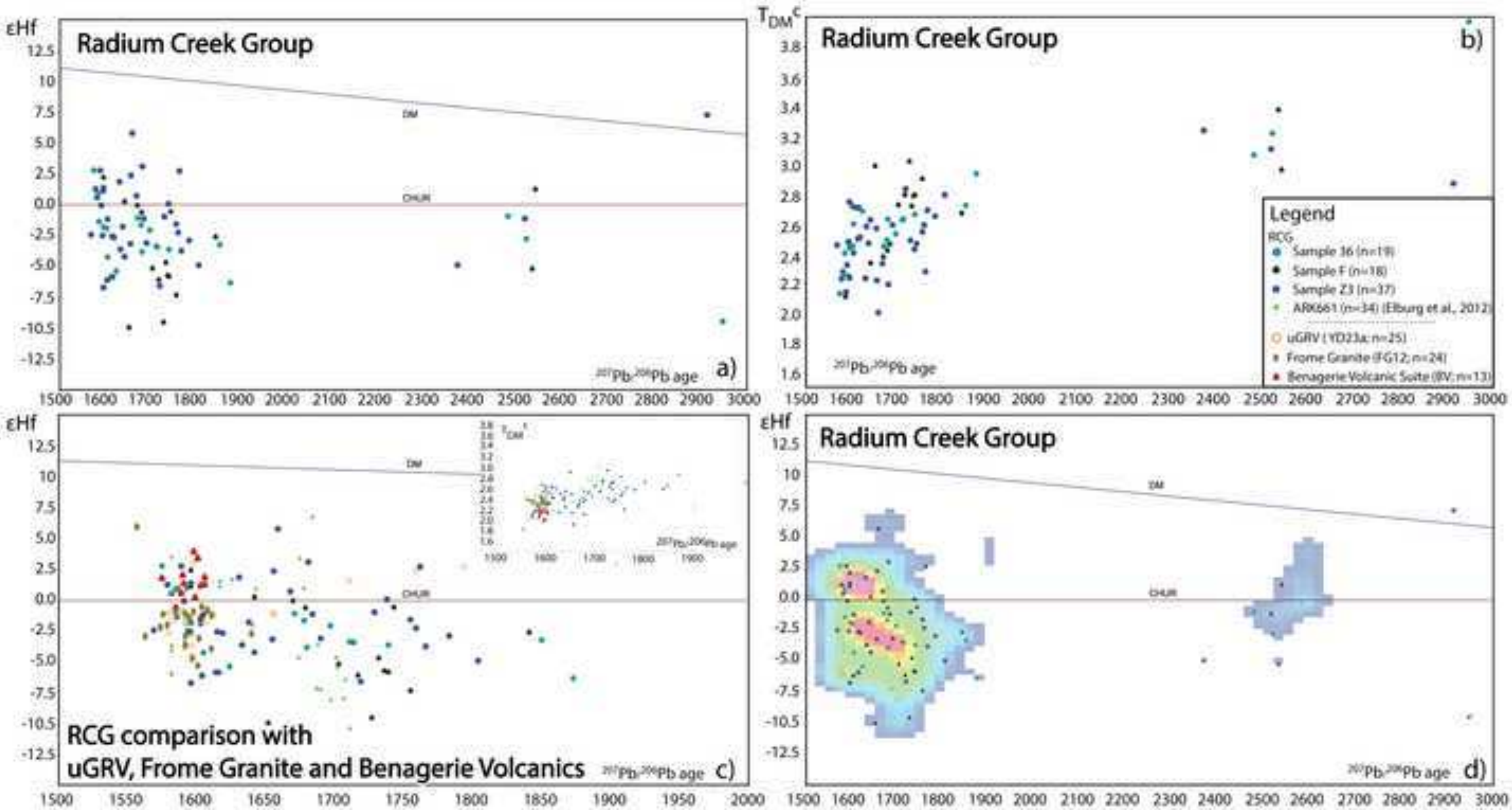

Figure 9
Click here to download high resolution image

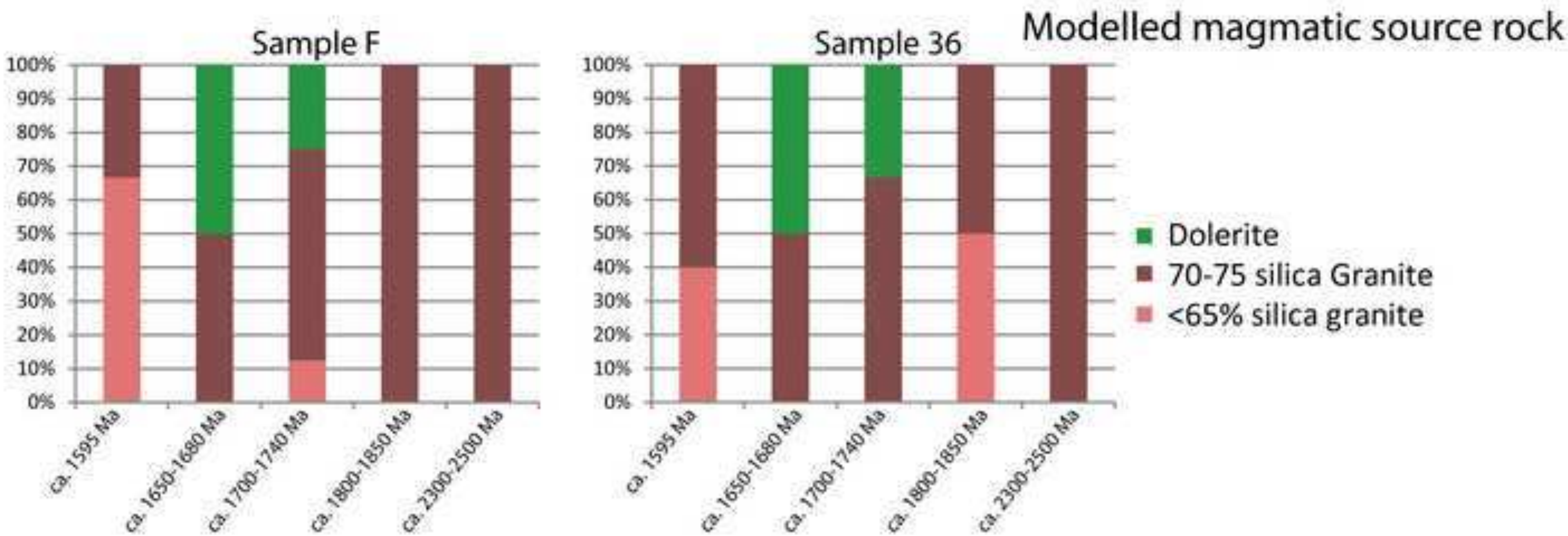

Figure 10

Click here to download high resolution image

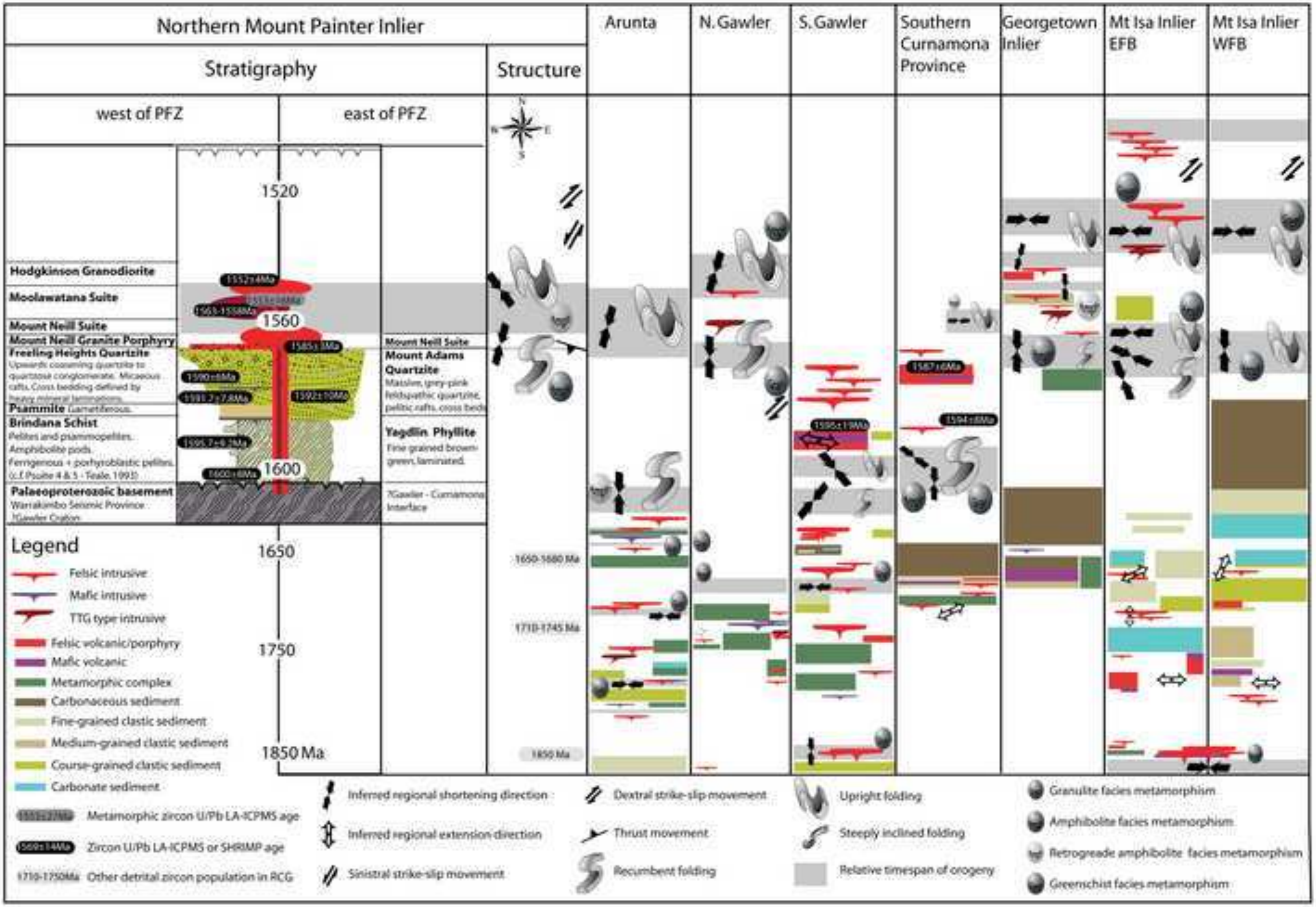

Figure 11

Click here to download high resolution image

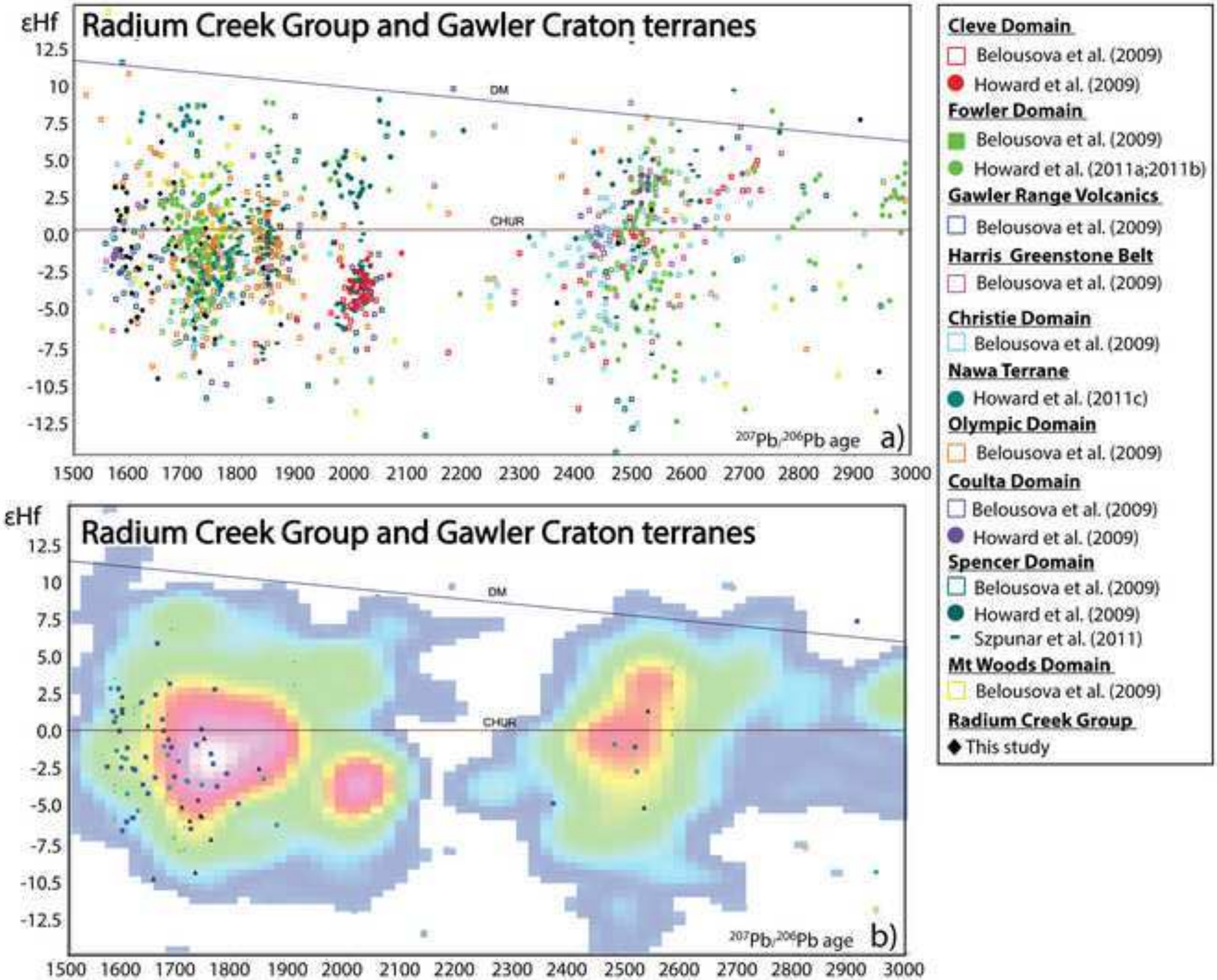

Figure 12
Click here to download high resolution image

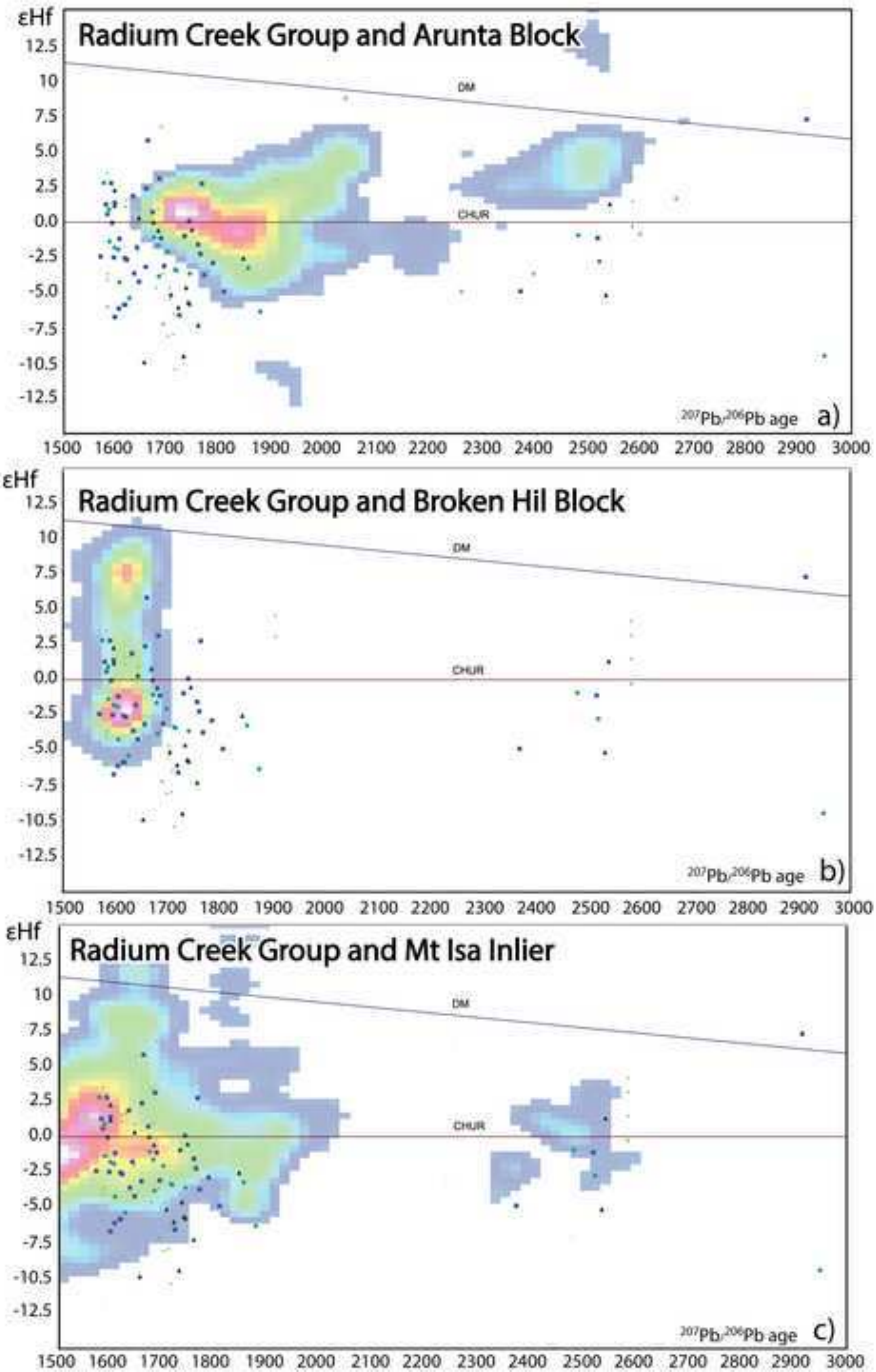

Figure 13

Click here to download high resolution image

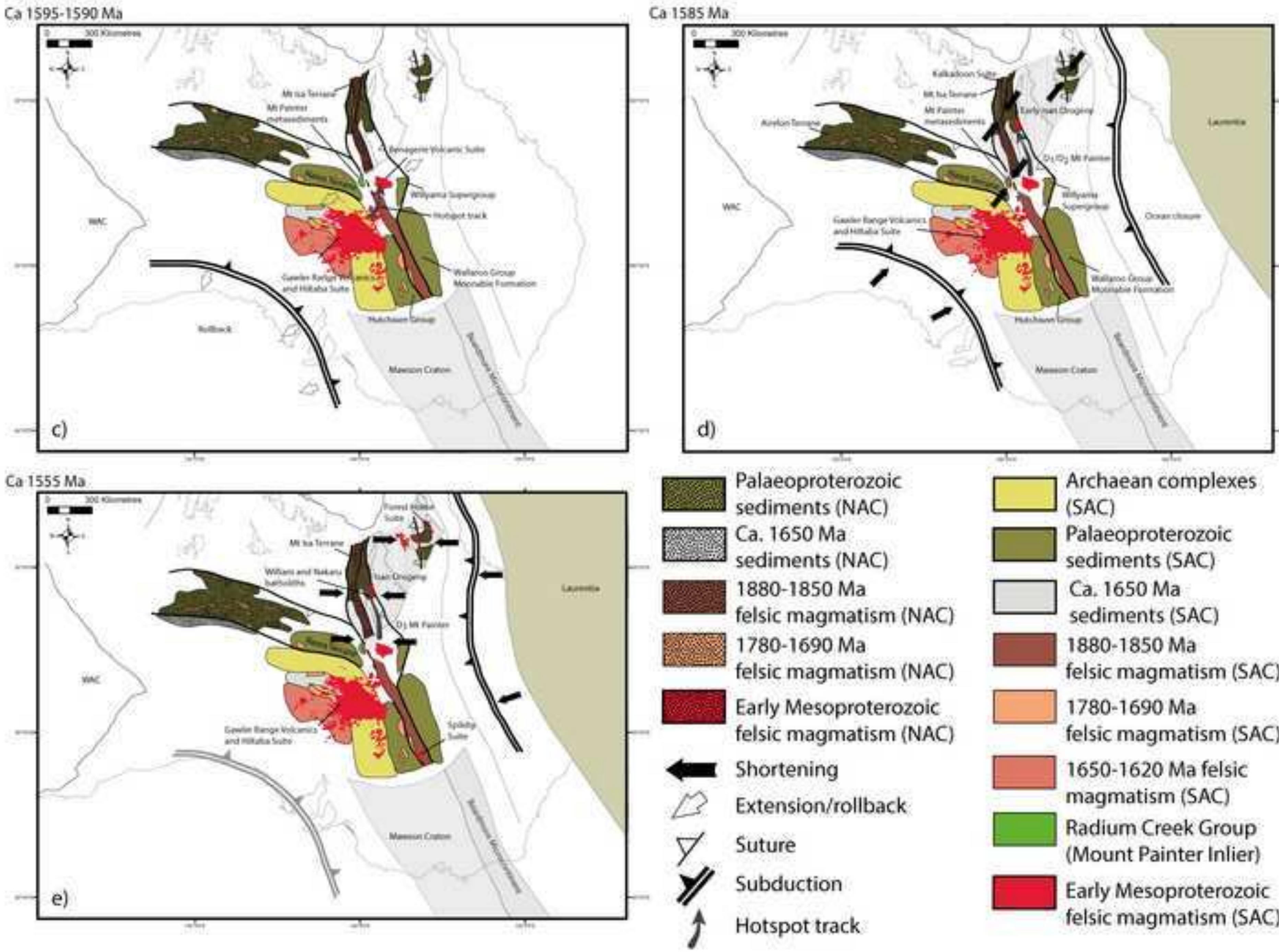

Figure 1 grey

Click here to download high resolution image

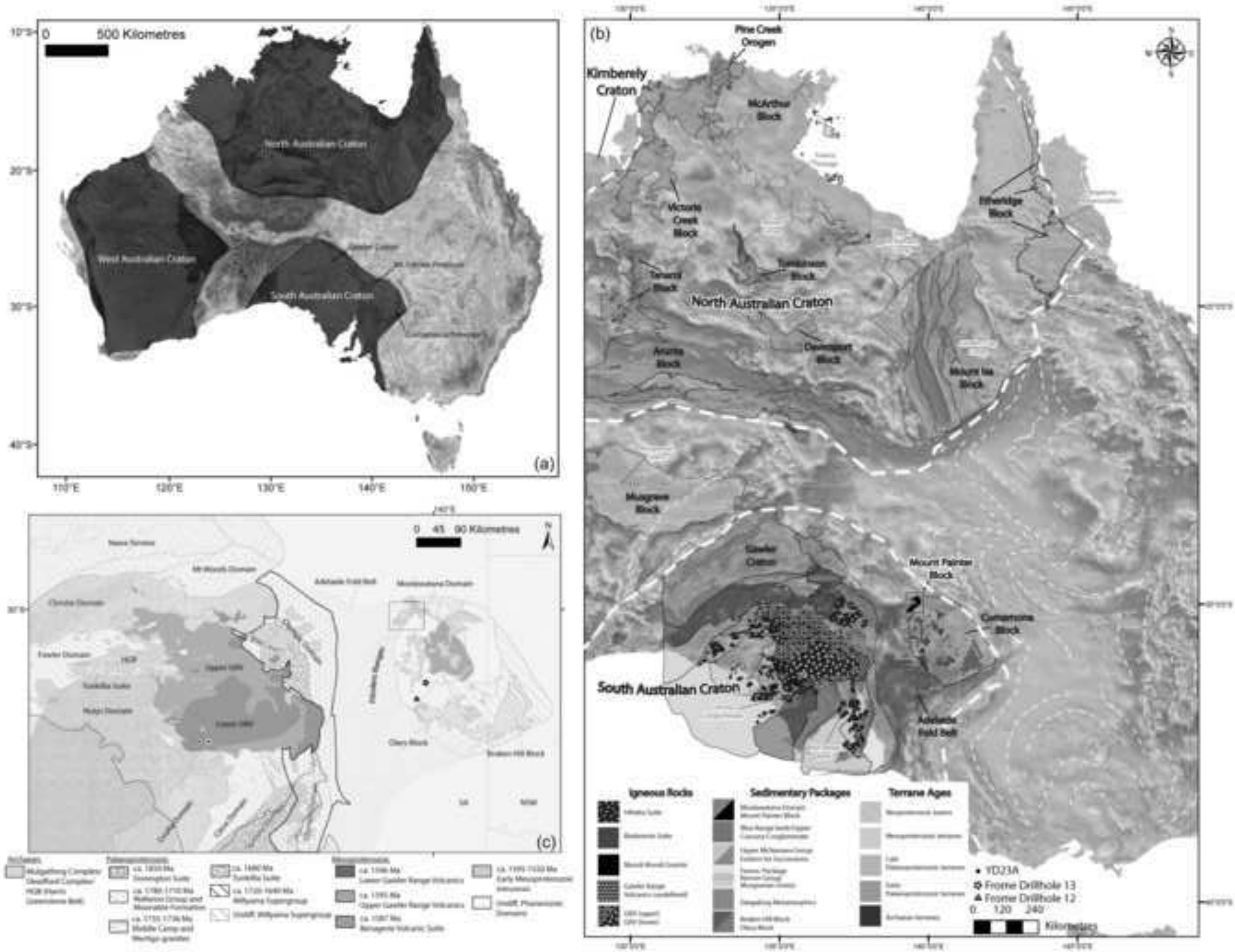

Figure 2 grey
Click here to download high resolution image

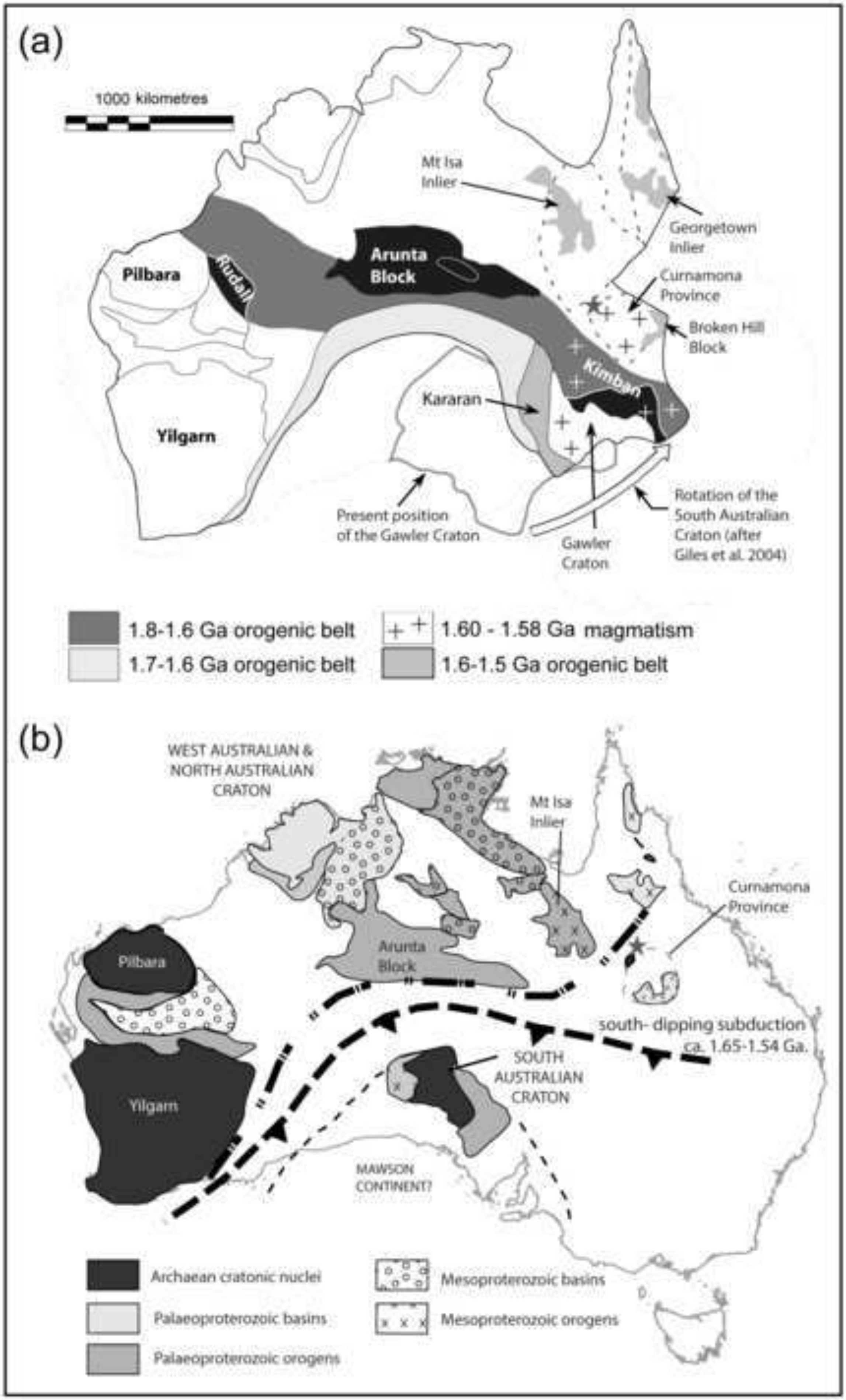

Figure 3 grey
Click here to download high resolution image

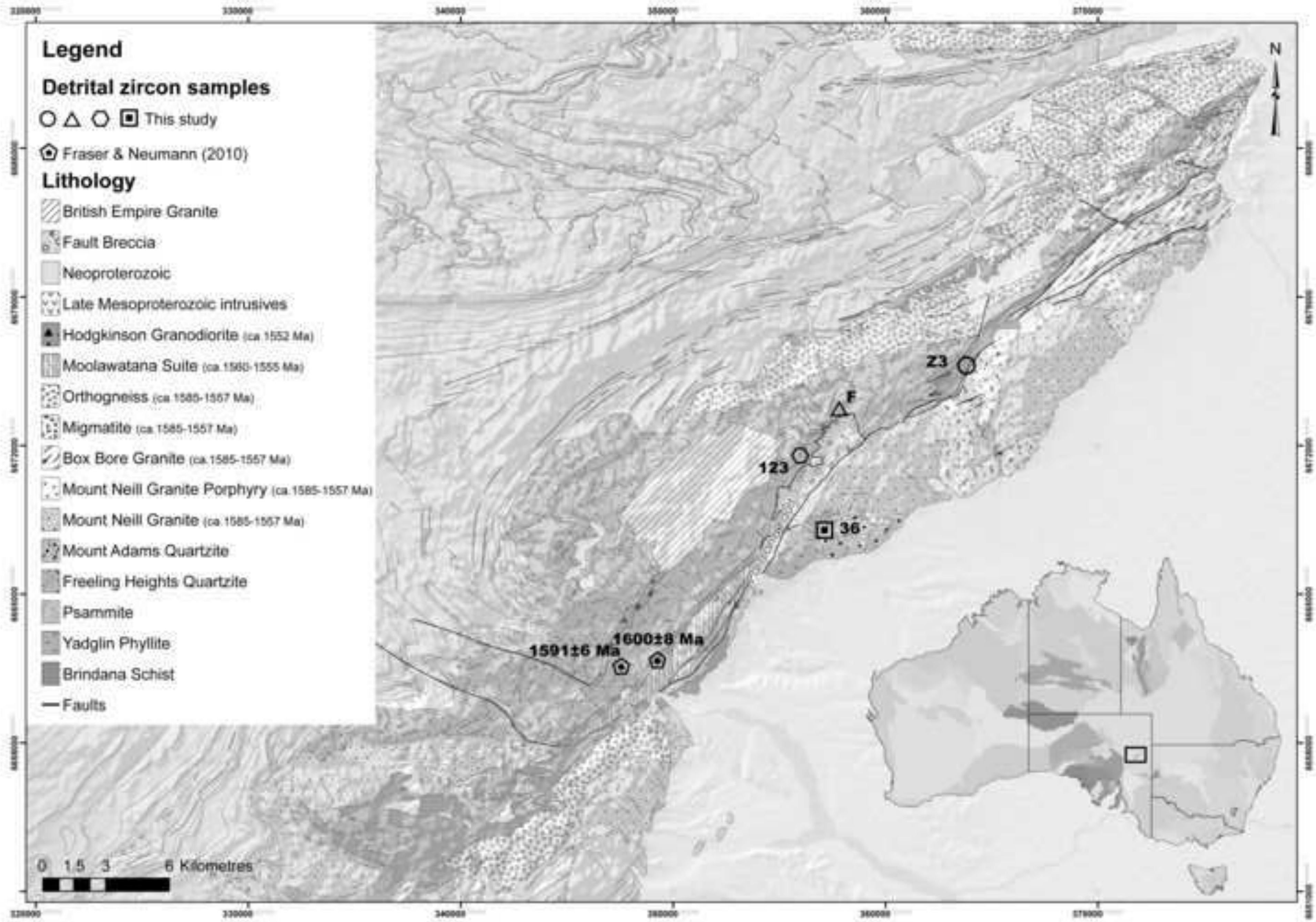

Figure 4 grey

Click here to download high resolution image

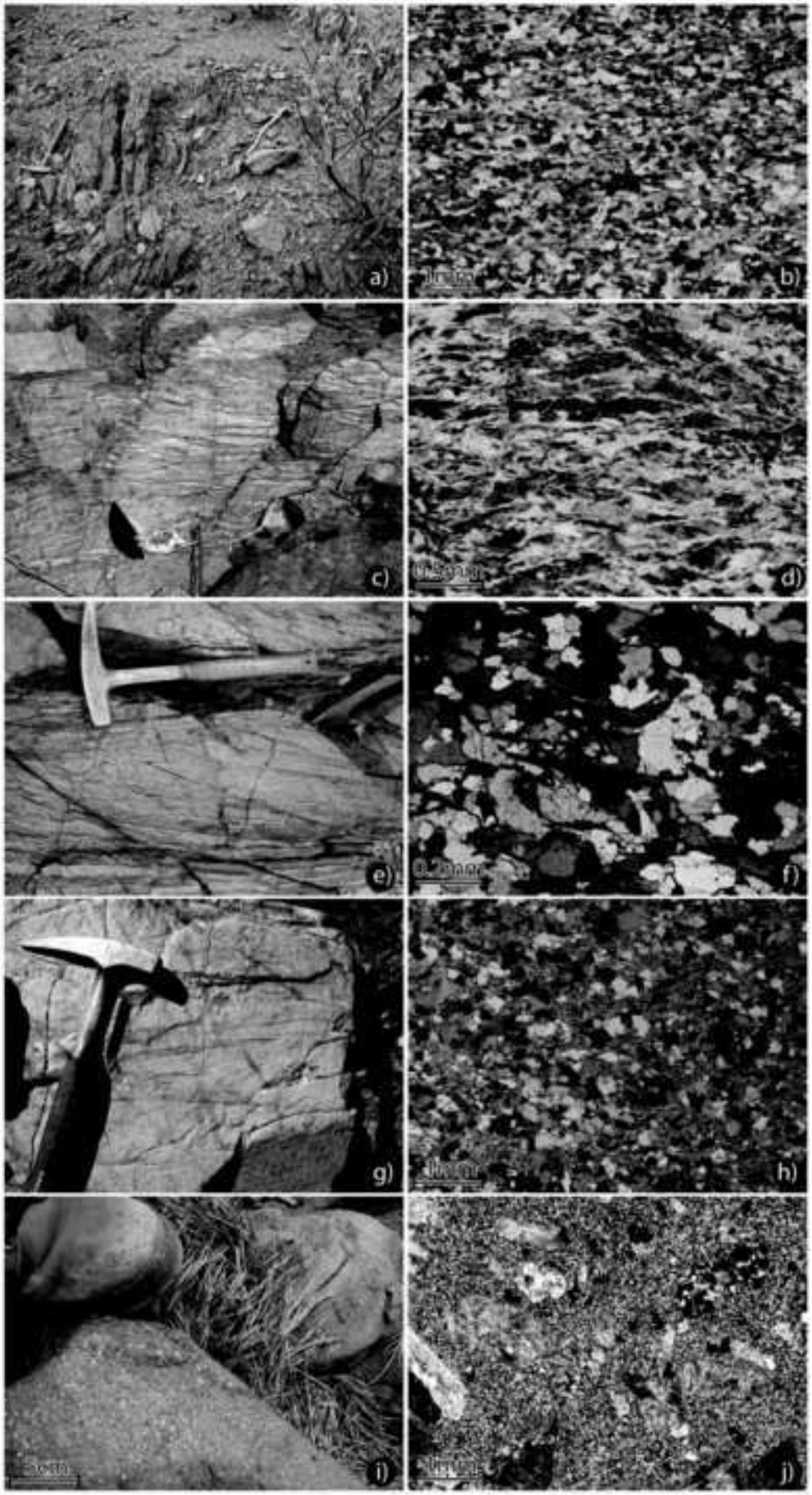

Figure 6 grey

Click here to download high resolution image

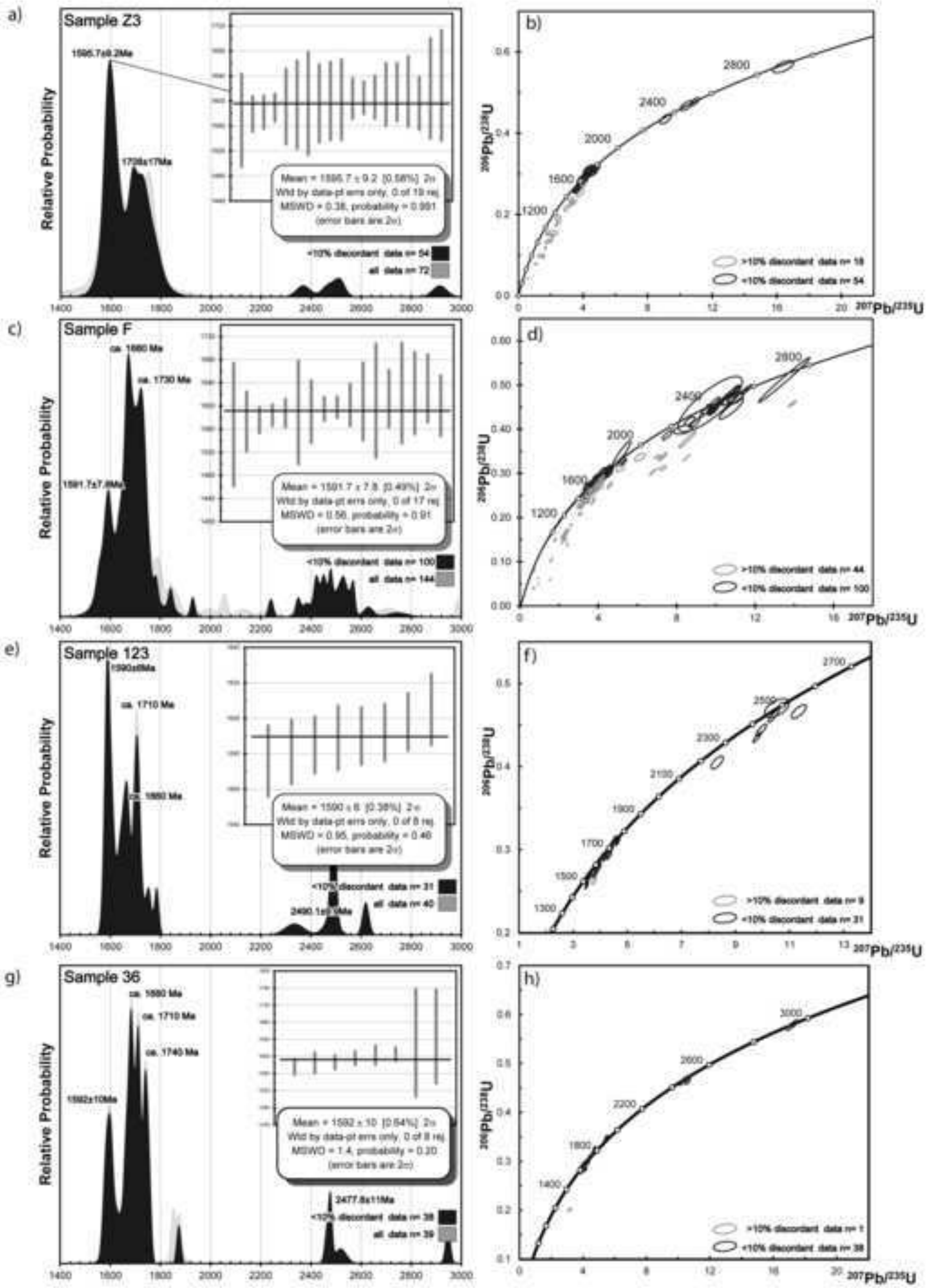

Figure 7 grey

Click here to download high resolution image

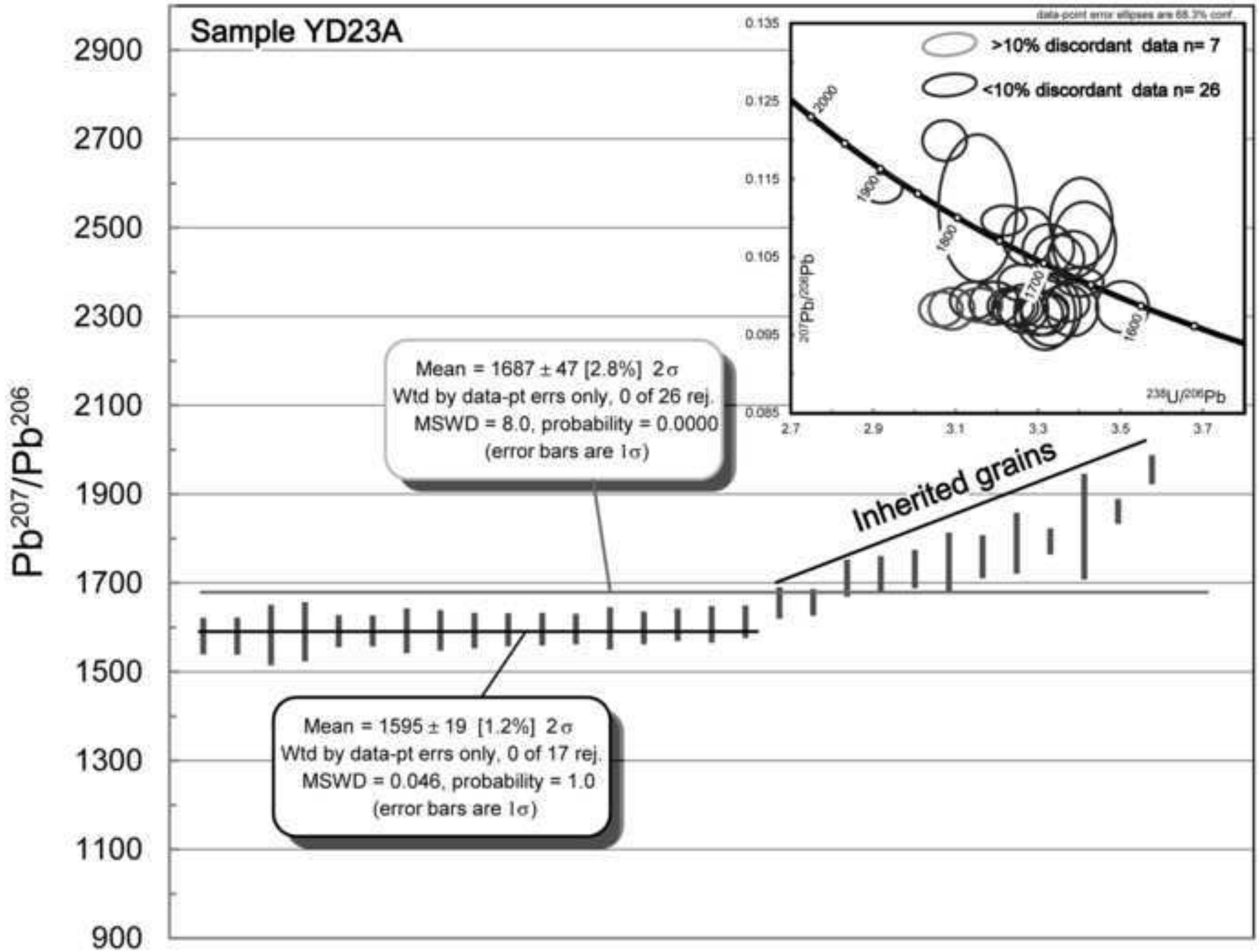

Figure 9 grey

Click here to download high resolution image

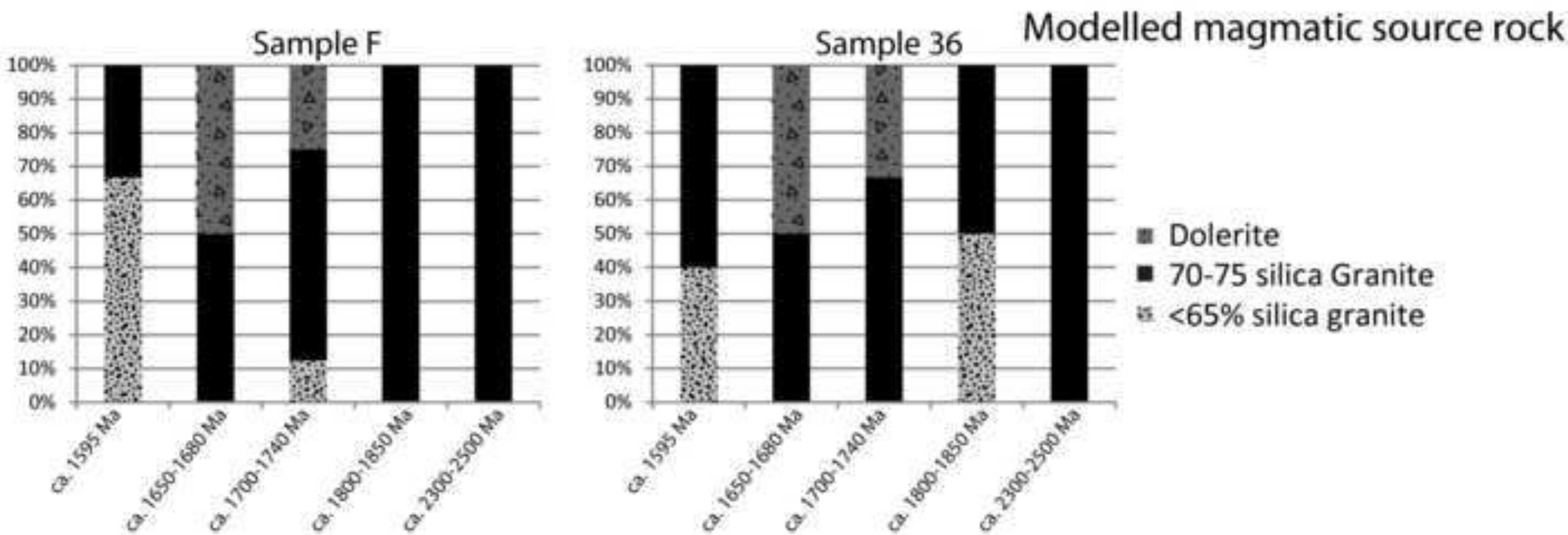

Figure 10 grey
Click here to download high resolution image

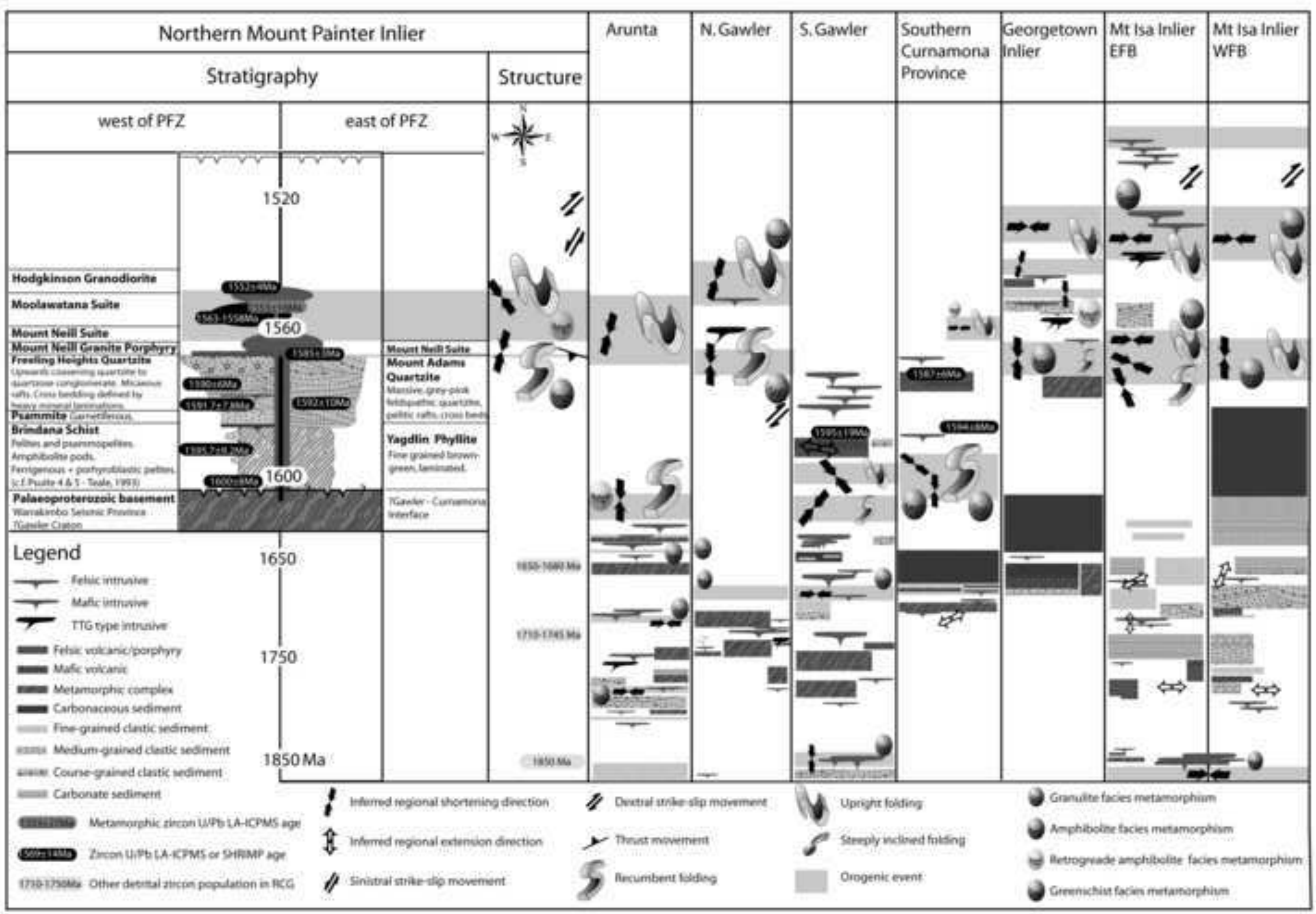

Figure 13 grey

Click here to download high resolution image

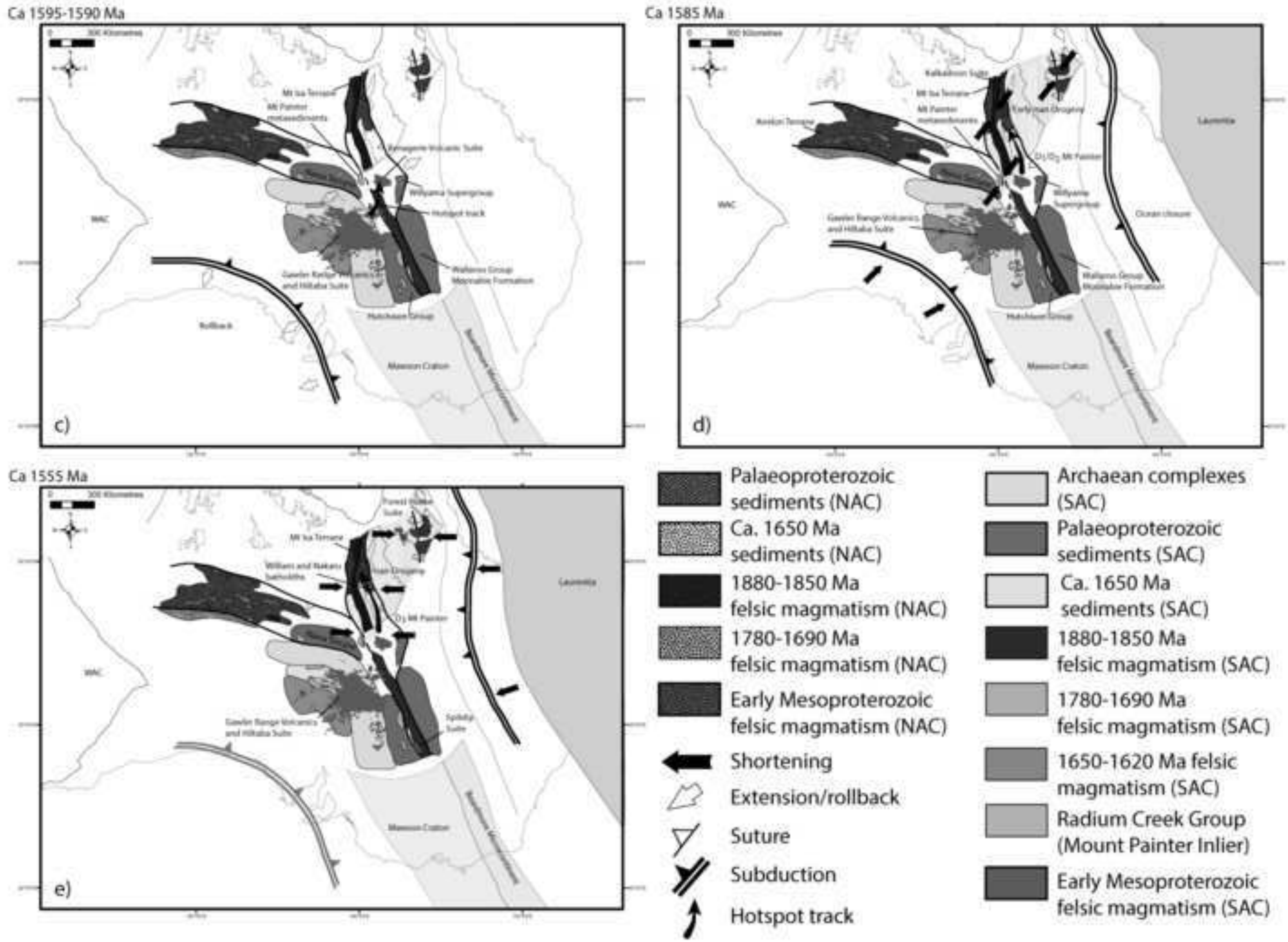

Figure Captions

Fig. 1: a) Map of Australia showing the geography-based nomenclature after Myer et al. (1996) in which the continent is divided into three major cratonic units, called the North, West and South Australian cratons draped over a composite of the bouguer gravity and first vertical derivative of the total magnetic intensity (TMI) map of Australia (geophysical data provided by Geoscience Australia); b) Map highlighting the location of the Mount Painter Block and other eastern Australian Proterozoic terranes in relation to the major geological provinces of Australia. These are draped across a composite total magnetic intensity (TMI) anomaly and first vertical derivative of the TMI map of Australia. This magnetic image was produced using a two kilometre grid spacing and by applying a low pass filter (upward continued six kilometres), which highlights the longer wavelengths/major structural elements of eastern Australia. Data provided by Geoscience Australia; c). Map showing the position of the Mount Painter Province (grey box) in respect to the major domains and Archaean to Mesoproterozoic geology of the Curnamona Province after Conor and Preiss (2008) and the Gawler Craton modified after Fairclough et al. (2003) and Hand et al. (2007).

Fig 2: a) Palaeogeographical reconfiguration model after Giles et al. (2004); Betts and Giles (2006) supporting a shared history for the South Australian Craton and the North Australian Craton between ca. 1800 and 1550 Ma. This configuration aligns contemporaneous orogenic belts across the Gawler Craton, Arunta Inlier, Mount Isa Inlier and the Curnamona Province.; b) Palaeogeographical reconfiguration model after Wade et al. (2006) in which the Gawler Craton and Curnamona Province are separated by a south-dipping subduction zone between ca.1600-1580 Ma with the Gawler Craton positioned in the overriding plate.

Fig. 3: Map of the Mount Painter Inlier showing sample locations and regional geology after Armit et al. (2012).

Fig. 4: a) Photograph of the steeply dipping, foliated psammopelites of the Brindana Schist unit at the base of Radium Creek Group, geo-pick shown for scale (sample Z3 363800E 6675681N); b) Photo-micrograph of a thin section of sample Z3 from the Brindana Schist in cross-polarised light, cut normal to the S_3 foliation. This view demonstrates overprinting, spaced foliations defined by muscovite ± biotite fabrics (sub-horizontal in photo-micrograph) and recrystallised polygonal quartz aggregate (microlithons); c) Photograph of the intensely crenulated, micaceous quartzite outcrop of the Freeling Heights Quartzite (sample F 357632E 6673138N); d) Photo-micrograph of a thin section of the Freeling Heights Quartzite in cross-polarised light. The section, taken normal to the S_3 foliation, highlights a spaced schistosity defined by muscovite with elongate relic quartz grains which display undulose extinction. A discrete crenulation cleavage overprints the existing schistosity; e) Photograph of quartzite unit of the Freeling Heights Quartzite (sample 123 355996E, 6672099N). Cross-beds defined by heavy minerals and distinct compositional layering (compare with bottom right of picture) record reverse grading. This indicates that younging is upwards and towards the west (head of the geo-pick is orientated E-W); f) Photo-micrograph of sample 123 in cross-polarised light. The section was cut normal to the S_3 foliation and highlights two spaced and overprinting foliations defined by biotite ± muscovite and polygonal quartz-rich microlithons; g) Photograph of the fine-grained pinky-grey micaceous quartzite outcrop of the Mount Adams Quartzite (Sample 36; 357161E, 6668472N). Cross beds defined by heavy minerals indicate upward younging; h) Photo-

micrograph of sample 36 in cross-polarised light shows fine grained muscovite, sercite and quartz-rich assemblage. A sub-horizontal spaced foliation, defined by fine-grained micaceous material, overprints an earlier mica fabric with polygonal undulose quartz and biotite microlithons; i) Photograph of a hand specimen from the Pondanna member of the upper Gawler Range Volcanics (573593E, 6405524N) showing porphyritic texture with phenocrysts of quartz and feldspar within a dark, aphanitic groundmass; j) Photo-micrograph of Sample YD23a from the Pondanna member of the upper Gawler Range Volcanics (573593E, 6405524N), section shows phenocrysts of k-feldspar, quartz, and pyroxene within a fine grained matrix .

Fig. 5: Cathodoluminescence and back scatter electron images (a-d & e-j respectively of representive zircon grains from each sample analysed in this study. The region ablated during analysis is indicated; a) Z1-29a,b zircon grains from sample Z3 (Brindana Schist). Z1-29a grain has a U-Pb age 1659 ±15 Ma and an εHf value of+5.80, Z1-29b grain has a U-Pb age of 1604 ± 16 Ma and a εHf value of -6.1; b) Z3-24 zircon grain from sample Z3 (Brindana Schist). This grain has a U-Pb age of 2369 ± 28 Ma and an εHf value of-4.89; c) F6 zircon grain from sample F (Freeling Heights Quartzite). This grain has a U-Pb age of 1670 ± 10 Ma and an εHf value of +0.01; d) F9 zircon grain from sample F (Freeling Heights Quartzite). This grain has a U-Pb age of 2539 ± 28 Ma and an εHf value of +1.29; e) 36-13 zircon grain from sample 36 (Mount Adams Quartzite). This grain has a U-Pb age of 1596 ± 8 Ma and an εHf value of -1.79; f) Back scatter electron image of 36-10 zircon grain from sample 36 (Mount Adams Quartzite). This grain has a U-Pb age of 1678 ± 29 Ma and an εHf value of -1.64; g) 123-17 zircon grain from sample 123 (Freeling Heights Quartzite). This grain has a U-Pb age of 1589 ± 9 Ma; h) 123-1 zircon grain from sample 123 (Freeling Heights Quartzite). This grain has a U-Pb age of 1712 ± 8 Ma; i) YD23a-7 zircon grain from sample YD23a (uGRV). This grain has a U-Pb age of 1596.2 ± 36 Ma and an εHf value of -2.74; j) YD23a-27 zircon grain from sample YD23a (uGRV). This grain has a U-Pb age of 1597.6 ± 47 Ma and a εHf value of -4.5.

Fig. 6: a) Probability plot of detrital zircons analysed from sample Z3. Inset: weighted mean $^{207}Pb/^{206}Pb$ (2σ) age plot for the youngest population in this sample, interpreted as the maximum depositional age.; b) Concordia plot for zircons analysed from sample Z3 ;c) Probability plot of detrital zircons analysed from sample F. Inset: weighted mean $^{207}Pb/^{206}Pb$ (2σ) age plot for the maximum depositional age of this sample; c) Zircon grains from sample F plotted on a U-Pb concordia plot; d) Concordia plot for zircons analysed from sample F; e) Detrital zircon probability plot from sample 123. Inset: weighted mean age $^{207}Pb/^{206}Pb$ ages (2σ) for the maximum depositional age ; f) Concordia diagram for zircons analysed from sample 123; g) Probability plots for zircon analysed from sample 36. Inset: weighted mean $^{207}Pb/^{206}Pb$ ages (2σ) for the maximum depositional age for this sample; h) U-Pb concordia plot for zircon analysed from sample 36.

Fig. 7: Weighted mean $^{207}Pb/^{206}Pb$ ages plot for sample YD23a showing the dominant population and older inherited grains. Inset: Tera-Wasserburg concordia plot shows the concordant (<10% discordant) analyses, as well as all data >10% discordant from this sample. Data error ellipses and error bars used are 1σ.

Fig. 8: a) Plot of ε $Hf_{(t)}$ versus $^{207}Pb/^{206}Pb$ ages for the Radium Creek Group samples; b) Plot of T_{DM}^{c} versus $^{207}Pb/^{206}Pb$ ages for the Radium Creek Group samples; c) Plot of ε $Hf_{(t)}$ versus $^{207}Pb/^{206}Pb$ ages for the Radium Creek Group samples including values for ARK661 sample from Elburg et al. (2012) compared with the values for the upper Gawler Range Volcanics, uGRV from the Gawler Craton (sample YD23a), and the Frome Granite of the Bimbowrie Suite (sample FG12) and Benagerie Volcanic Suite (sample BV) from the Curnamona Province (see Fig. 1c-d for sample locations). Insert shows a plot of T_{DM}^{c} versus $^{207}Pb/^{206}Pb$ ages for these samples; d) Field for the Radium Creek Group ε $Hf_{(t)}$ values plotted as gridded density and data points for comparison. Density grid constructed

using cell size of 20 Myr in the X direction and 0.5 ε Hf units in the Y direction, a threshold level of 0.05 and a smoothing level of 3.

Fig. 9: Comparison of zircon crystallisation rock type, modelled from in-situ trace chemistry after Belousova et al. (2002) to determine the source rock type of zircon grains across the Paralana Fault. Sample F (357632E 6673138N) is from the Freeling Heights Quartzite to the west (Hangingwall) of the Paralana Fault. Sample 36 (357161E, 6668472N) is from the Mount Adams Quartzite to the east (Footwall) of the Paralana Fault. The modelled source rock type is predominantly felsic and indistinguishable across the Paralana Fault.

Fig. 10: Stratigraphic and structural framework of the Mount Painter Inlier using data from this study and Armit et al. (2012). Proterozoic magmatic ages determined using U-Pb geochronology by LA-ICPMS and SHRIMP where available. Mount Neill Granite and porphyry age from Teale (1987, unpublished), Elburg et al. (2003), Neumann (2001), Neumann et al. (2009) and Fraser and Neumann (2010). Northern Gawler tectonism from Payne et al. (2008), Fanning et al. (2007), Thomas et al. (2008), Swain et al. (2005b) and Skirrow et al. (2007). Southern Gawler tectonism from Stewart and Betts (2010), Webb et al. (1986) and Parker et al. (1993). Southern Curnamona Province tectonism from Conor and Preiss (2008), Forbes et al. (2008), Betts et al. (2002), Stüwe and Ehlers (1997), Forbes and Betts (2004), Forbes et al. (2004), Stevens et al. (1988), Wilson and Powell (2001), Page et al. (2000, 2005), Rutherford et al. (2007), Marjoribanks et al. (1980) and Clarke et al. (1987, 1995). Georgetown tectonism from Black et al. (1979), Withnall et al. (1996), Hills (2004), Cihan et al. (2006), Davis (1996), Betts et al. (2009), Boger and Hansen (2004), Black and Withnall (1993), Black et al. (1998), Withnall et al. (1988), Withnall et al. (1996), Blewett et al. (1998) and Bell and Rubenach (1983). Tectonism in the Eastern Fold Belt of the Mount Isa Inlier from Betts et al. (2006), MacCready et al. (1998), Giles et al. (2006a), O'Dea et al. (2006), Page and Sun (1998), Giles and Nutman (2002), Hand and Rubatto (2002), Giles and Nutman (2003), De Jong and Williams (1995), Betts et al. (2006), Connors and Page (1995) and O'Dea et al. (1997). West Fold Belt tectonism from O'Dea and Lister (1995), O'Dea et al. (1997), Lister et al. (1999), Hand and Rubatto (2002), Connors and Page (1995), O'Dea et al. (1997), MacCready et al. (1998), Betts et al. (2006) and Blenkinsop et al. (2008). Tectonism in the Arunta Block after (Claoué-Long et al., 2008; Collins and Shaw, 1995; Collins and Williams, 1995; Maidment et al., 2005; Scrimgeour et al., 2005). Stratigraphy after Armit and Betts(2011) and references therein.

Fig. 11: a) Plot of ε $Hf_{(t)}$ versus $^{207}Pb/^{206}Pb$ ages for Archaean to Mesoproterozoic zircon populations for the major domains of the Gawler Craton from Belousova et al. (2009); Howard et al. (2009;2010;2011a;2011b); Szpunar et al. (2011), compared with the samples from the Radium Creek Group (this study); b) Field for the Gawler Craton ε $Hf_{(t)}$ values from Belousova et al. (2009); Howard et al. (2009;2010;2011a;b); Szpunar et al. (2011) plotted as gridded density and data points for comparison with the samples from the Radium Creek Group plotted as points. Density grid constructed using cell size of 20 Myr in the X direction and 0.5 ε Hf units in the Y direction, a threshold level of 0.05 and a smoothing level of 3.

Fig. 12: a) Plot of ε $Hf_{(t)}$ versus $^{207}Pb/^{206}Pb$ ages for Archaean to Mesoproterozoic zircon populations from the Arunta Block (Hollis et al. 2010) displayed as a gridded density field compared with the samples from the Radium Creek Group shown as points; b) Plot of ε $Hf_{(t)}$ versus $^{207}Pb/^{206}Pb$ ages for Archaean to Mesoproterozoic zircon populations from the Broken Hill Block of the Curnamona Province (Condie et al. 2005) displayed as a gridded density field, compared with the samples from the Radium Creek Group shown as points; c) Plot of ε $Hf_{(t)}$ versus $^{207}Pb/^{206}Pb$ ages for Archaean to Mesoproterozoic zircon populations from the Broken Hill Block of the Mount Isa Inlier (Griffin et al. 2006) displayed as a gridded density field compared with the samples from the Radium Creek Group shown as points. All U-Pb dates shown as $^{207}Pb/^{206}Pb$ ages, Hf isotope values recalculated using a

decay constant of 1.865E10^{-11}/yr. Density grids for the Radium Creek Group, Gawler Craton, Curnamona Province and Mount Isa Inlier are constructed using cell size of 20 Myrs in the X direction and 0.5 ε Hf units in the Y direction, a threshold level of 0.05 and a smoothing level of 3.

Fig 13: a) Palaeogeographical reconstruction of eastern Proterozoic Australia at ca. 1595 Ma adapted after Giles et al. (2004); Betts and Giles (2006); Betts et al. (2006;2007;2009). In this model the Radium Creek Group are deposited in an extensional back-arc basin and sourced from the Felsic large igneous province (FLIP) preserved on the Gawler Craton; b) Rapid tectonic switching to shortening ca. 1585 Ma and back to extension is driven by perturbations in the convergent margins along the southern margin of Australia; c) Renewed crustal shortening at ca. 1555 Ma is related to subduction along the eastern margin of the continent.

Table 1: Lu-Hf values for standards run to determine instrumentation precision and accuracy.

Table 2: U-Pb values for standards run during the study acquisition period and longer-term averages indicating the level of reproducibility and instrument stability obtained.

Table 3: Summary of the U-Pb dating and Hf isotope analysis.

Table 4: Zircon crystallisation rock type, modelled rock type from in-situ trace element chemistry after Belousova et al. (2002).

U-Th-Pb and Lu-Hf data

Click here to download Supplementary material for on-line publication: Appendix A_FINAL.xlsx

Major and trace geochemistry

Click here to download Supplementary material for on-line publication: Appendix B_FINAL.xlsx